JPL PUBLICATION 84-62

Flow of Nitrogen-Pressurized Halon 1301 in Fire Extinguishing Systems

D.G. Elliott
P.W. Garrison
G.A. Klein
K.M. Moran
M.P. Zydowicz

November 1, 1984

Prepared for
U.S. Army Tank-Automotive Command
Through an agreement with
National Aeronautics and Space Administration
by
Jet Propulsion Laboratory
California Institute of Technology
Pasadena, California

JPL PUBLICATION 84-62

Flow of Nitrogen-Pressurized Halon 1301 in Fire Extinguishing Systems

D.G. Elliott
P.W. Garrison
G.A. Klein
K.M. Moran
M.P. Zydowicz

November 1, 1984

Prepared for
U.S. Army Tank-Automotive Command
Through an agreement with
National Aeronautics and Space Administration
by
Jet Propulsion Laboratory
California Institute of Technology
Pasadena, California

The research described in this publication was carried out by the Jet Propulsion Laboratory, California Institute of Technology, and was sponsored by the U.S. Department of the Army through an agreement with the National Aeronautics and Space Administration.

ABSTRACT

Halon 1301 is a halocarbon fire extinguishing agent ($CBrF_3$) used by the U.S. Army for vehicle fire suppression. Halon 1301 is discharged under nitrogen pressure, and the Halon-nitrogen mixture is a two-phase, two-component mixture that obeys compressible fluid laws and exhibits choking effects. A computer model was developed for analyzing the discharge of Halon and nitrogen from a storage bottle through pipes and nozzles. The model agrees well with data from Halon 1301 discharge tests. According to the model the discharge time depends mainly on nozzle area and pipe volume, for given bottle initial conditions. Graphs were developed for estimating discharge times. In tests of dispersion nozzles, conventional orifice-type nozzles gave only narrow-angle coverage, but a nozzle employing multiple concentric converging-diverging nozzles was developed which gave hemispherical coverage.

ACKNOWLEDGEMENTS

The work on Halon - nitrogen flow was sponsored by the U.S. Army Tank-Automotive Command (TACOM) under Military Interdepartmental Purchase Request No. W56HZV-4-IRRD-6 (NASA Task Order RE-182, Amendment 51). The TACOM project manager was Charles Beaudette. Technical guidance from TACOM was provided by Charles Beaudette, Edward Rozniecki, and Karl Brobeil. Dr. Harry Johnson of NASA White Sands Test Facility cooperated in fire-suppression aspects of the study.

The work was performed in the JPL Propulsion Systems Section, Winston Gin, Manager.

Test technician support was provided by James Arnold, instrumentation support by Joseph Carames and Russell Hansen, and photography by Robert Hansen. Programs for processing the data tapes were provided by Richard Cowley.

CONTENTS

Figures

Tables

I. INTRODUCTION

"Halon" is the name given by the U.S. Army to fire extinguisher agents containing halogens (Ref. 1). "Halon 1301" is bromotrifluoromethane, $CBrF_3$. The numerals "1301" stand for one carbon, three fluorines, no chlorine, and one bromine. A Halon 1301 concentration of only 7 percent by volume in air extinguishes fires by a combination of cooling and interference with the chemical reaction chain of fuel and oxygen (Refs. 2-5).

Halon 1301 is a clear liquid with a vapor pressure of 1.4 MPa (200 psia) at room temperature. To speed expulsion, Halon is stored under nitrogen pressure. The Army has adopted a standard storage pressure of 5.2 MPa (750 psia) at 20°C (Ref. 6).

Figure 1 is a photograph of Halon 1301 discharging from a 3750 cm^3 bottle. The liquid discharge time, with only the bottle valve restricting the flow as in this test, is 0.17 s. The subsequent venting of nitrogen and Halon vapor takes another 0.2 s. To the eye the discharge is a puff of white vapor. High speed movies show an opaque white plume that steadily diminishes in size but does not change in density. In particular, there is no change in appearance, with either front lighting or back lighting, when the liquid flow stops and vapor venting begins, because the vapor condenses and continues to form a vapor cloud.

A Halon fire extinguisher system may consist of only a bottle and a nozzle, or a complex arrangement of pipes and nozzles. In any case, the design problem is to determine the bottle, nozzle, and pipe sizes that will deliver the desired amount of Halon at each discharge point in the desired time. A necessary design tool for this task is a flow model for predicting Halon flow rate versus time as

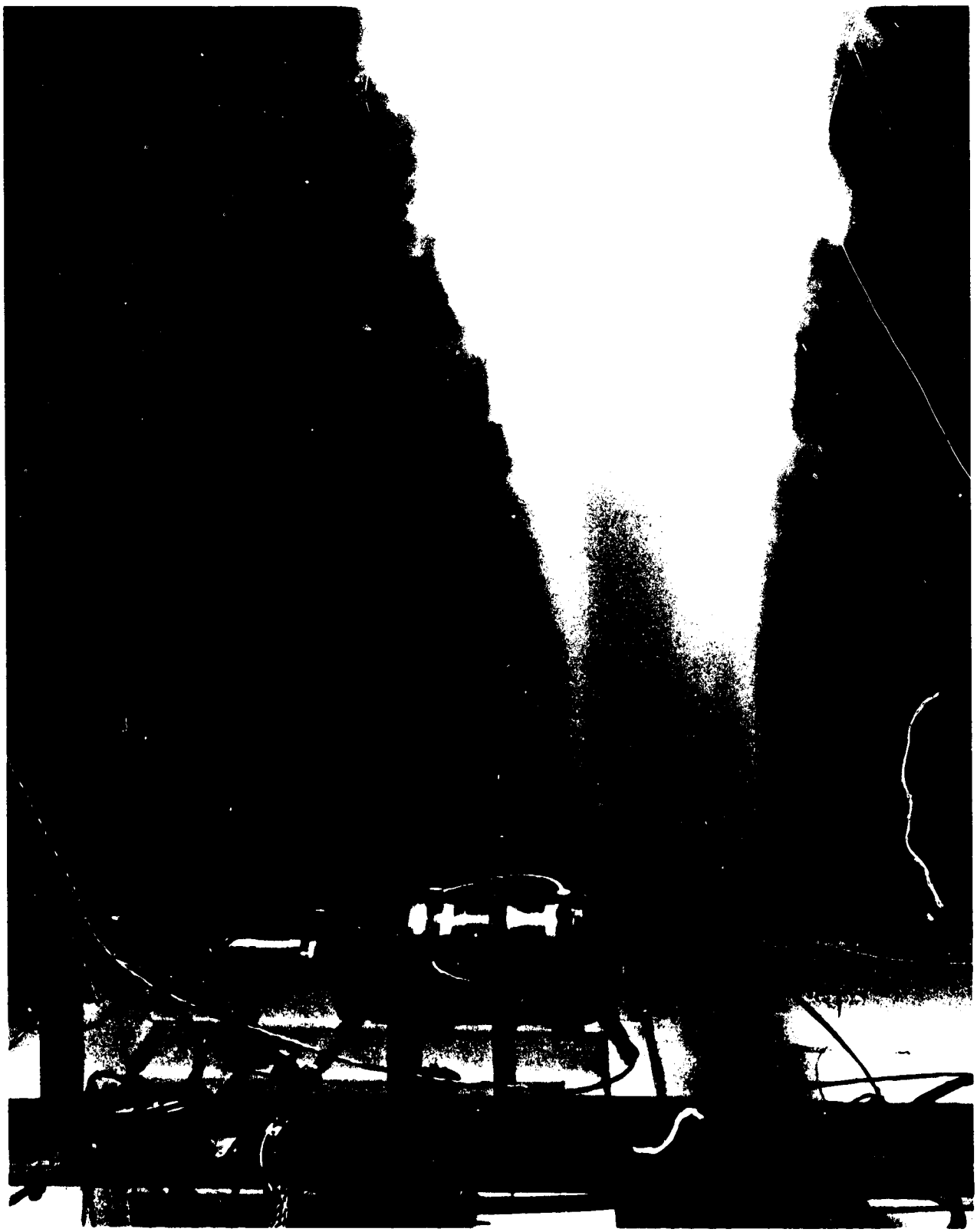

Figure 1. Halon 1301 discharge

a function of bottle, pipe, and nozzle sizes. Such a flow model was the primary goal of this project. In addition, the flow distribution from dispersion nozzles was investigated. Tests were also conducted on valves, burst discs, flow deflectors, safety plugs and pressure gages; those tests were reported in Ref. 7.

One benefit of a theoretical flow model is to provide a detailed understanding of the processes occurring during Halon flow. Section II describes how nitrogen-pressurized Halon expands out of a bottle and through pipes and nozzles, based on the model. Section II also shows the verification of the model by comparison of theoretical and experimental pressure-time curves.

Section III shows how to calculate Halon flow rate using the computer program and how to estimate discharge time using graphs calculated by the program.

Section IV describes tests of Halon dispersion nozzles. Appendix A gives the derivation of the theoretical model. Appendix B presents equations for the properties of Halon and nitrogen mixtures. Appendix C describes work done toward modifying a steam blowdown program as an alternate approach to calculating Halon flow. Appendix D summarizes the bottle discharge tests made to provide a data base.

II. NITROGEN-PRESSURIZED HALON FLOW

The purpose of this Section is to describe the behavior of Halon flow expanding from a bottle and flowing through pipes and orifices, based on the theoretical model. Comparisons between theoretical and measured pressure-time curves will be used to validate the model.

A. Bottle Discharge Tests

Figure 2 shows a typical pressure-time curve for a Halon discharge test (Test 146) and the apparatus used. The bottle had an electric pilot-operated valve. Nozzles or pipes could be connected to the valve exit. A pressure transducer and a thermistor temperature probe were mounted at the top of the bottle, and another temperature probe was mounted at the bottom.

Before each run the bottle was loaded with the desired mass of liquid Halon (typically filling 60 percent of the bottle) and pressurized with nitrogen. The bottle was rocked and nitrogen added until the pressure stayed constant at the desired level, showing that the dissolved nitrogen concentration (about 2.3 percent by mass) was in equilibrium with the nitrogen gas.

The recorders were started, the valve was actuated and the pressure and temperature traces were recorded. The pressure dropped to atmospheric in times ranging from a fraction of a second to several seconds, depending on nozzle size.

In most tests the pressure-time curve had visible slope changes marking two key events in the run. The curve in Fig. 2 shows these slope changes clearly. The first slope change is a pressure recovery from 3.9 MPa to 4.1 MPa at 0.2 s.

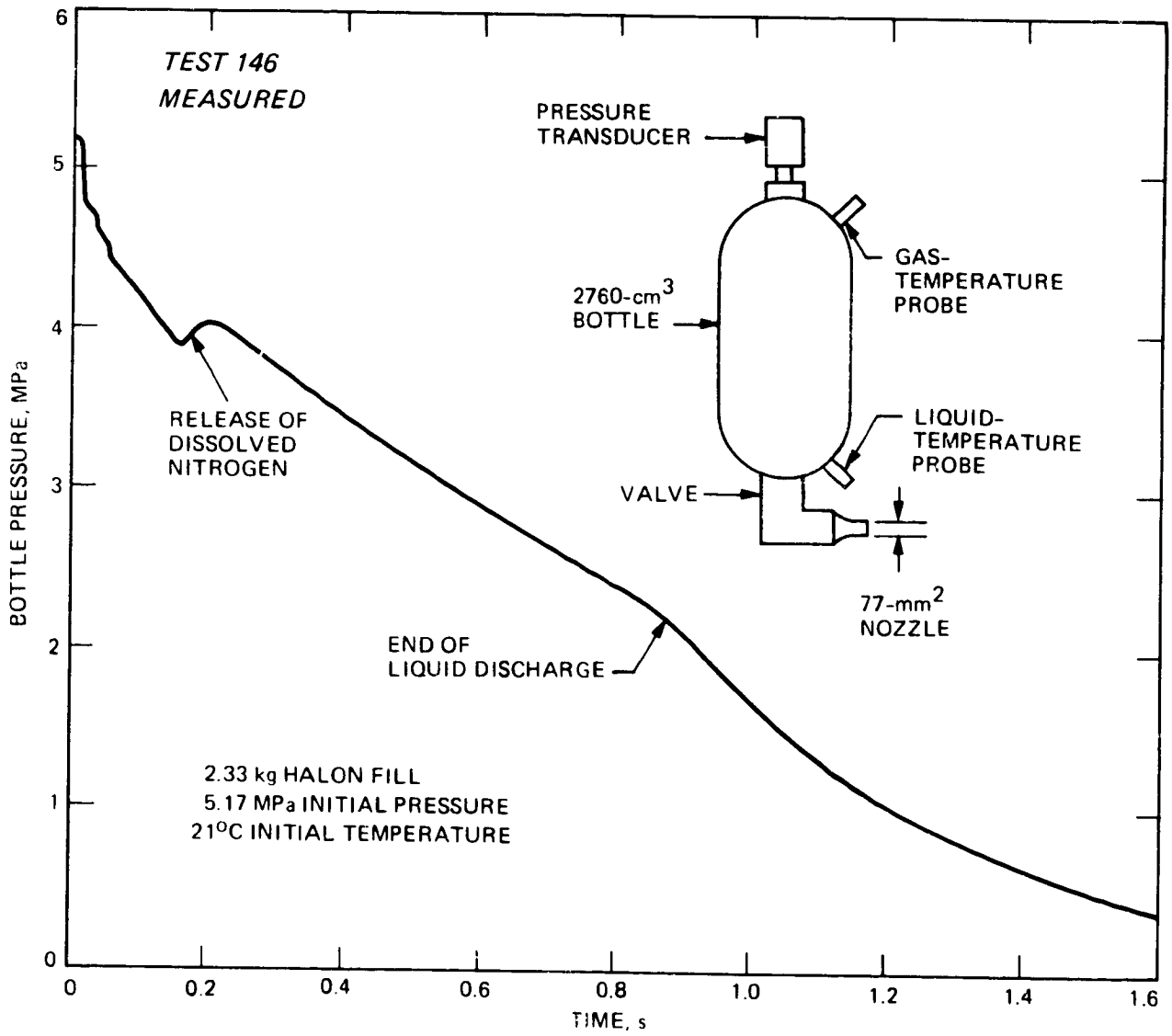

Figure 2. Typical pressure data

The second change is an increase in pressure decay rate at 0.85 s. The pressure recovery at 0.2 s is due to a sudden release of dissolved nitrogen. The slope change at 0.85 s marks the point at which the bottle runs out of liquid and venting of nitrogen gas and Halon vapor begins. The identification of these slope changes with nitrogen release and liquid runout is based entirely on the theoretical model; there was no experimental observation of nitrogen release or liquid runout.

The measured temperatures are shown in Fig. 3. The temperature measured by the top probe is considered to be the gas temperature, and the temperature measured by the bottom probe is considered to be the liquid temperature. The measured temperatures drop gradually until liquid runout at 0.85 s. Then the temperatures drop more rapidly until limited by heat input from the warm bottle walls.

B. Bottle Discharge Predictions

The theoretical flow model predicts the pressure decay curve shown in Fig. 4 for Test 146. Numbers on the curve identify several events predicted by the model. During the first part of the run, from Point 1 to Point 2, nitrogen stays dissolved in the Halon as a non-equilibrium supersaturated solution, and the Halon remains a clear liquid. At Point 2 the pressure has dropped sufficiently to allow nitrogen bubbles to form. Once the bubbles form, all of the excess dissolved nitrogen quickly comes out of solution into the bubbles. The bubbles raise the Halon liquid level by about 25 percent and recompress the ullage gas to the pressure at Point 3.

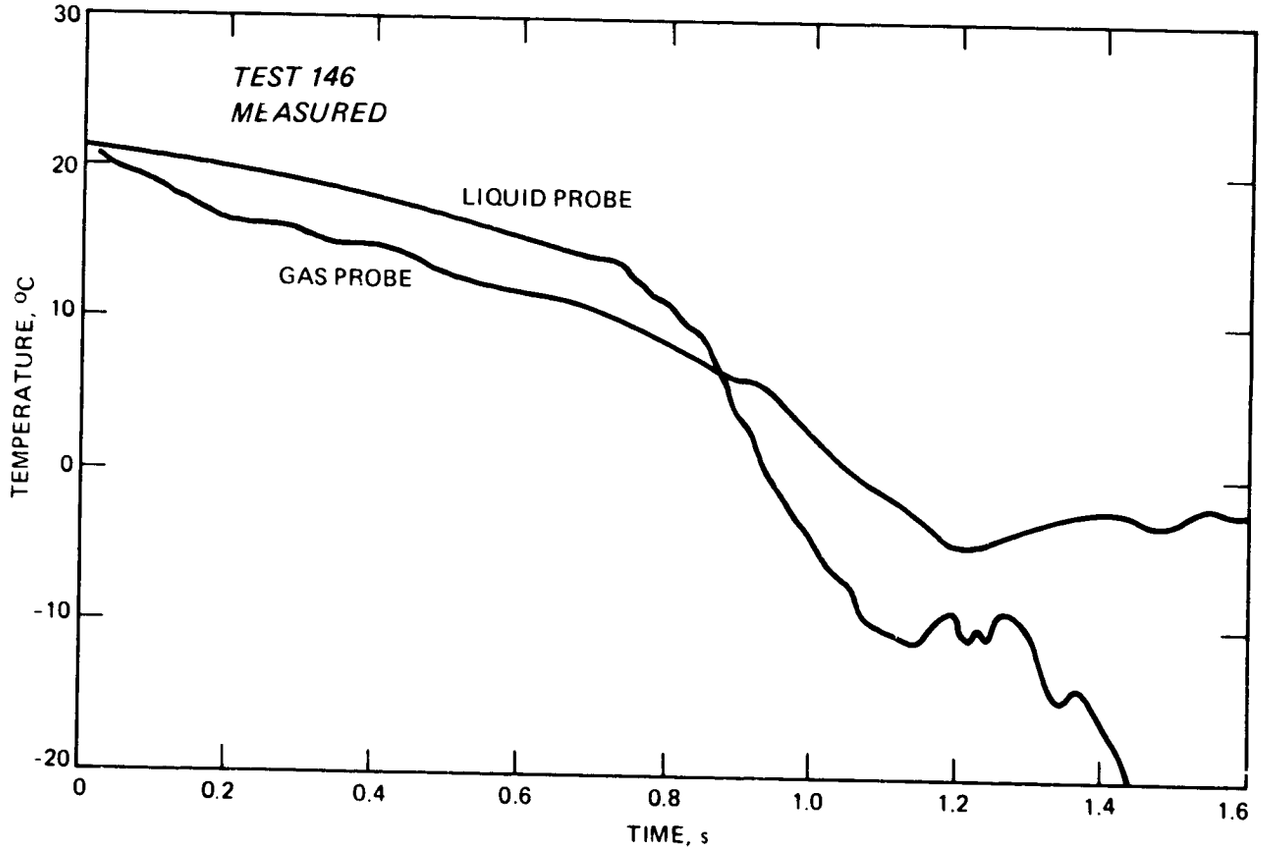

Figure 3. Typical temperature data

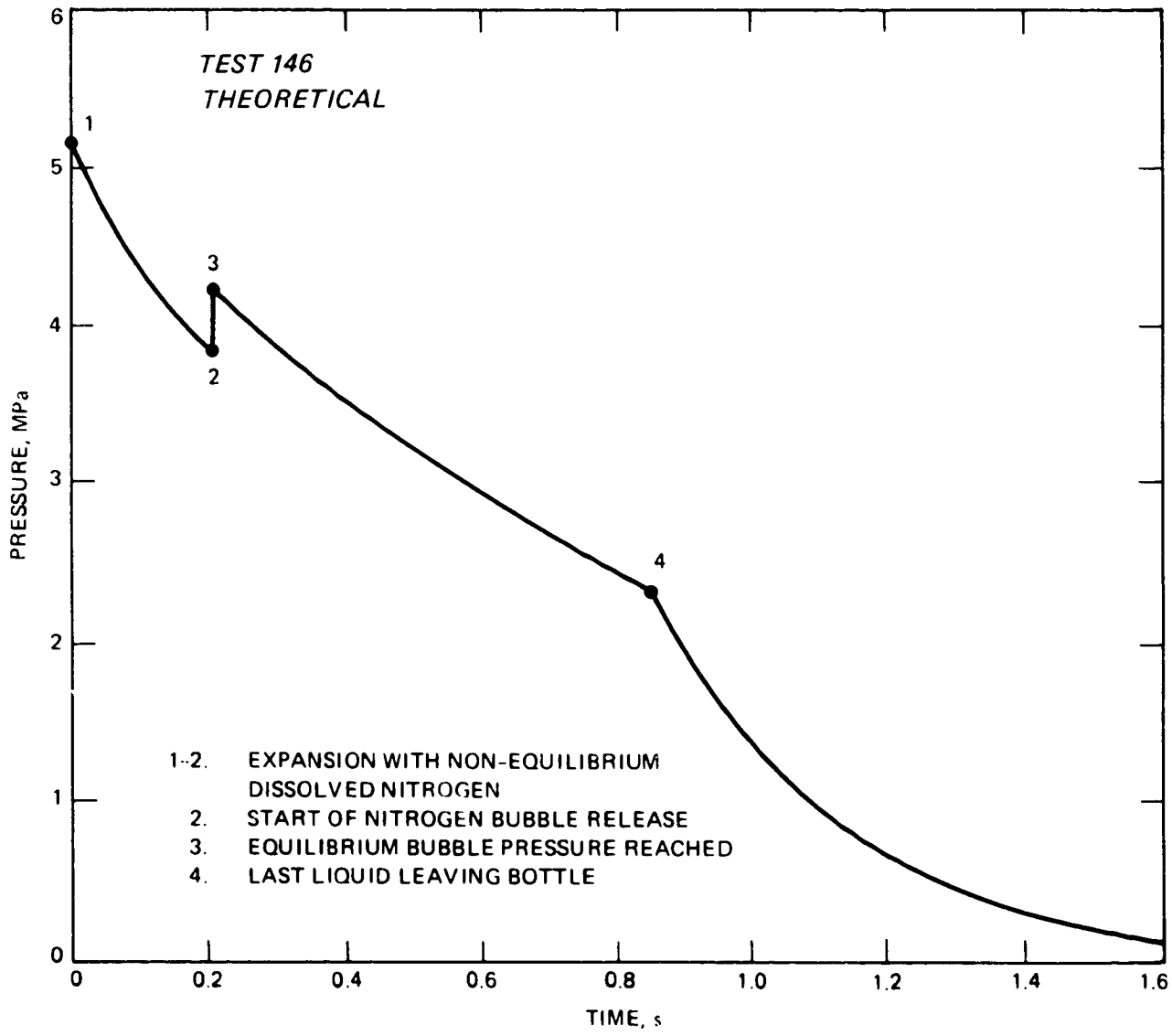

Figure 4. Theoretical pressure-time curve

The last liquid leaves the bottle at Point 4. The rate of pressure decay then increases because the gas is less dense than the liquid and allows a higher volume flow rate through the nozzle.

"Outage fraction" is the mass fraction of the original Halon fill that has been discharged from the bottle at any given time. Figure 5 shows the theoretical increase of outage fraction with time. At liquid runout the outage fraction is 0.93; only 7 percent of the Halon remains in the bottle.

C. Nitrogen Release Pressure

The pressure at which the nitrogen starts coming out of solution, the "nitrogen release pressure" (identified by Point 2 in Fig. 4), depends on the Halon surface tension. As the pressure drops from Point 1 to Point 2, microscopic nitrogen bubbles are continually forming throughout the liquid due to random agglomeration of nitrogen molecules. The pressure of the nitrogen in these nucleation bubbles is equal to the initial nitrogen pressure, because the dissolved nitrogen concentration has not changed. However, the bubbles do not grow when the bottle pressure drops, because the surface tension of the Halon produces an additional inward pressure. Bubble growth only starts when the bottle pressure falls below the nucleation bubble pressure by an amount equal to the surface-tension pressure. Once this bottle pressure is reached the bubbles start to grow, and the surface-tension pressure on the bubbles decreases due to the increasing radius of curvature. The bubble growth accelerates, and the excess nitrogen in solution is quickly released.

The difference between nucleation bubble pressure and bottle pressure at the start of nitrogen release (Point 2) is plotted as a function of Halon temperature for several runs in Fig. 6. As shown by the inset pressure-time

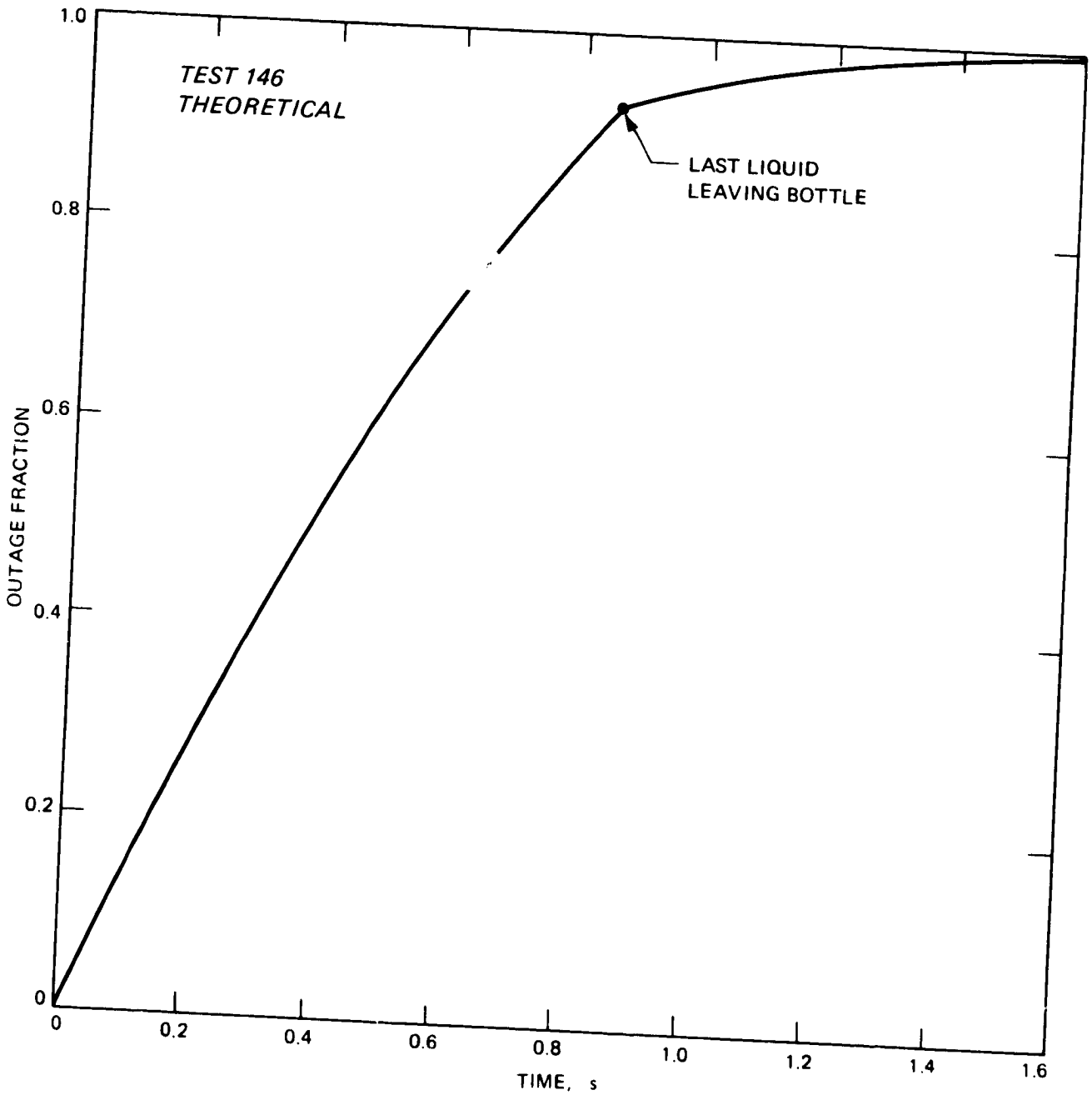

Figure 5. Theoretical outage fraction

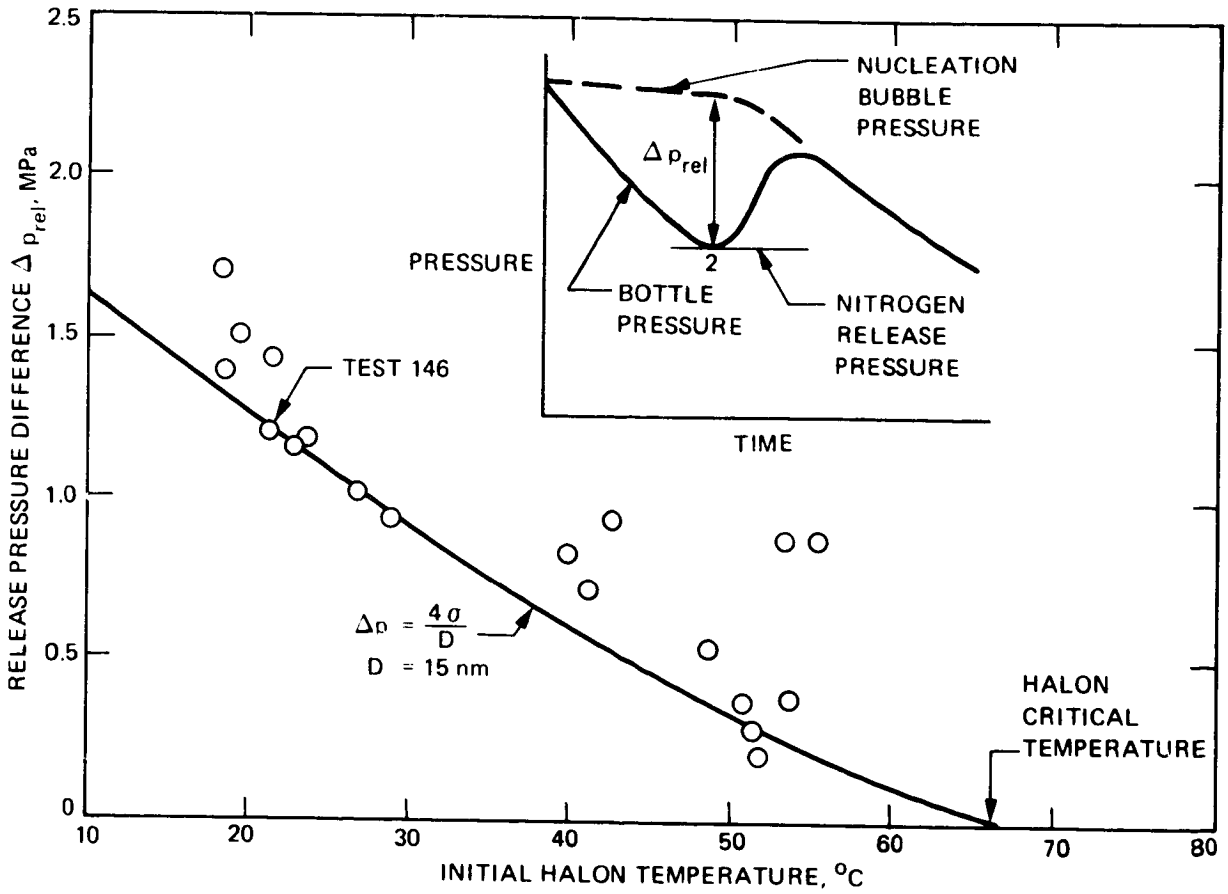

Figure 6. Nitrogen-release pressures and fitted curve

curve in Fig. 6, the nucleation bubble pressure, which is the sum of the Halon vapor pressure and the initial nitrogen pressure, decreases slightly during expansion from Point 1 to Point 2 because the Halon vapor pressure decreases. The pressure difference Δp_{rel} at the start of nitrogen release decreases with increased Halon temperature, because the surface tension decreases. At 20°C the release pressure difference is about 1.5 MPa. At the critical temperature of Halon 1301, 67°C, the surface tension is zero and the observed pressure difference Δp_{rel} at nitrogen release is also zero. There is considerable scatter in the data; the pressure difference required for nitrogen release is three times as great in some runs as in others at the same temperature.

The pressure difference due to the surface tension of the liquid surrounding a bubble is $4\sigma/D$, where σ is the surface tension and D is the bubble diameter. As shown in Fig. 6, a nucleation bubble diameter of 15 nm gives a pressure difference that agrees with the lowest release pressure differences observed. That value of nucleation bubble diameter is used in the model, because it also gives the best agreement with the data between 20°C and 30°C where most of the tests were run.

D. Theory and Data Comparison

For comparing theoretical and experimental pressure-time curves it is necessary to match the starting times. The procedure adopted is to match the curves a short time after the valve-opening transients are over, about halfway between Point 1 and Point 2.

Figure 7 compares the theoretical and experimental pressure-time curves for Test 146. The curves agree well up to the point of liquid runout, Point 4.

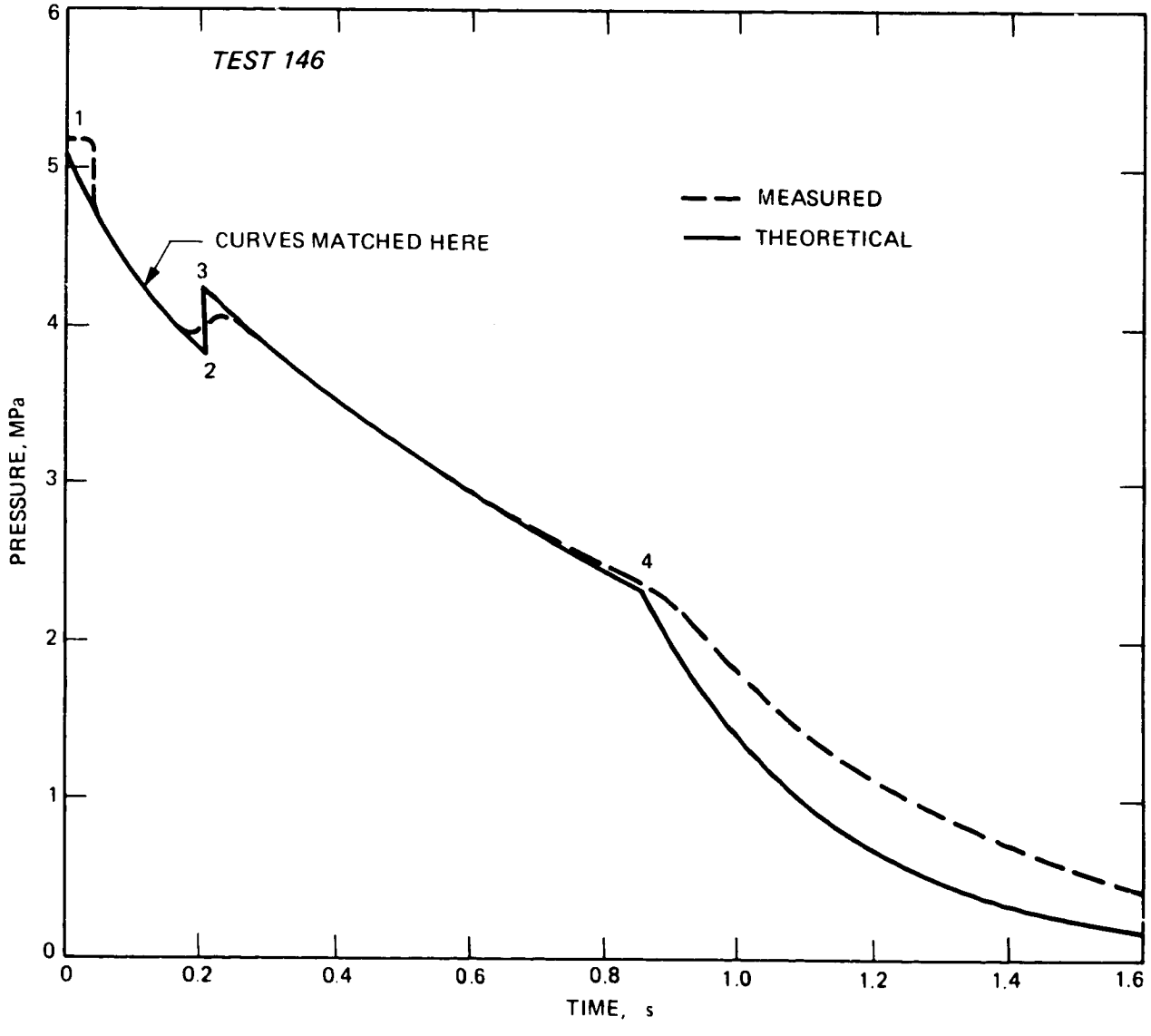

Figure 7. Comparison between theoretical and experimental pressure-time curves

During subsequent vapor venting the measured pressure falls more slowly than the theoretical pressure. The slower decay could be due to liquid draining from the bottle walls and raising the density of the nozzle flow.

The theoretical and experimental temperatures are compared in Fig. 8. In the model the gas and liquid temperatures are equal and there is no heat transfer from the bottle. The theoretical temperature falls more rapidly than the measured temperatures especially during vapor discharge. During vapor venting the theoretical temperature drops to -80°C whereas the measured temperatures remain above -20°C. The warmer measured temperatures are attributed to heat transfer into the gas and into the temperature probes from the bottle walls.

Figure 9 compares the theoretical and experimental pressure traces for Test 102, a test with no nozzle, using only the valve to restrict the flow. The valve flow area cannot be measured directly because of the complicated shape of the valve flow passage. Instead, the flow area used in Fig. 9 is the one that gives the best agreement between the theoretical and experimental pressure curves, 500 mm^2. The flow area measured in water flow tests was less, 400 mm^2. Test 102 can be considered a calibration of the effective flow area of the valve with Halon. The question of determining flow areas for use in the theoretical model will be discussed further in Section III.

Because of the substantial agreement between the theoretical and measured pressure-time curves for Test 146, and other tests to be discussed (especially up to the time of liquid runout), it is concluded that all other quantities calculated by the model are also correct. It is unlikely that quantities such

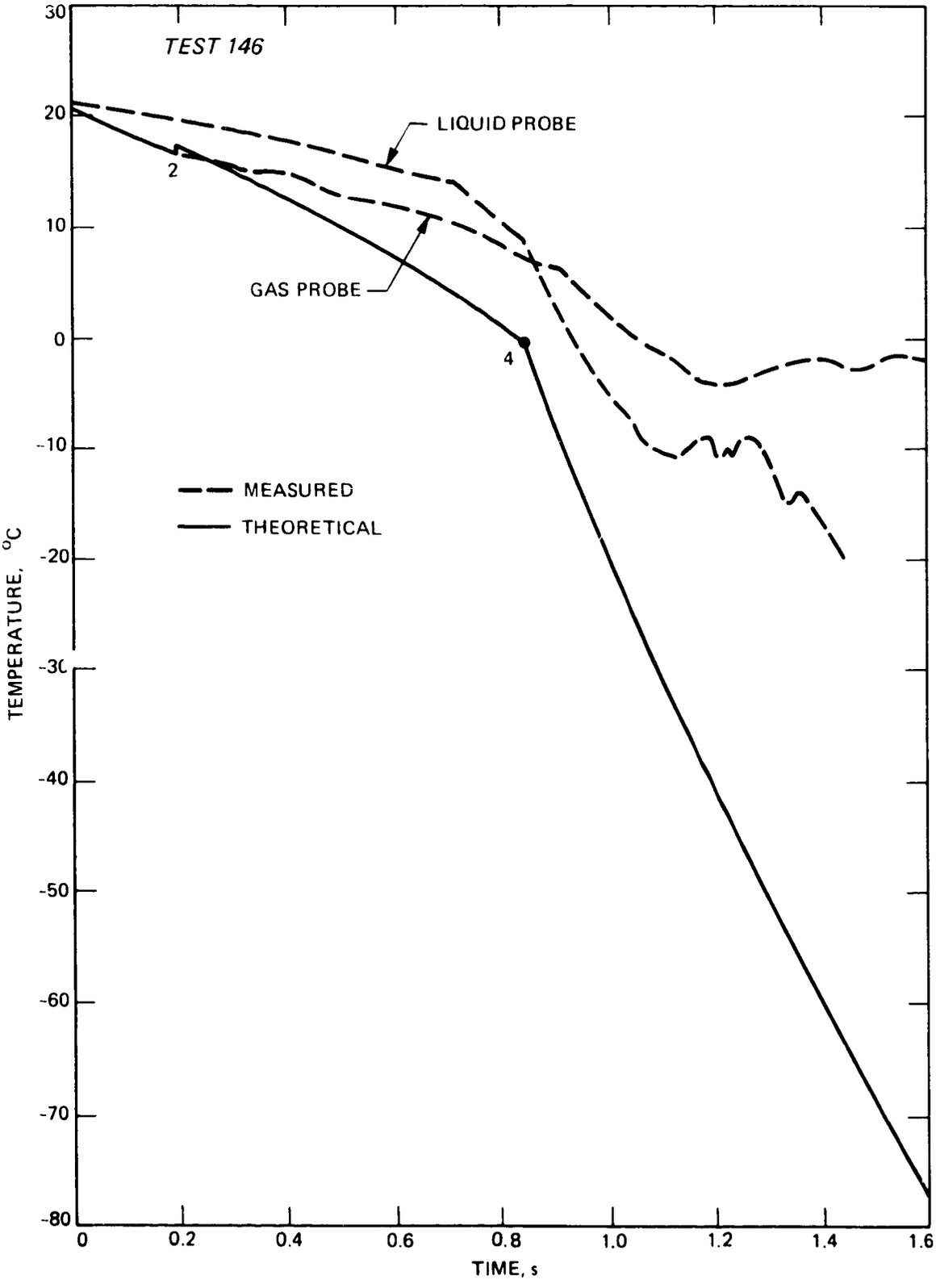

Figure 8. Comparison between theoretical and experimental temperature-time curves

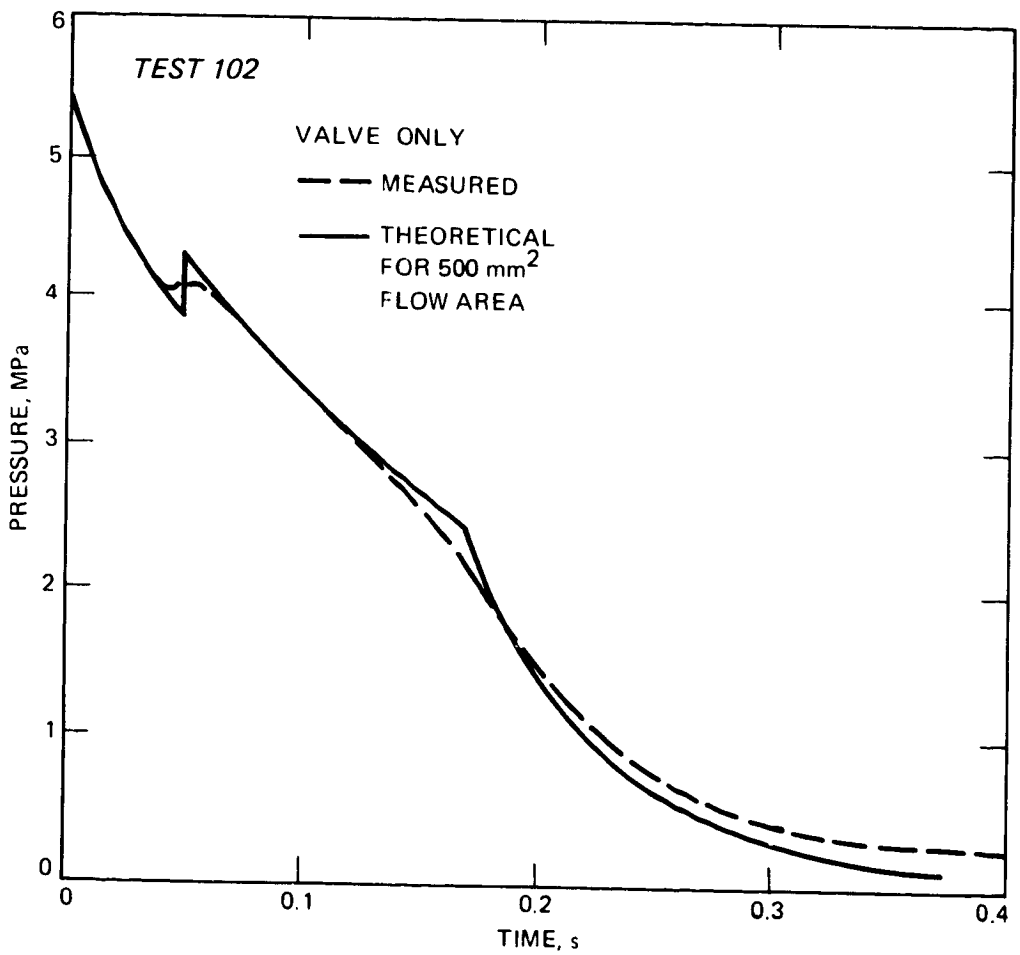

Figure 9. Comparison, with valve only, between theoretical and experimental pressures

as void fraction, quality, temperature, and nitrogen concentration could be significantly in error and the pressure-time curve still be correct. After liquid runout, the model is less accurate, as evidenced by the slower pressure decay and lower temperatures than measured.

E. Bottle Expansion Process

The theoretical model calculates many details of the Halon discharge process in addition to the pressure, temperature, and outage values that have been presented. A study of these other quantities provides useful insight into the nature of the flow. The processes occurring inside the bottle, as calculated by the theoretical model, will be considered first.

Figure 10 presents sketches of the interior of the Halon bottle at four key times during discharge, with corresponding points marked on pressure and outage curves. Initially, at Point 1, the bottle is about 60 percent full of liquid. The ullage volume above the liquid contains nitrogen gas and Halon vapor. The region below the liquid surface, which will be referred to as the "liquid layer," consists of liquid Halon and dissolved nitrogen. The dissolved nitrogen initially has a concentration of about 2.3 percent by mass. When the valve is opened, fluid flows from the liquid layer through the valve and nozzle to atmosphere. Nitrogen bubbles form somewhere between the valve entrance and the nozzle exit as the pressure in the flow stream falls below the nitrogen release pressure.

As the bottle empties, Halon evaporates and supplies vapor to the growing ullage volume. The nitrogen dissolved in the evaporated Halon also contributes a small amount of additional nitrogen to the ullage. In addition, the dissolved nitrogen that is very close to the surface (within a few mm) probably comes out

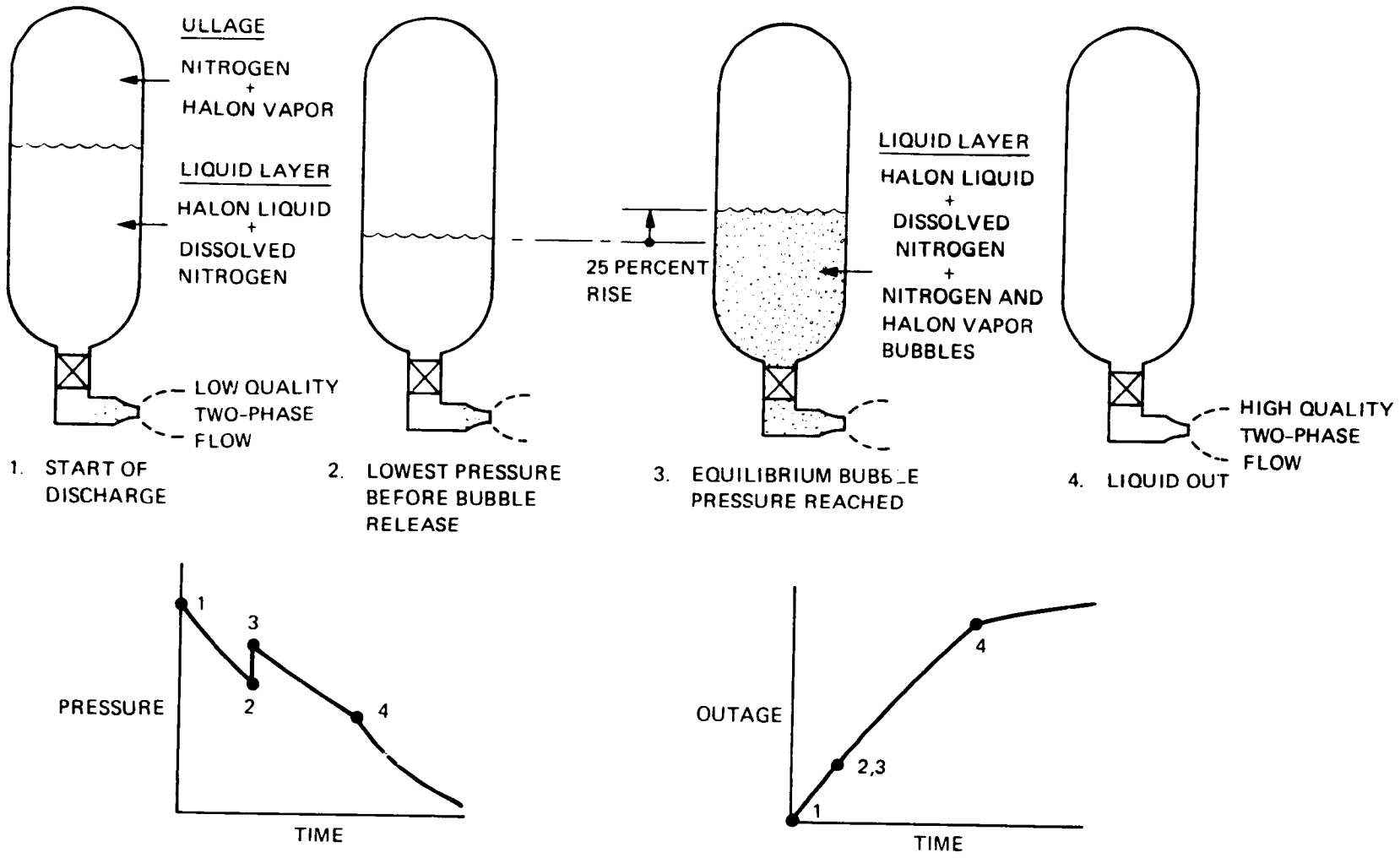

Figure 10. Bottle expansion steps

of solution and enters the ullage, but this effect is ignored in the model. The bulk of the dissolved nitrogen is too far below the surface to diffuse to the surface and is only released when bubbles form throughout the liquid at the nitrogen release pressure. Sketch 2 in Fig. 10 shows the conditions just before nitrogen release and Sketch 3 shows the conditions just after equilibrium concentration is reached.

During bubble formation the liquid layer expands by about 25 percent, compressing the ullage gas and raising the pressure to Point 3. The liquid layer is now a two-phase mixture of (1) a liquid phase consisting of Halon and dissolved nitrogen and (2) a gas phase (distributed as bubbles) consisting of nitrogen gas and Halon vapor.

The liquid layer continues to discharge from the bottle until all of the liquid has left the bottle at Point 4. At that time the ullage gas starts to flow out of the bottle. As the gas in the ullage cools, the Halon vapor starts to condense, and the flow leaving the bottle becomes an increasingly wet mixture of nitrogen gas, Halon vapor, and Halon liquid.

The conditions inside the bottle depend only on the amount of Halon that has been discharged, and not on time, under the assumption of adiabatic flow. Figure 11 shows how the pressure and temperature decrease as the outage fraction increases, for typical initial conditions. The pressure drops to 3.8 MPa at an outage of 0.30 before the first nitrogen bubbles form (based on a 15-nm nucleation bubble diameter). The temperature drops to 15°C at the same time. As shown in Fig. 12, the mass of liquid in the bottle (Halon plus dissolved nitrogen) has dropped to 2.1 kg at this point. The mass of gas in the ullage

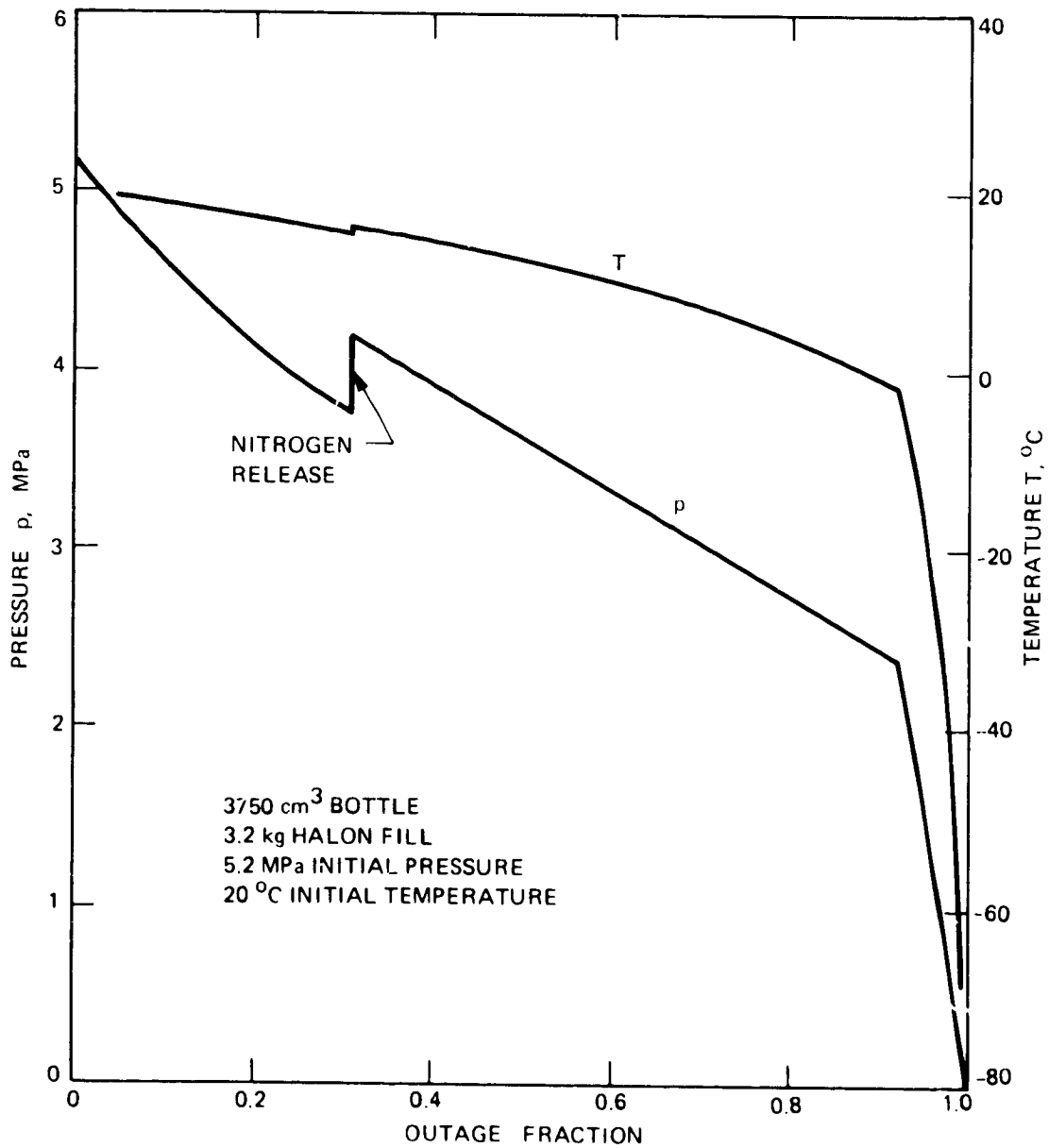

Figure 11. Bottle pressure and temperature during discharge

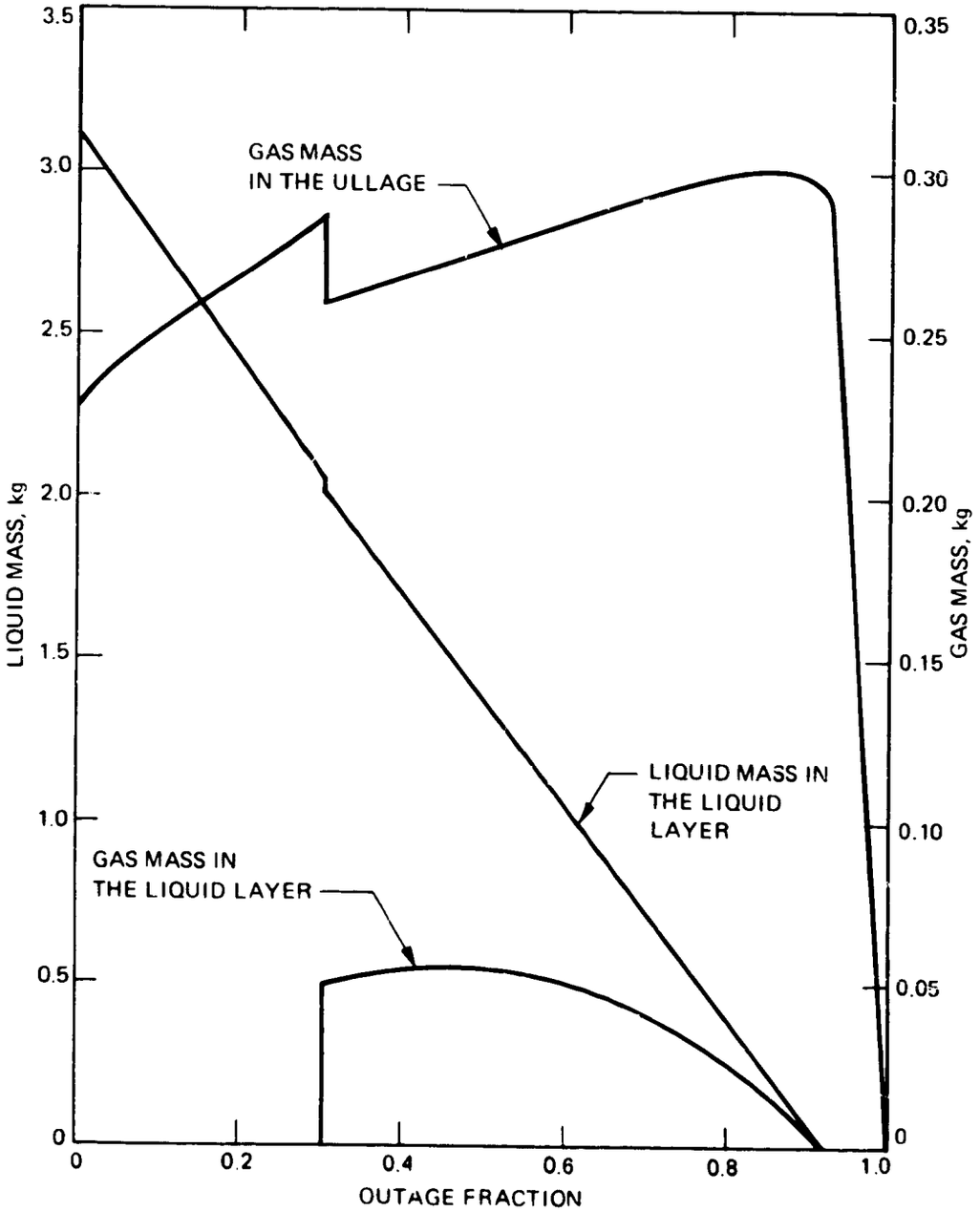

Figure 12. Bottle masses during discharge

has risen from an initial 0.22 kg to 0.29 kg because of Halon evaporation.

When the nitrogen bubbles form, the pressure increases by 0.4 MPa, the temperature increases by $1^{o}C$, the liquid mass decreases by 0.1 kg, and the ullage gas mass decreases by 0.03 kg (due to Halon vapor condensation). The mass of bubbles produced is 0.05 kg. As shown in Fig. 13, the exit flow becomes a two-phase mixture having 0.02 quality and 0.2 void fraction.

The mass of gas in the liquid layer reaches a maximum of 0.06 kg at 0.49 outage. The mass of gas in the ullage reaches a maximum of 0.30 kg at 0.86 outage. The last liquid leaves the bottle at an outage of 0.90; 10 percent of the Halon remains as vapor. The quality of the last of the liquid layer leaving is 0.07 and the void fraction is 0.60.

After the last liquid leaves the bottle the ullage gas follows a pressure and temperature path that causes condensation of Halon vapor. The quality of the exit flow starts at 1.0 at liquid runout and drops to 0.75 as the pressure drops to atmospheric. The void fraction only drops to 0.998. The final outage fraction is 0.995; 0.5 percent of the Halon remains in the bottle at atmospheric pressure.

F. Nozzle Flow

The flow rate out of the bottle depends on the response of the external flow components to the bottle conditions. An important case is a nozzle connected directly to the valve. The nozzle may have multiple passages to disperse the Halon, but the net effect is an area restriction through which the Halon must pass. As the area decreases in the flow direction, the stream

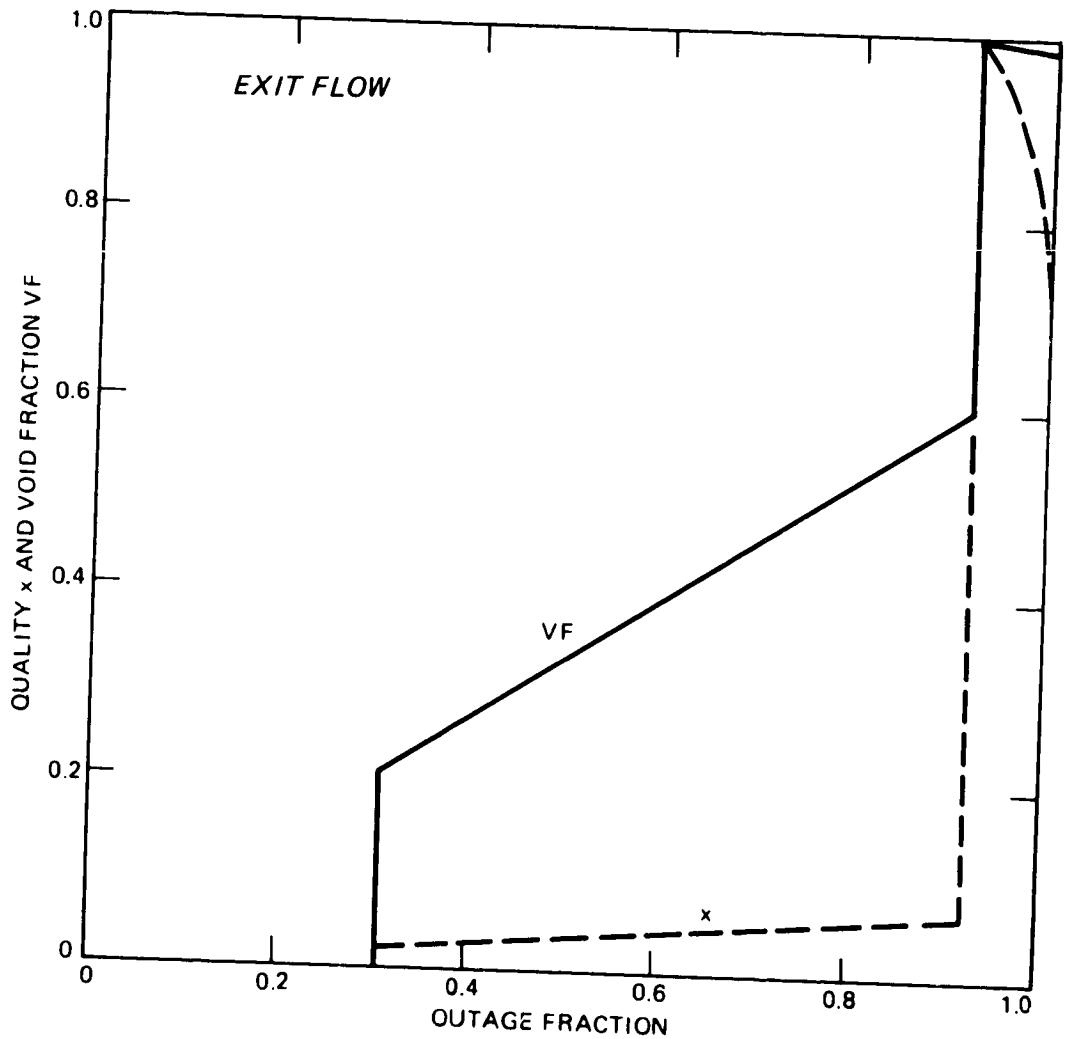

Figure 13. Exit flow conditions during discharge

pressure drops, but the pressure cannot reach atmospheric in a converging passage because the flow is compressible and sonic conditions are reached at about half the nozzle inlet pressure. Sonic flow is reached at the minimum-area point, or "throat" in the nozzle. The nozzle can either be cut off at that point for unguided fluid expansion to atmospheric pressure (as in Fig. 1, where the valve acts as a converging nozzle) or the nozzle can have a diverging section for guided expansion.

Figure 14 shows the calculated flow conditions in a typical converging-diverging nozzle (or in a converging nozzle cut off at the throat). The inlet conditions are the bottle conditions of Fig. 11 at 0.5 outage fraction: 3.6 MPa, 12°C, 0.04 quality, and 0.34 void fraction. The pressure decreases to 2.4 MPa at the throat. The quality increases to 0.09 and the void fraction to 0.66. The velocity at the throat is 56 m/s. The throat temperature is 7°C.

As the flow proceeds through the diverging section (or to atmosphere in an unguided expansion) the quality, void fraction and velocity continue to increase. When atmospheric pressure is reached (at a flow area 11 times the throat area) the quality is 0.47, the void fraction is 0.996, and the velocity is 200 m/s. If the nozzle is cut off at the throat, the same conditions would be reached except that the gas phase may expand laterally away from the liquid, leaving a slow liquid core surrounded by a higher-velocity gas sheath.

The flow rate set by the 314 mm^2 throat area at 3.6 MPa nozzle inlet pressure is 10.4 kg/s. The flow rates at other times during the bottle blowdown are plotted as a function of time in Fig. 15. The initial flow rate is 15 kg/s. The flow rate increases when the pressure rises at the time of nitrogen release. The flow rate drops abruptly when the liquid runs out and gas venting begins.

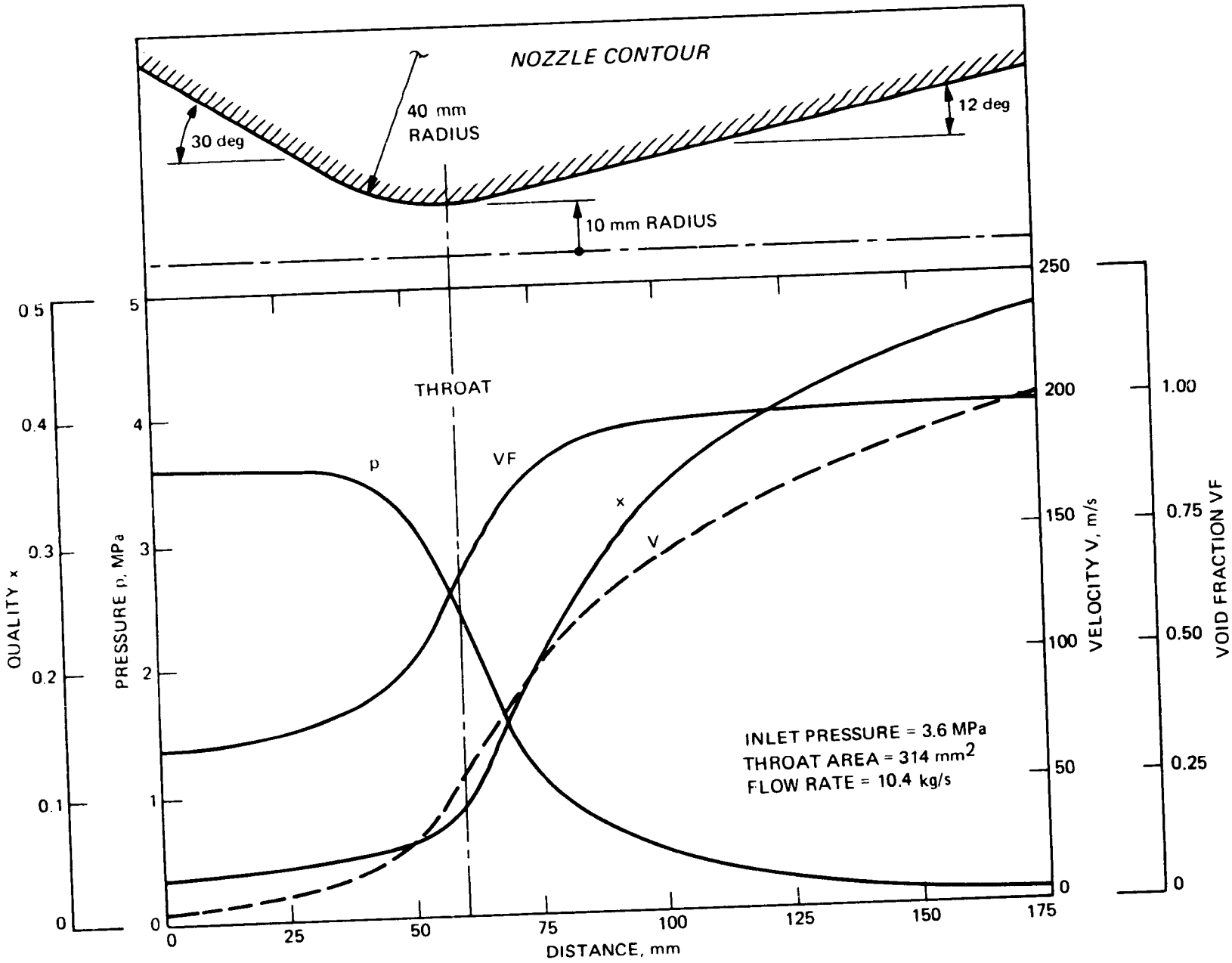

Figure 14. Typical flow conditions in a nozzle

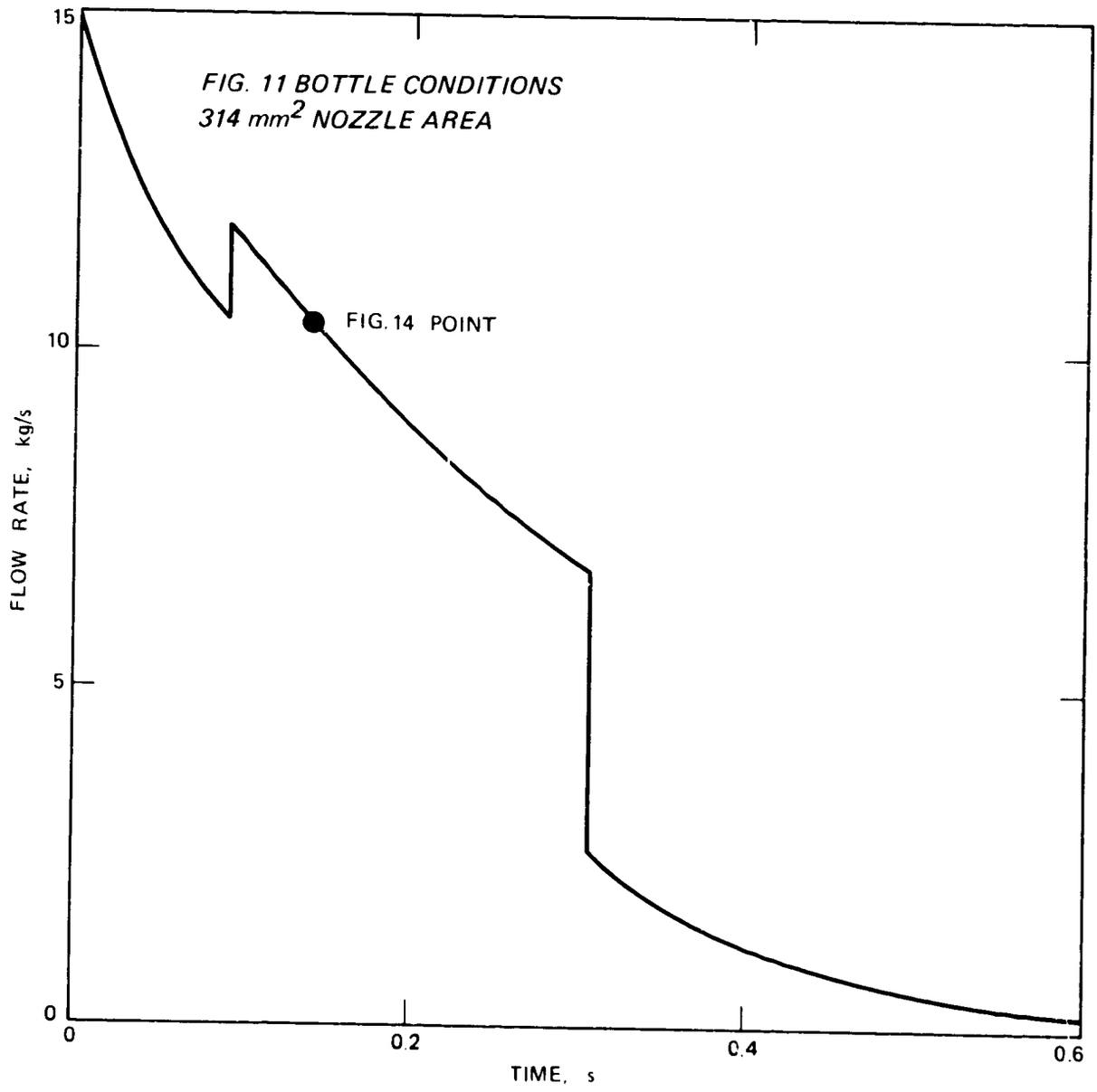

Figure 15. Flow rate variation during discharge

G. Pipe Flow

Another important type of flow component is a pipe leading from the bottle to atmosphere or to nozzles at a distance. The leading edge of the Halon traveling down the pipe forms a "liquid front" consisting of a two-phase Halon-nitrogen mixture traveling at soric velocity. If the pipe leads to atmosphere without a nozzle the flow at the exit remains sonic after the pipe is full.

Figure 16 shows the theoretical variation of pressure along a 314 mm^2 pipe at the same inlet conditions as in Fig. 14. The calculations apply to the instant the liquid front has traveled 2.4 m down a long pipe or when steady flow has been established at the end of a 2.4-m pipe.

The pressure falls to 3.3 MPa at the pipe inlet and to 1.7 MPa at the liquid front or pipe exit. The velocity is 25 m/s at the pipe inlet and 59 m/s at the exit. The main acceleration takes place as the flow approaches the liquid front or pipe exit.

The flow rate set by choked flow in the pipe is 6.9 kg/s, a 34 percent reduction from the 10.4 kg/s with a nozzle of the same area. Thus, as a 314 mm^2, 2.4-m pipe fills, the flow rate starts at 10.4 kg/s and decreases to 6.9 kg/s.

H. Pipe Pressurization

If there is a nozzle or other restriction at the end of a pipe, the pipe exit pressure starts to rise when the liquid front reaches the end. The pressure rises until the flow rates into and out of the pipe are balanced at a lower flow rate. The theoretical pressures along the pipe at various stages during the filling and pressurization process are illustrated in Fig. 17, for

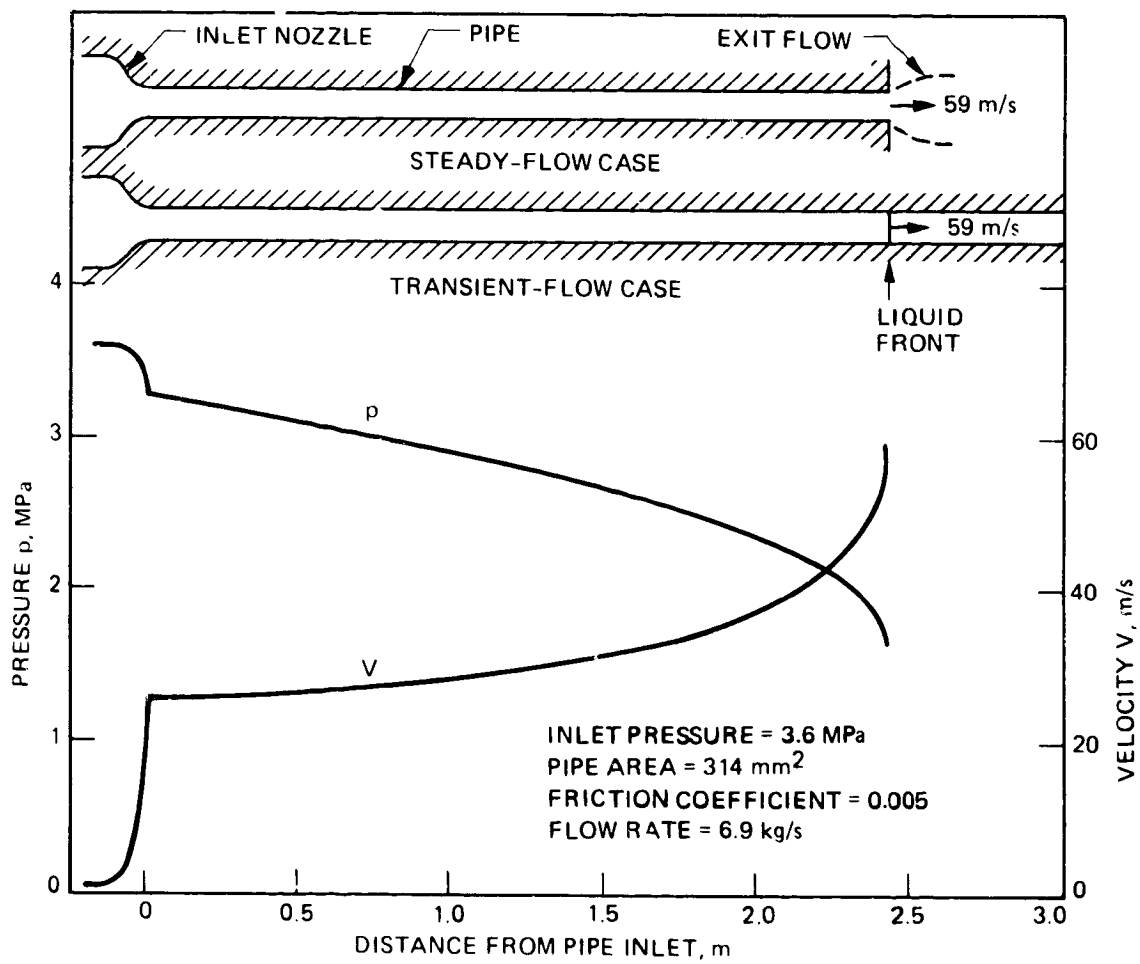

Figure 16. Choked flow conditions in a pipe

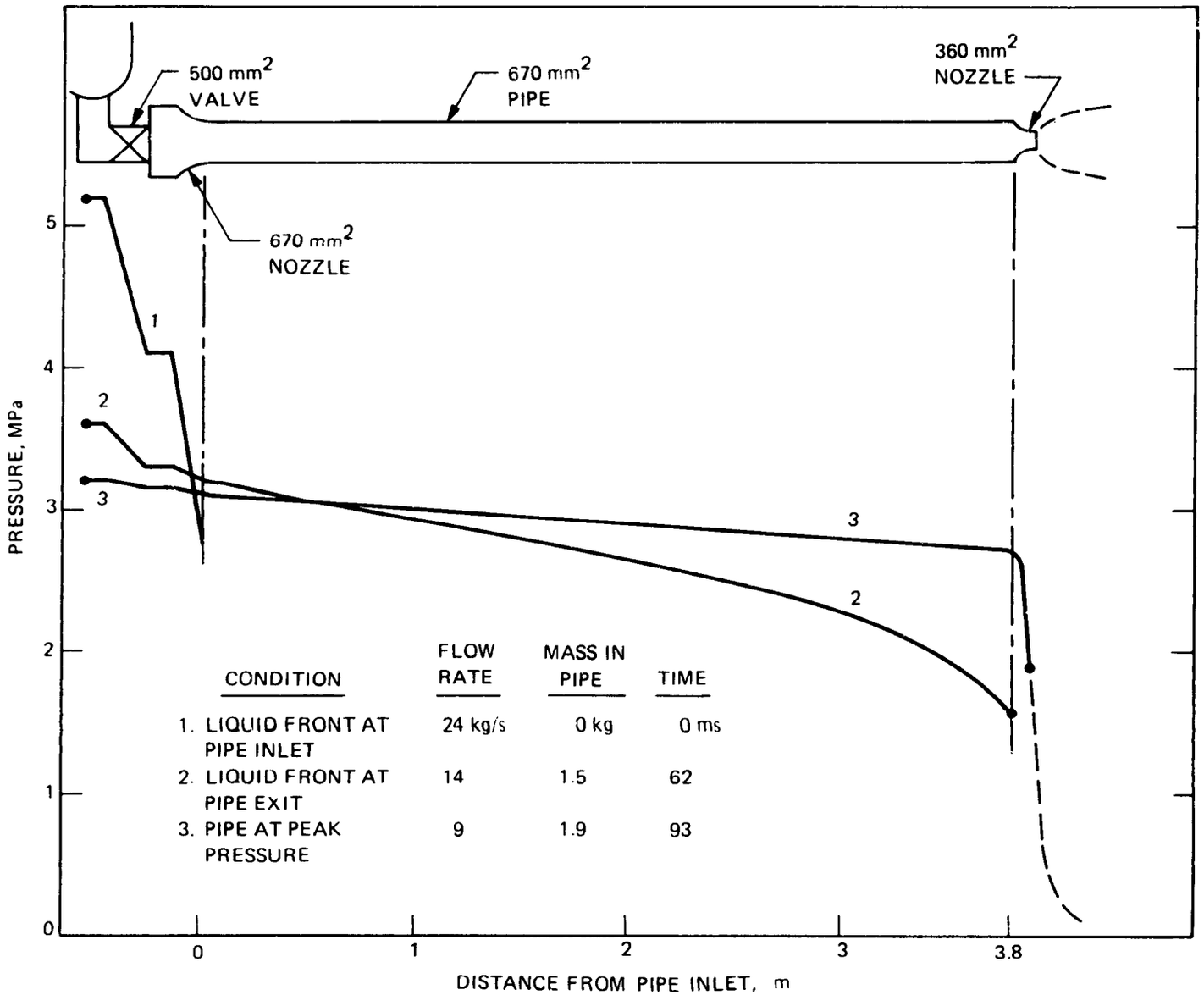

Figure 17. Pressure profiles in a pipe during discharge

Halon discharging from a 3750 cm^3 bottle into a 2550 cm^3 pipe with a 360 mm^2 nozzle at the end. The initial bottle pressure is 5.2 MPa. When the valve is opened the Halon quickly reaches the pipe inlet and establishes sonic flow at that point; the pressure profile is shown by Curve 1. The pressure at the valve exit at that time is 4.1 MPa and the pressure at the pipe inlet is 2.8 MPa. The flow rate is 24 kg/s.

The liquid front proceeds down the pipe at 60 m/s and reaches the end in 62 ms. As shown by Curve 2, the bottle pressure has dropped to 3.6 MPa, but the pipe inlet pressure has increased to 3.3 MPa. The pressure at the liquid front (on the liquid side) is 1.6 MPa. The flow rate is 14 kg/s. The mass of fluid in the pipe is 1.5 kg, 47 percent of the Halon fill.

The Halon then encounters a nozzle with a throat area about half the pipe area. The flow decreases and the pipe exit pressure increases. The exit pressure reaches a peak 31 ms after the arrival of the liquid front (Curve 3). The bottle pressure at that time is 3.2 MPa, the pipe exit pressure is 2.7 MPa, and the flow rate is 9 kg/s. The amount of Halon stored in the pipe is 1.9 kg, 60 percent of the Halon bottle fill. About 6 percent of the Halon has been discharged from the nozzle by this time.

I. Pipe and Nozzle Discharge Tests

To verify the theory, flow tests were made with a 670-mm^2, 3.8-m long pipe and various nozzles. Figure 18 is a sketch of the apparatus. The theoretical and experimental pressure curves, for both the bottle pressure and the pipe exit pressure, are compared in Fig. 19 for Test 175, in which a 360 mm^2 nozzle was used. The agreement is good. Several events predicted by the model are marked along the curves. At Point 1 the liquid front reaches the end of the pipe and

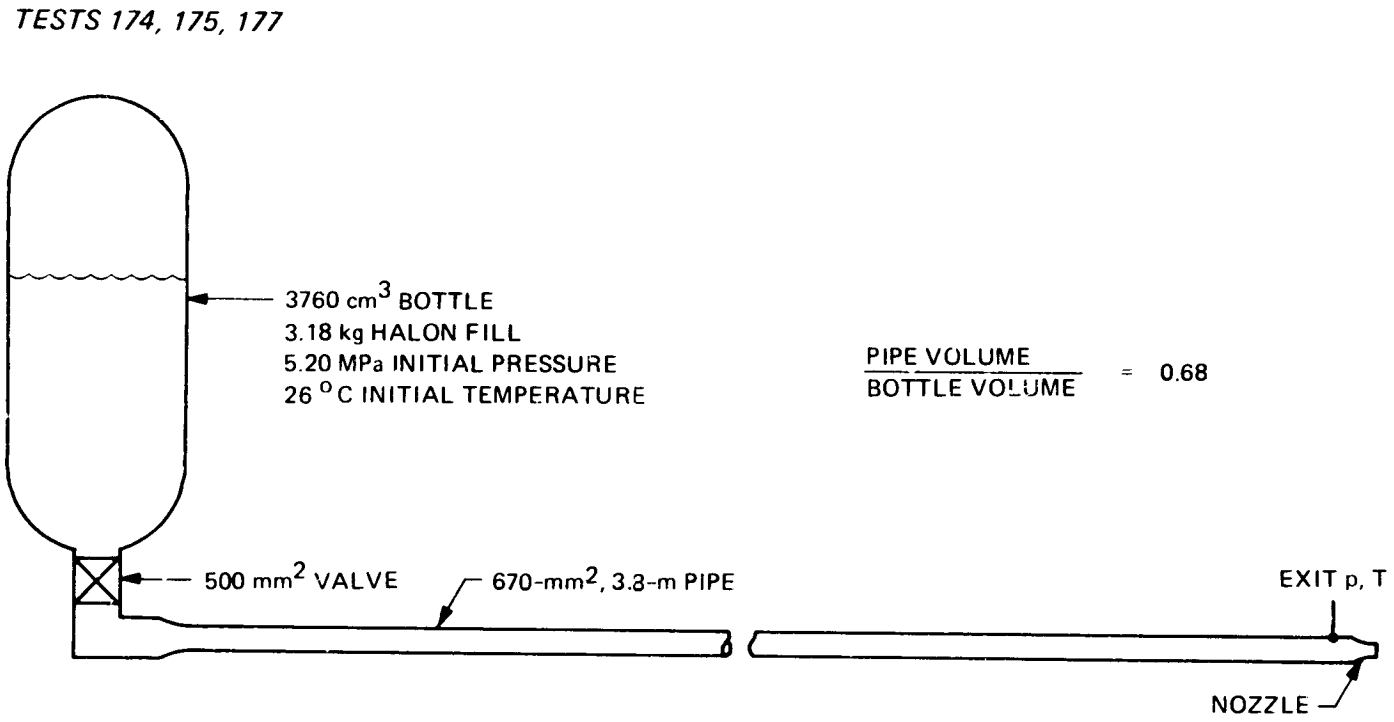

Figure 18. Pipe and nozzle flow system

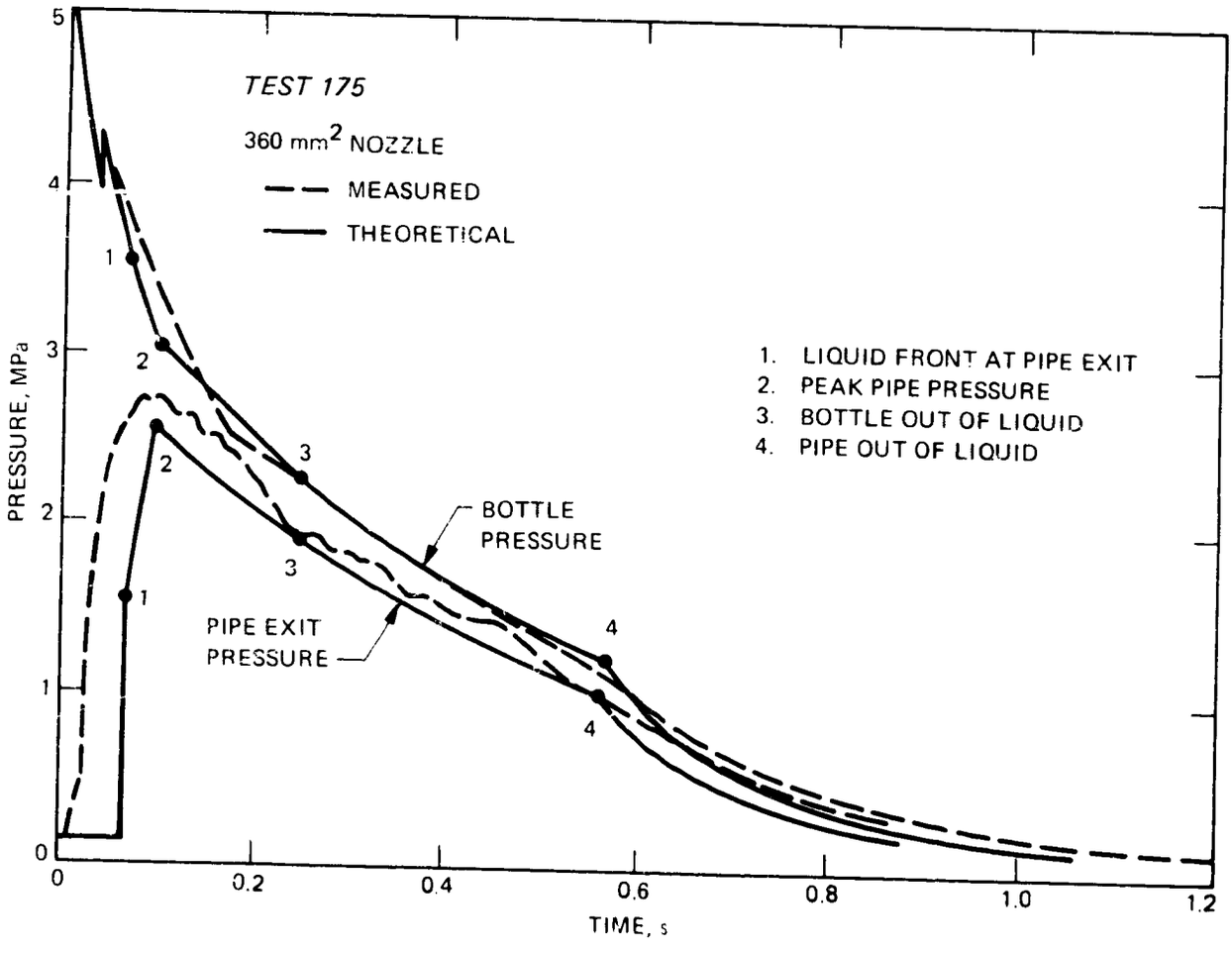

Figure 19. Comparison, with a large nozzle, between theoretical and experimental pressure-time curves

the pipe exit pressure starts to rise. In the test the exit pressure rises earlier due to air pushed ahead of the Halon.

Point 2 is the instant of peak pipe exit pressure. At Point 3 the last liquid has left the bottle, and vapor is following the liquid down the pipe. At Point 4 the last liquid has left the pipe. The abrupt change in slope at liquid runout predicted by the theory is not observed in the test.

The theoretical and experimental temperatures at the end of the pipe are compared in Fig. 20. The model predicts an initial temperature reading of 0 ^{o}C when the liquid front reaches the end of the pipe, followed by an increase to 12^{o}C as the pipe pressurizes. The measurements, however, show a 50^{o}C spike due to the pulse of air preceding the Halon. The measured temperatures during gas venting (after Point 4) do not drop as low as predicted by the model, presumably because of heat transfer from the bottle and pipe.

Theoretical and experimental pressures for Test 174, with a smaller nozzle, are compared in Fig. 21(a) for the bottle pressure and Fig. 21(b) for the pipe exit pressure. The characteristic differences are again evident: no sharp break in slope at liquid runout in the test and a longer venting time. Also, the measurements show oscillations in the pressure after the liquid reaches the end of the pipe; in fact, the pipe exit pressure is alternately higher and lower than the bottle pressure.

Fig. 22 compares the theoretical and experimental pressures for a test with no exit nozzle. The flow expands directly from the pipe exit. Events 1 and 2 (the liquid front reaching the exit and the pipe reaching peak pressure) are

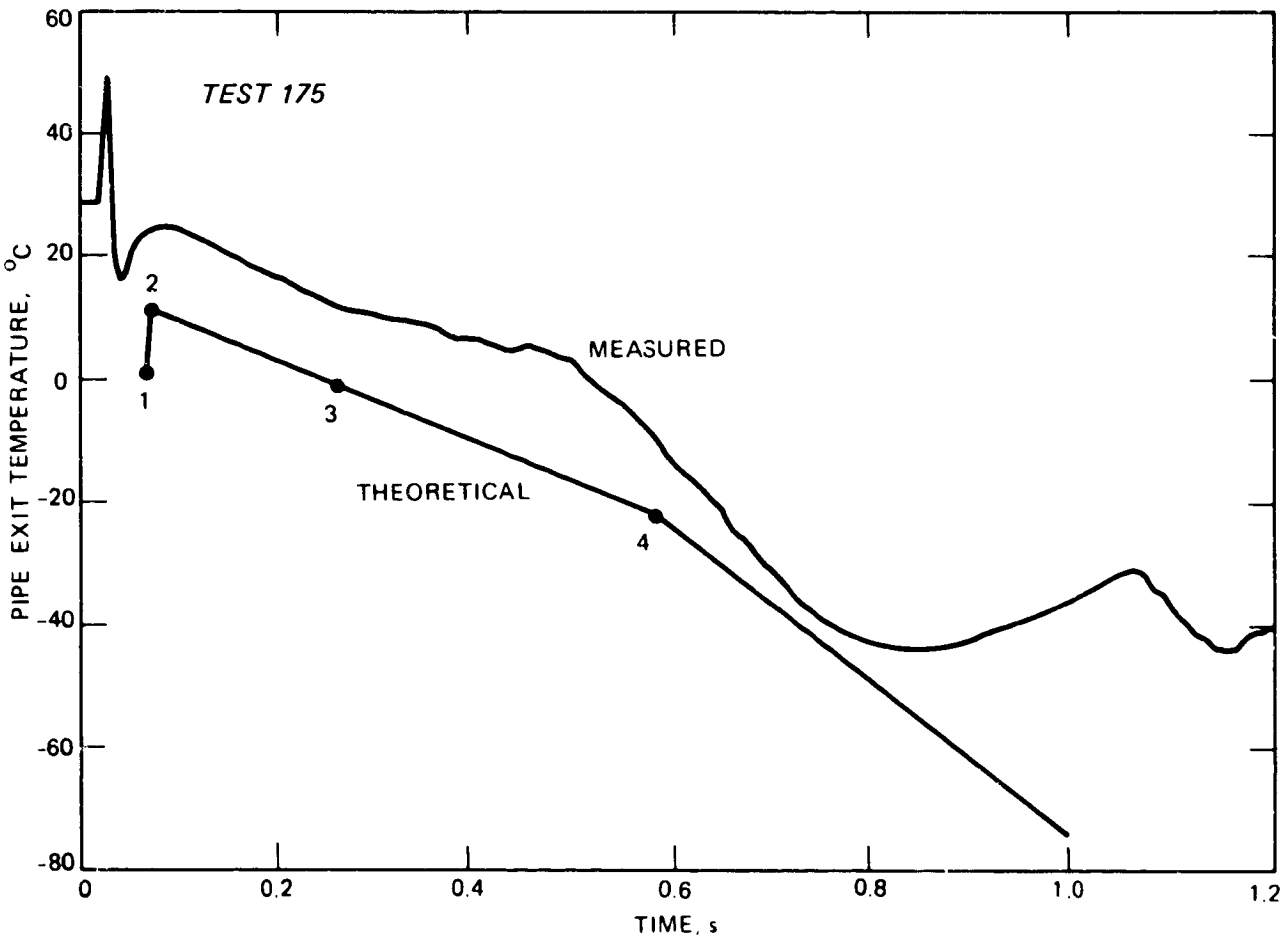

Figure 20. Comparison between theoretical and experimental pipe exit temperatures

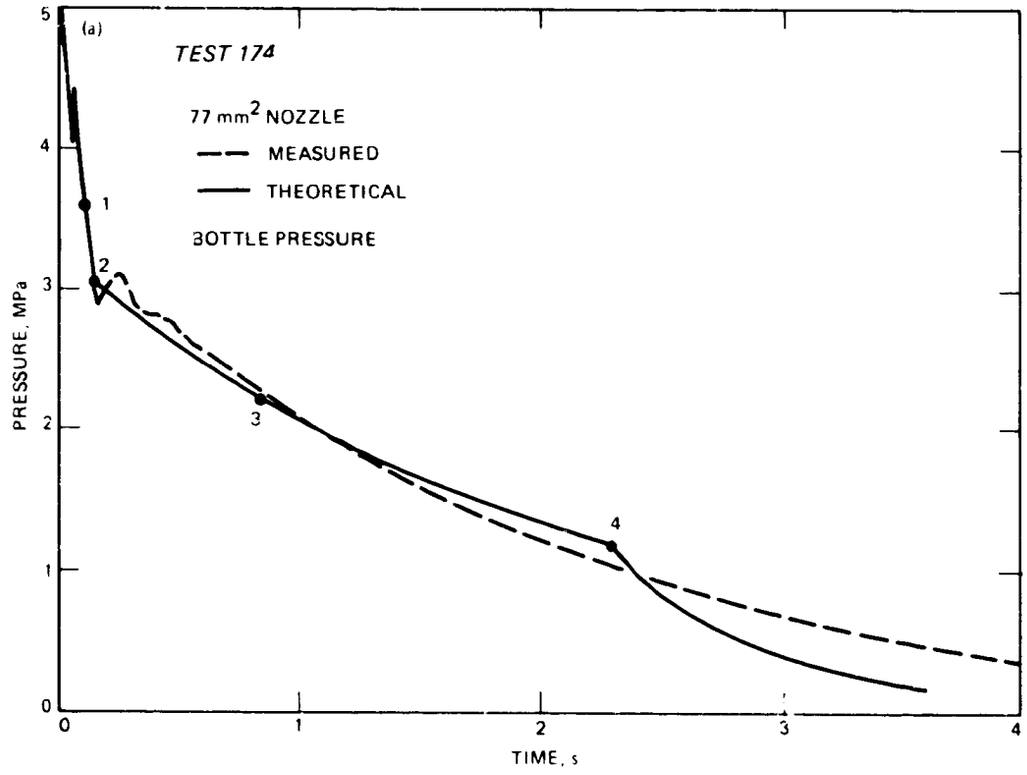

Figure 21. Comparison, with a small nozzle, between: (a) Theoretical and experimental bottle pressure-time curves

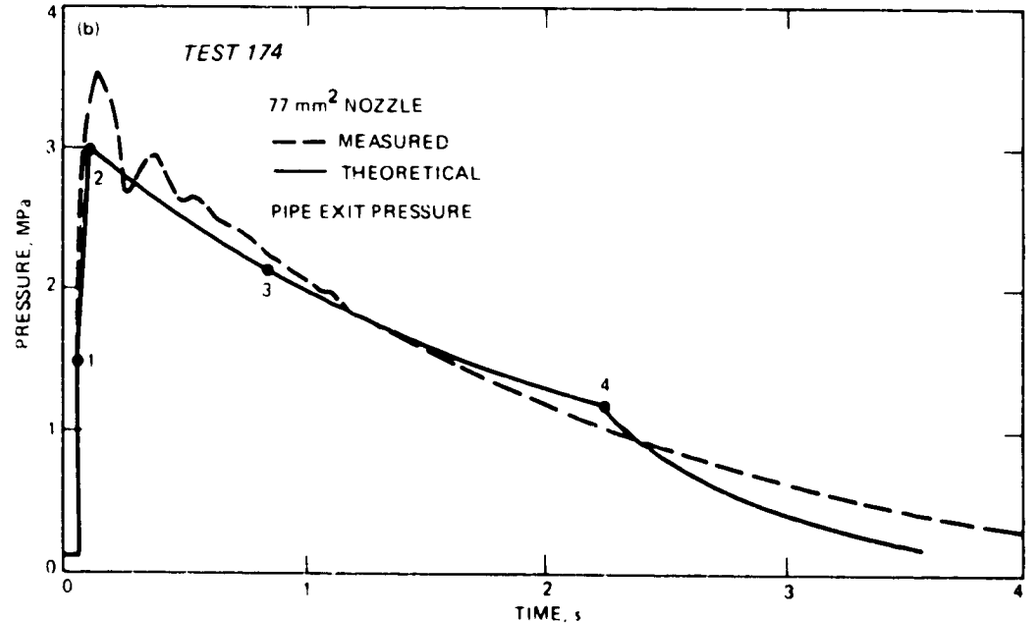

Figure 21. Comparison, with a small nozzle, between: (b) Theoretical and experimental pipe pressure-time curves

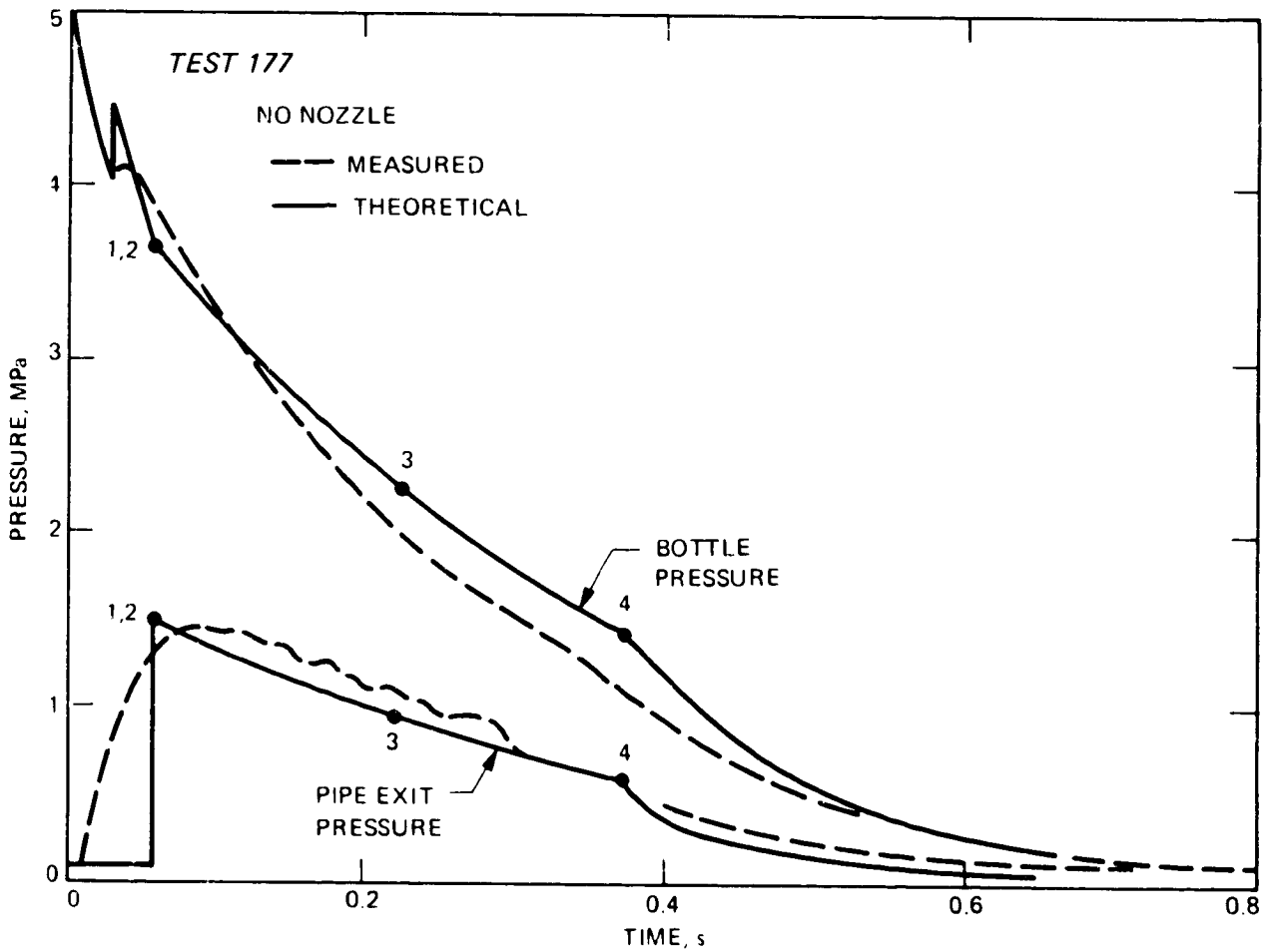

Figure 22. Comparison, with no nozzle, between theoretical and experimental pressure-time curves

simultaneous. The agreement between theory and experiment is still good in this extreme case of a large pressure drop in the pipe.

J. Multibranch Flow Systems

A Halon distribution system may consist of several pipes and nozzles delivering Halon to multiple locations. The computer model was developed to the point of handling a single pipe leading to a manifold, with any number of pipes leading from the manifold to discharge nozzles.

Two double-branch distribution systems were assembled to test the model. Figure 23 shows System 1 which had a 3.73-m pipe leading from the bottle to a tee and two pipes of different lengths leading to nozzles of different diameters. The inlets to the pipes, tee, and nozzles had rounded entrances to avoid any uncertainty about flow area.

Figure 24 presents the theoretical pressure-time curves for the bottle, tee, and nozzles, and Fig. 25 shows theoretical Halon mass discharged versus time from each nozzle. As shown in Fig. 24, the liquid front reaches the nozzles very quickly. Traveling at about 60 m/s, the Halon reaches the most distant nozzle, 8 m from the bottle, in only 0.13 s. The piping system reaches peak pressure only 0.2 s after valve opening. Once nozzle flow begins, there are only small pressure drops in the pipes: 3 percent from bottle to tee, 7 percent from the tee to the small nozzle, and 13 percent from the tee to the large nozzle.

The bottle runs out of liquid at 1.0 s and the main pipe at 2.1 s. The short branch runs out of liquid at 2.3 s, clearing a vapor path from bottle to atmosphere and starting a more rapid pressure decay. Because of the diminishing

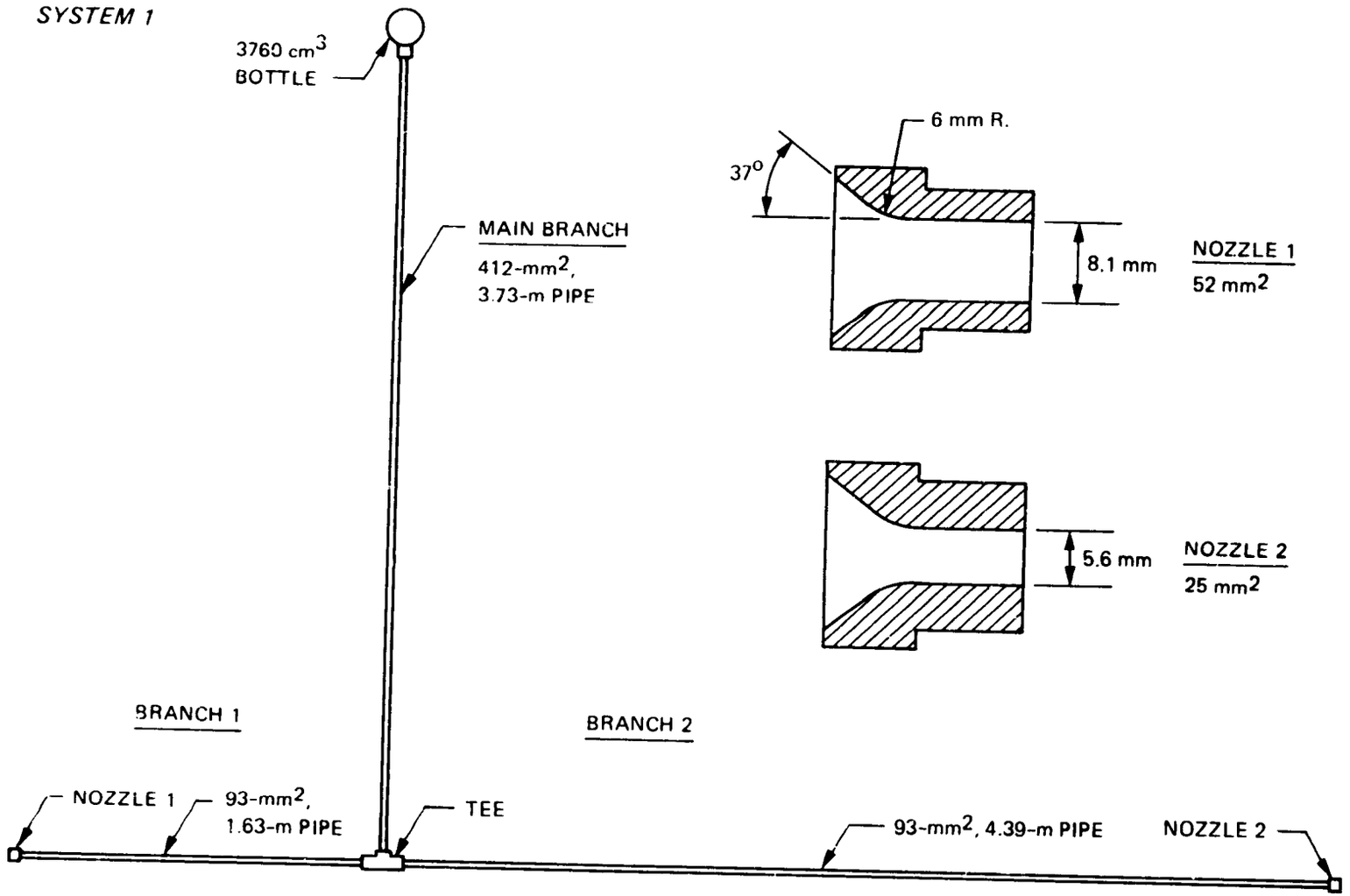

Figure 23. Two-branch distribution system 1

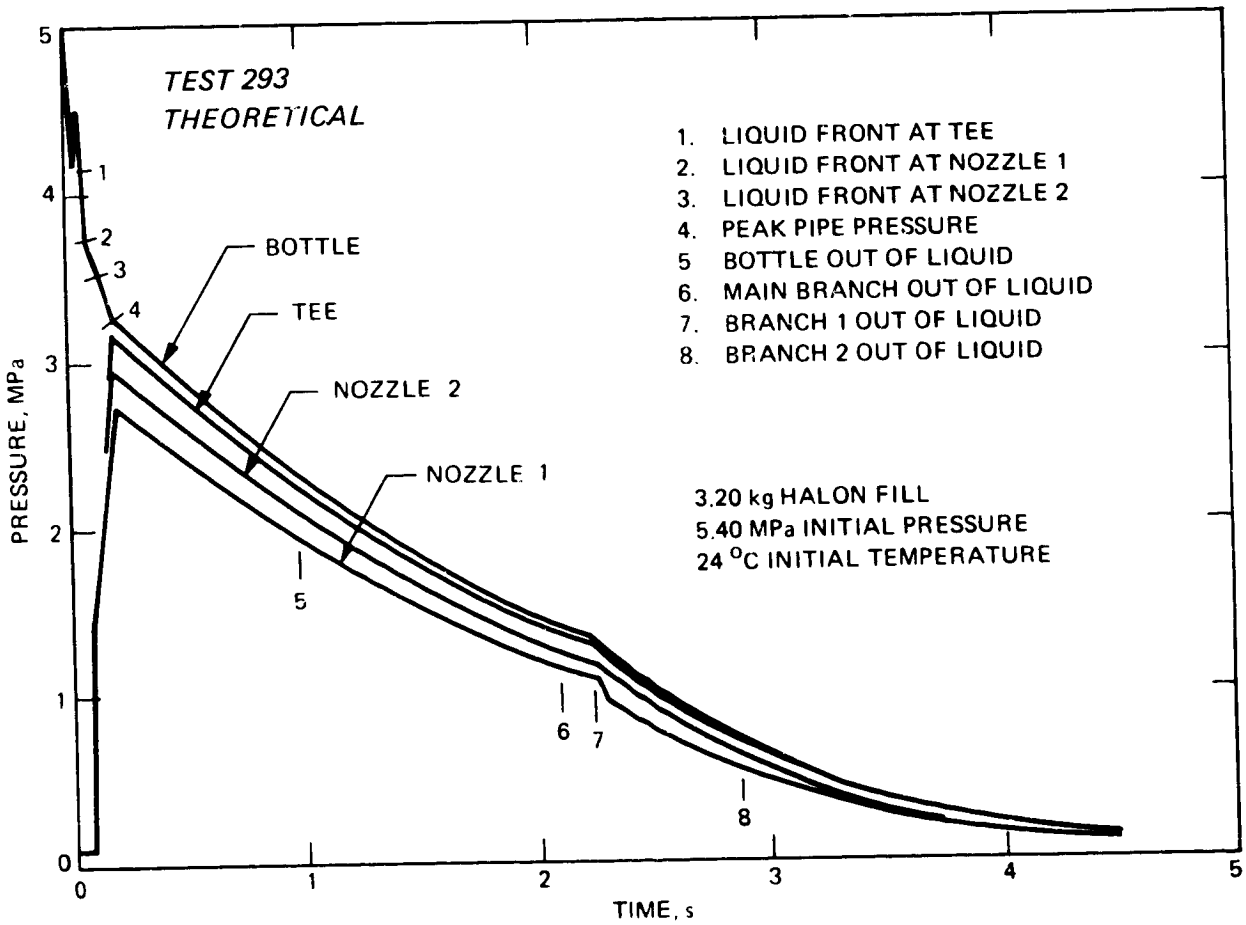

Figure 24. Theoretical pressure-time curves for distribution system 1

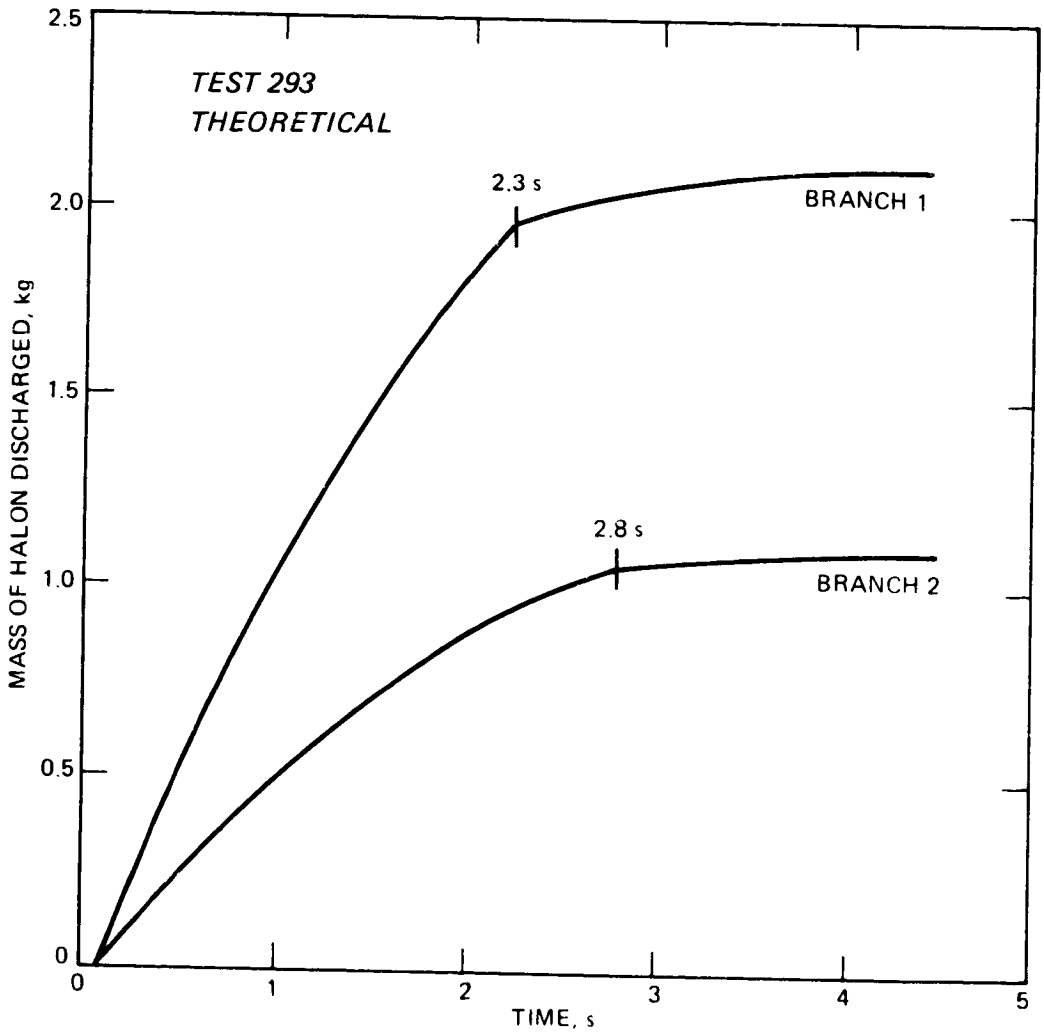

Figure 25. Theoretical discharge flows for distribution system 1

pressure, the longer branch does not run out of liquid until 2.8 s.

The amount of Halon theoretically discharged from each nozzle (Fig. 25) is proportional to the nozzle area. At the time of liquid runout in the short branch, 89 percent of the Halon has been discharged. At the time of liquid runout in the long branch, 96 percent of the Halon has been discharged.

Figures 26(a)-(d) compare the theoretical pressure-time curves with the measured pressure-time curves. The general agreement is good. Specific differences are that the theoretical bottle pressure does not show the observed undershoot when the system fills, and the theoretical pressures fall slightly below the data for most of the run, especially during vapor venting.

The second multibranch system tested is sketched in Fig. 27. This system was designed to be an extreme example of a large length and high volume. The distance from bottle to nozzles is 9.8 m, and the piping volume is 6 percent greater than the bottle volume. The multibranch option of the computer program would not run with such a large volume without further programming effort. Instead, the system was analyzed as an equivalent single-branch system using the rules for equivalent pipe and nozzle sizes presented in the next Section.

Figure 28 compares the theoretical and experimental pressure-time curves for this multibranch system 2. Because of the large pipe volume the bottle runs out of liquid before the pipes are fully pressurized. Nozzle flow does not start until all of the Halon has been transferred to the pipes and the bottle pressure has dropped to 2.1 MPa. The agreement between the theoretical and experimental pressures is reasonably good, with the theoretical pressures again

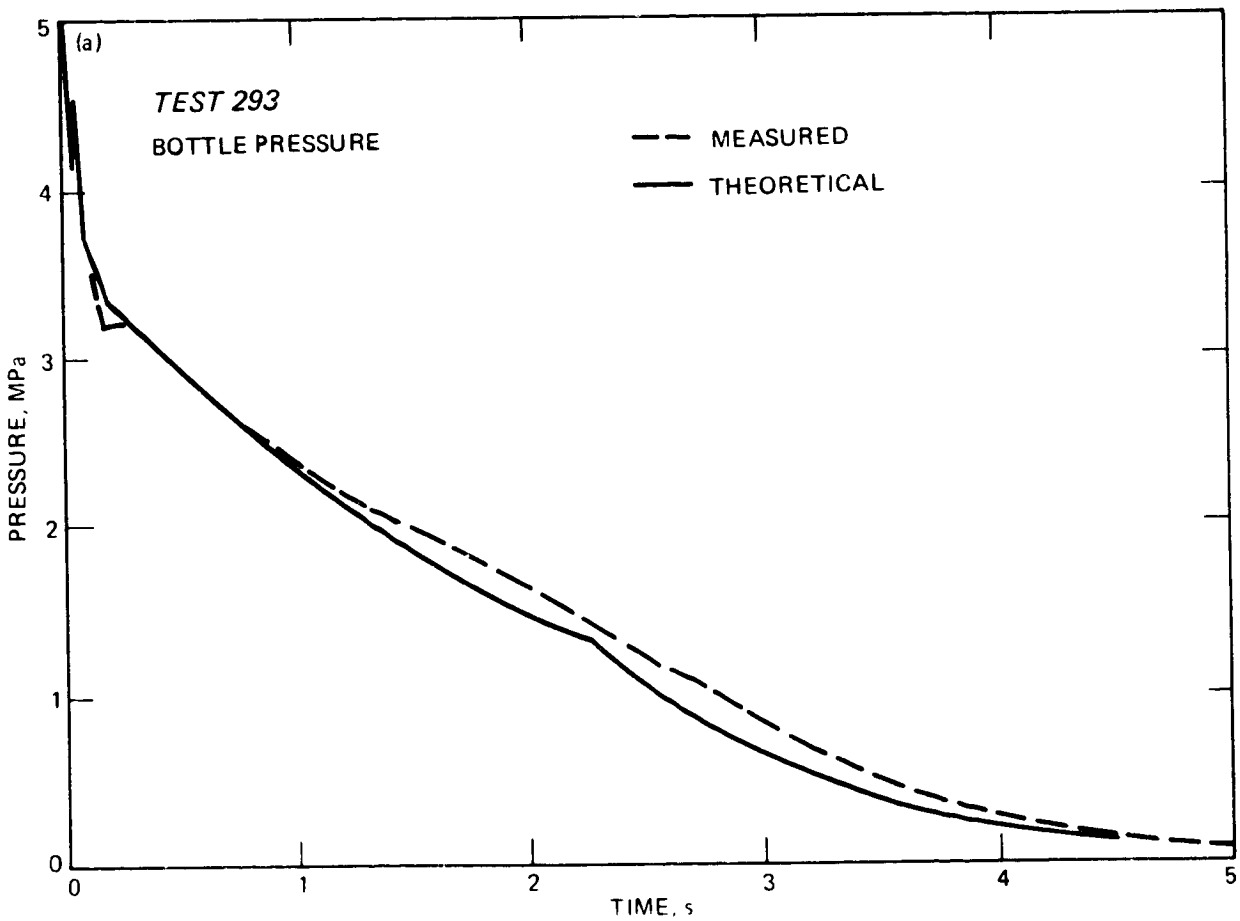

Figure 26. Comparison, for distribution system 1, between: (a) Theoretical and experimental bottle pressure-time curves

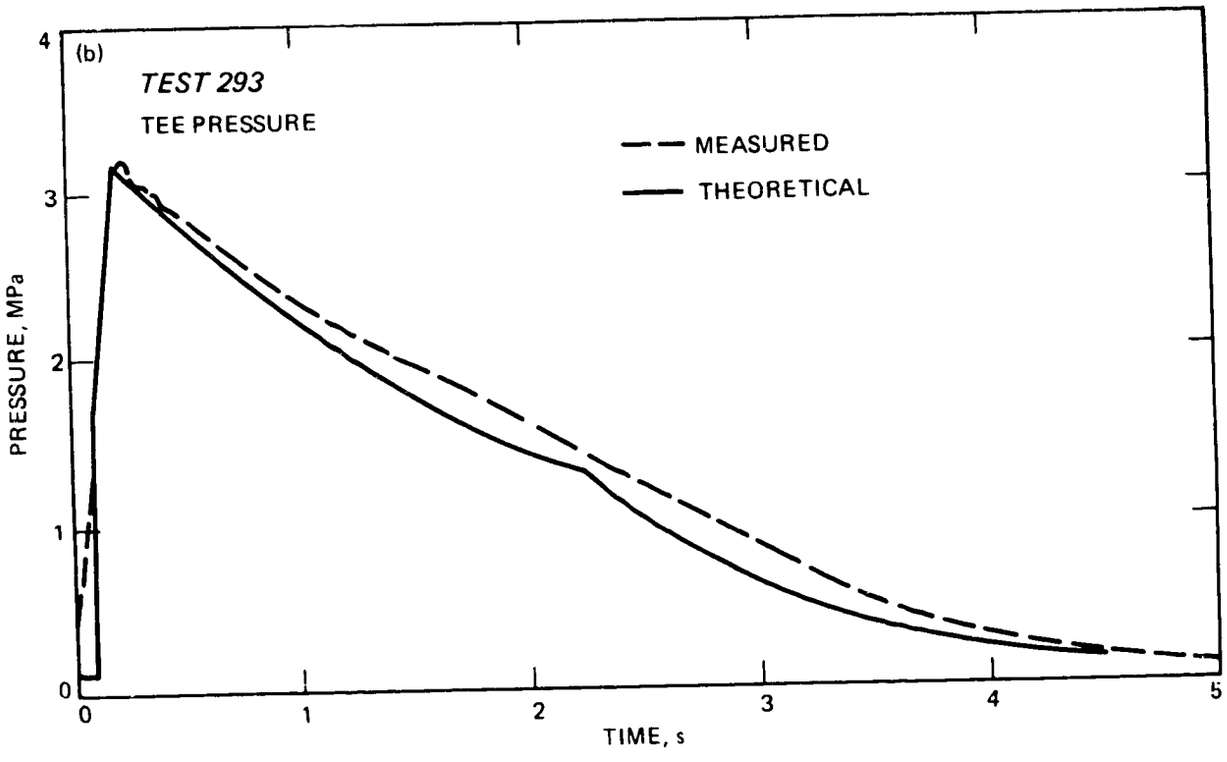

Figure 26. Comparison, for distribution system 1, between: (b) Theoretical and experimental tee pressure-time curves

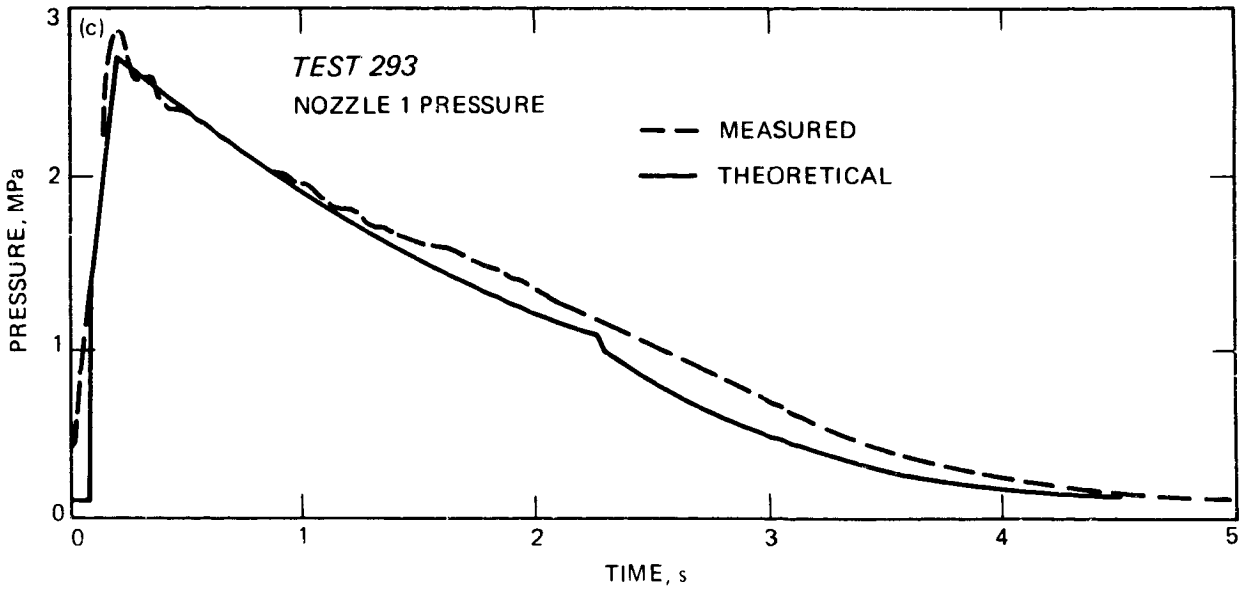

Figure 26. Comparison, for distribution system 1, between: (c) Theoretical and experimental nozzle 1 pressure-time curves

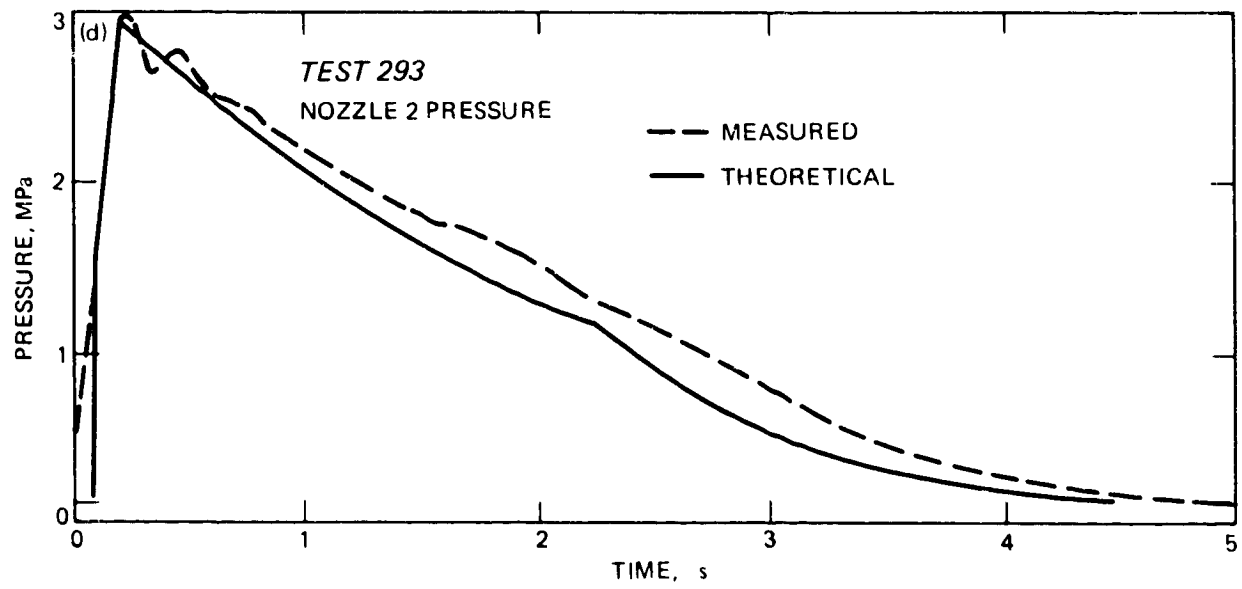

Figure 26. Comparison, for distribution system 1, between: (d) Theoretical and experimental nozzle 2 pressure-time curves

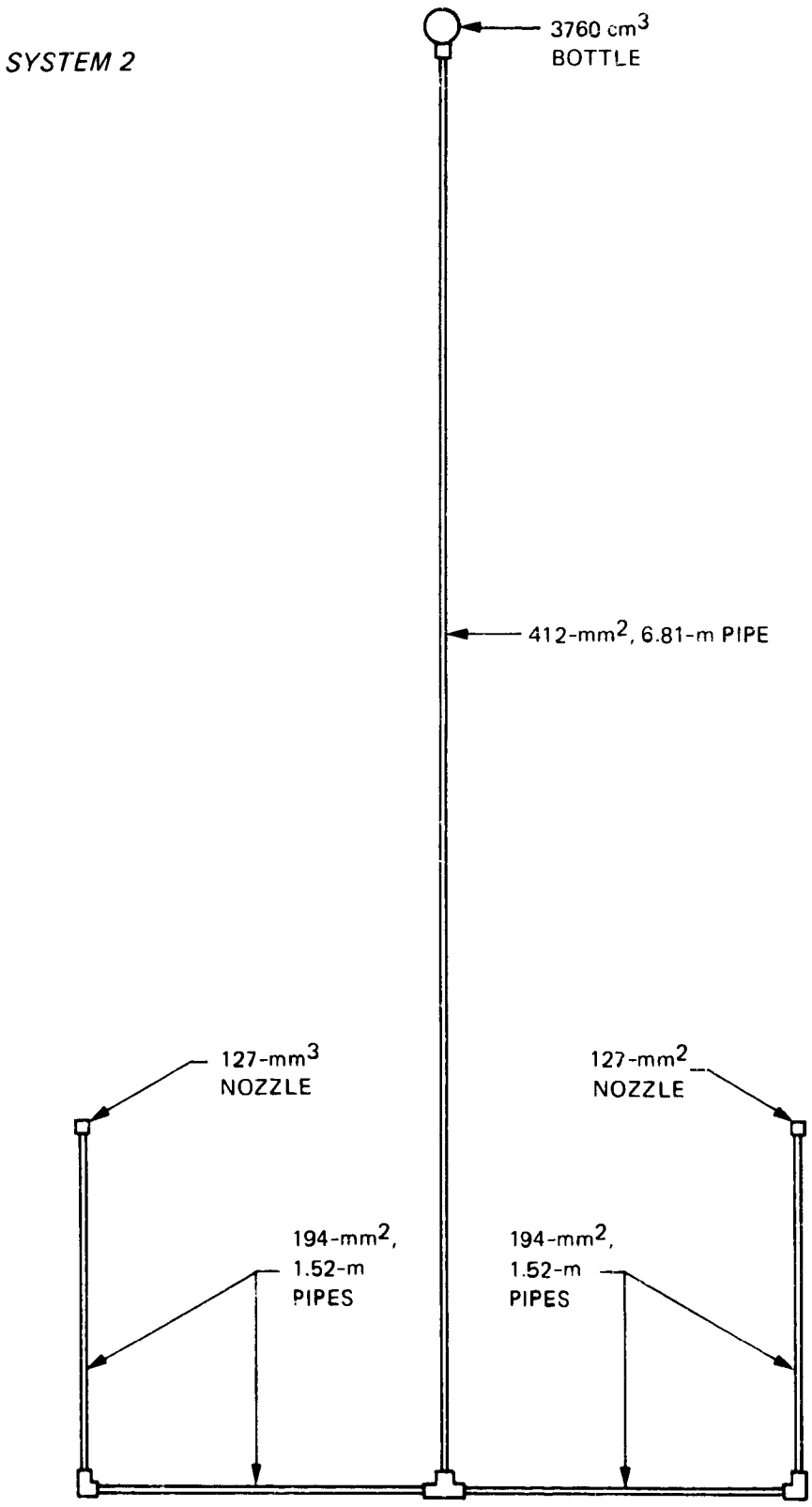

Figure 27. Two-branch distribution system 2

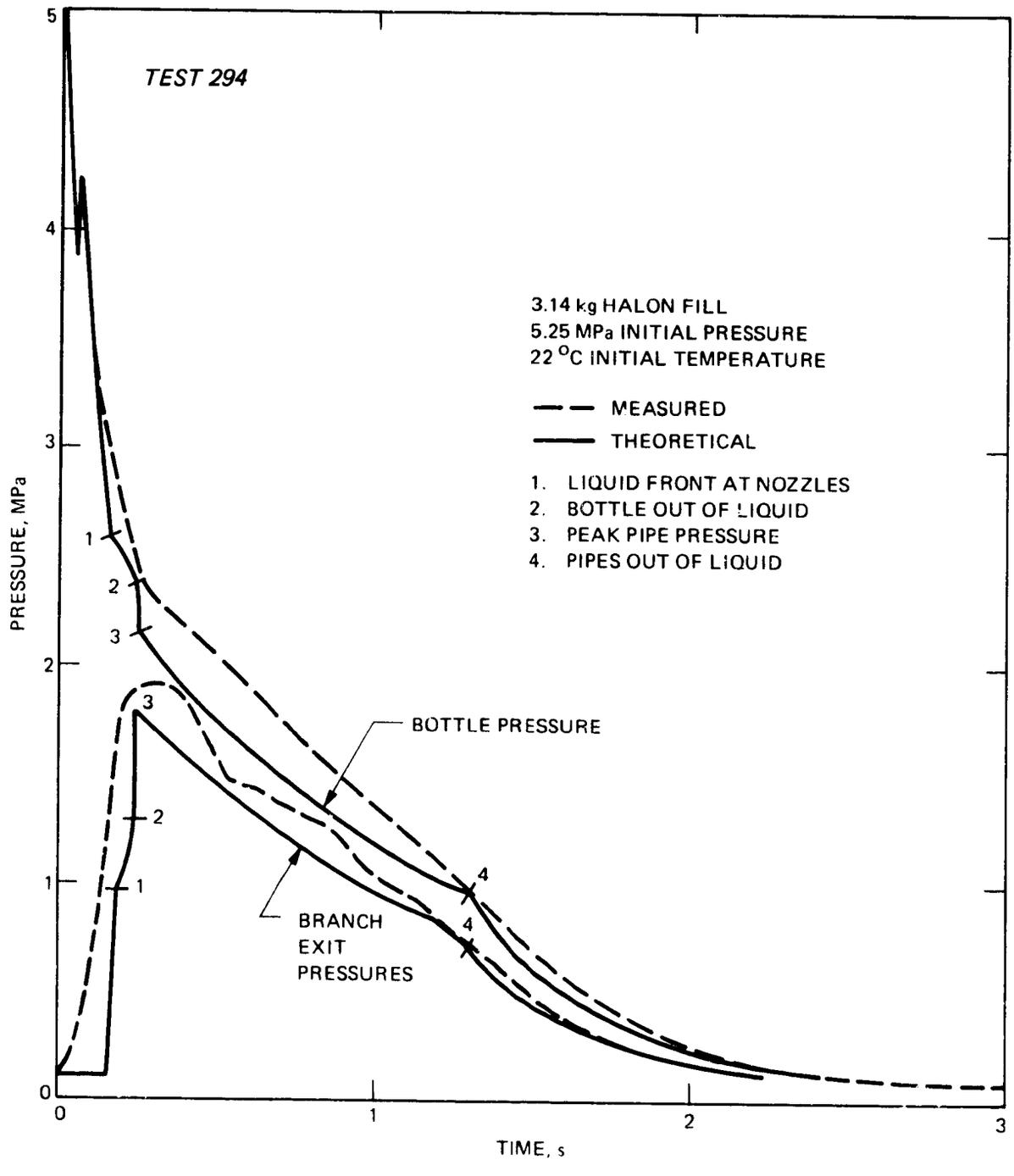

Figure 28. Comparison, for distribution system 2, between theoretical and experimental pressure-time curves

being somewhat lower than experimental.

K. Summary

The results presented in this Section have shown that the theoretical model predicts the pressure-time behavior of Halon discharge reasonably well. Other behavior predicted by the model, such as mass discharged versus time, is, therefore, probably also correct. Based on the model, a clearer picture of Halon discharge behavior emerges. After valve opening, the Halon travels rapidly to the discharge nozzles, and rapidly pressurizes the piping system. These steps are completed before any significant amount of Halon has been discharged and in a time that is short compared with the total discharge time. During discharge, the flow rates through the individual nozzles are divided in proportion to nozzle throat areas. The discharge time with a pipe between the bottle and nozzles is increased, compared with the discharge time for a nozzle only, by both pipe friction and by the loss of pressure due to filling the pipes.

III. FLOW CALCULATION METHODS

Two methods of calculating Halon and nitrogen flow were developed during this project. One method was a modification of a steam-and-water blowdown program developed at the Los Alamos National Laboratory (LANL), which was run on the LANL computer. Results of that approach are discussed in Appendix C. The other method was a program called HFLOW, written specifically for Halon and nitrogen discharge, and run on the JPL computer. The two methods agreed, but the HFLOW program was more convenient to use and was the model used for the theoretical calculations that have been presented in this report.

The multibranch version of HFLOW is limited in the piping geometries it will handle. However, multibranch systems can be reduced to single-branch systems by rules that will be presented, and the program runs well for single branches. For estimation of discharge time it is possible to use the computer program to prepare graphs of discharge time as a function of pipe length for various pipe and nozzle diameters. Such a graph can be prepared for each bottle condition of interest, and an example will be presented. Further simplification is possible if the flow system uses optimum pipe sizes. A time-estimation graph and formula will be presented for that case.

A. Program HFLOW

To run HFLOW for a single-branch system the following inputs are required: bottle volume, Halon mass, initial pressure, initial temperature, valve flow area, pipe length, pipe area, and nozzle area. The program prints various quantities at each of 100 pressure steps, including time, flow rate, mass discharged, mass stored in the pipe, and temperatures and pressures in the bottle and at the pipe exit.

Determining the flow areas to be used in the program may be difficult for some types of nozzles and certainly for the bottle valve. The flow area can be known accurately only for orifices having a well-rounded entrance, with a radius equal to at least half the orifice diameter, in which case the flow area can be assumed to be equal to the physical area.

If the orifice has a sharp entrance or only a small radius, the effective flow area can be as little as 60 percent of the physical area. In such cases the flow area (or the discharge coefficient, which is the ratio between the effective flow area and physical area) can be determined from flow tests with the type of fluid to be used. Discharge coefficients for some orifice shapes can be found in hydraulics handbooks.

Flow areas determined from water or gas flow tests or from handbook coefficients can be in error by 10 to 20 percent for two-phase flow, and the calculations using HFLOW will reflect that error. However, for flow components upstream of the final discharge nozzle, such as the valve, the effect of flow-area errors is usually small. If the discharge nozzle has a flow area less than 70 percent of the upstream restrictions, 90 percent or more of the pressure drop from the bottle to atmosphere will take place across the discharge nozzle, making it only necessary to provide the program with an accurate flow area for the discharge nozzle.

If the final discharge is through a complex restriction, such as the valve itself, then either a water calibration can be used, with uncertain accuracy for two-phase flow, or a Halon discharge test can be used as a calibration. As

shown earlier (Fig. 9), the best-fitting valve flow area for a Halon discharge test was 500 mm^2 whereas the valve flow area from a water calibration was 400 mm^2.

The equations used in program HFLOW are derived in Appendix A. The overall organization of the program is summarized in Fig. 29. The program has two sections. The first section calculates bottle conditions as a function of bottle pressure. The second section calculates flow rates and times.

The bottle section has a main program that calls subroutines for fluid properties, nitrogen release, and equation solving. The program proceeds stepwise through 100 pressure increments from the initial bottle pressure to atmospheric pressure. At each pressure step the temperature of the fluid in the bottle is guessed. The subroutines calculate the properties of the Halon and nitrogen mixture at that temperature and pressure. The main program calculates the amount of fluid that must be discharged in each step to reach the new pressure. The energy equation is then checked: change of internal energy of the bottle fluid equals enthalpy of the flow discharged. If the two quantities are not equal the subroutine SFABZ (subroutine to find a bounded zero) is called to furnish a new temperature guess. Iterations continue until the correct temperature is found.

When the pressure reaches the nitrogen release pressure, based on 15 nm nucleation bubble diameter, the nitrogen release subroutine calculates the conditions after transition to equilibrium nitrogen concentration at constant internal energy. The pressure steps then continue.

The result of the bottle section of the program is a table of the fluid

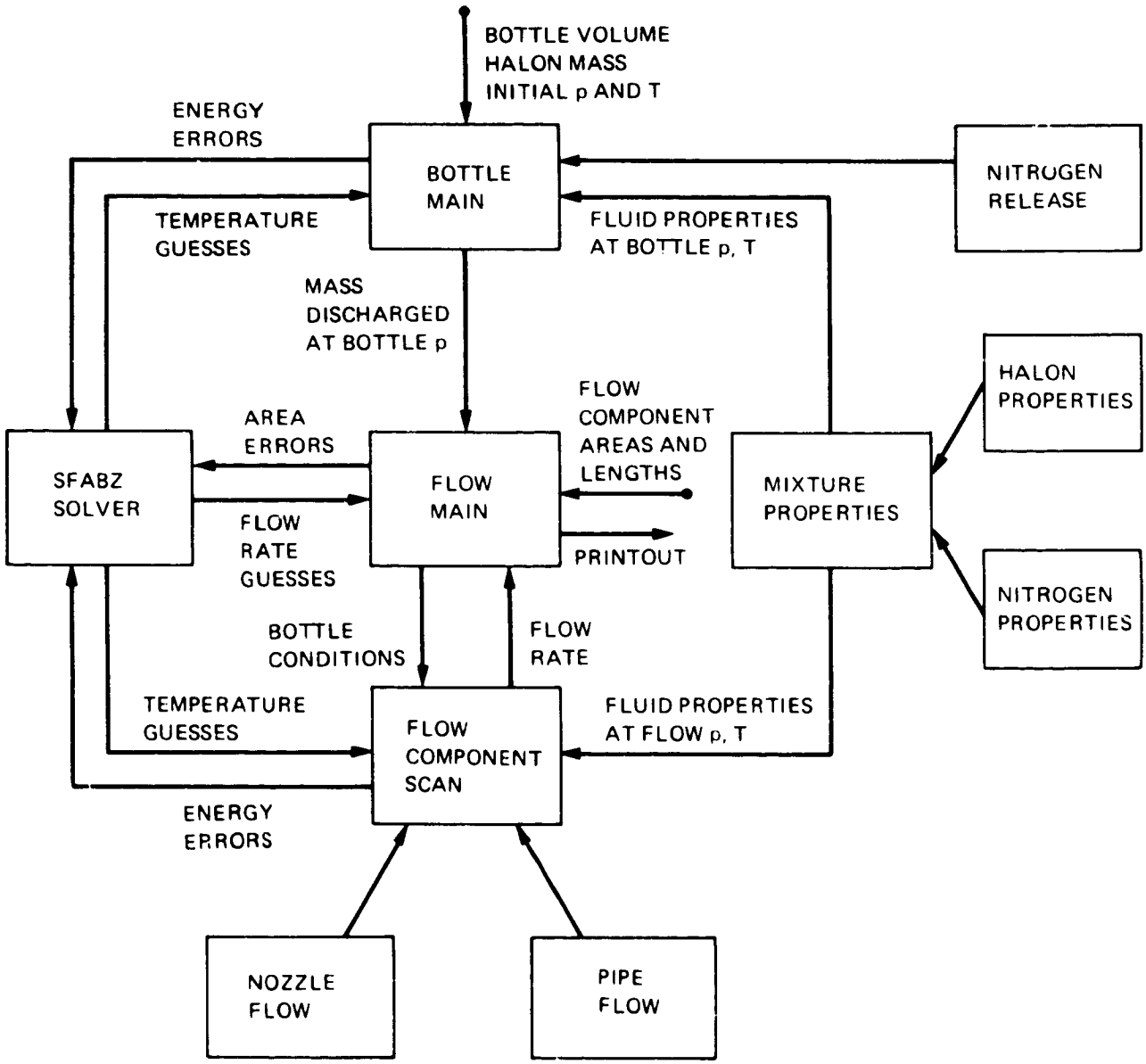

Figure 29. Organization of computer program HFLOW

mass increments discharged in each pressure step, and values of the pressure, temperature and quality of each mass increment discharged. These results are used by the flow section of the program.

The flow section of the program has a main program th . calls subroutines for fluid properties, component pressure drops, and equation solving. At each pressure step the main program guesses a flow rate. A downward pressure scan is made through each flow component (valve, pipe, and orifice) that is carrying flow at that time. At each pressure step the temperature of the fluid at that point is guessed, the property routines are called, the energy equation is checked, and SFABZ is called to furnish a new temperature guess to satisfy the energy equation. When the point in the flow that is at sonic conditions is reached the required flow area is calculated and compared with the actual flow area of the flow component that is limiting the flow at that time (the pipe area, if the liquid front has not reached the end of the pipe, and the nozzle area after that). If the required and actual areas are different, subroutine SFABZ supplies a new flow rate guess.

Once the correct flow rate is found, and added to the rate of fluid mass change in the pipe, the time required to discharge the required flow increment from the bottle is calculated and added to the elapsed time. If the liquid front has not reached the end of t.e pipe, the front is then advanced by its travel distance in that time increment.

The result of the flow section of the program is a printout of elapsed time at each step of bottle pressure, together with values of temperatures and pressures, fluid front positions and other quantities in the bottle and pipes.

B. Reducing Multibranch to Single Branch Systems

Most distribution systems have relatively small pressure drops from bottle to nozzles once nozzle flow begins. Therefore, the pressure in the bottle and pipes at the start of nozzle flow depends mainly on the total pipe volume and not on how the volume is distributed throughout the system. In addition, the flow rate out of the bottle is the sum of the nozzle flow rates, plus the rate of storage change in the pipe volume, and the bottle discharge flow rate does not depend greatly on nozzle location.

Since the locations of the pipe volumes and nozzle areas are of secondary importance, it should be possible to calculate the bottle and nozzle discharge flow rates for a multibranch system by treating the multibranch system as a single branch system with (1) the single branch having the same volume as the multiple pipes and (2) the single nozzle having the same total area as the multiple nozzles.

The nozzle areas to be used are effective areas reduced from the actual nozzle areas by factors that account for pressure drop in the pipes. Reduction factors for Halon flow at typical mean bottle conditions during discharge (3.0 MPa, 10°C and 4 percent quality) are plotted in Fig. 30 as a function of length/diameter ratio for pipes having areas of 1.5, 2, 3, and 4 times the nozzle area.

An example of reducing a multibranch system to a single branch system will be presented for the system of Fig. 23. For Branch 1 the pipe/nozzle area ratio is 1.8 and the pipe L/D is 150. From Fig. 30 the area reduction factor is 0.90, giving an effective nozzle area of 47 mm^2. For Branch 2 the area ratio is 3.7, the L/D is 400, the reduction factor is 0.96, and the effective area is 24 mm^2. The total effective area of the branches is thus 71 mm^2.

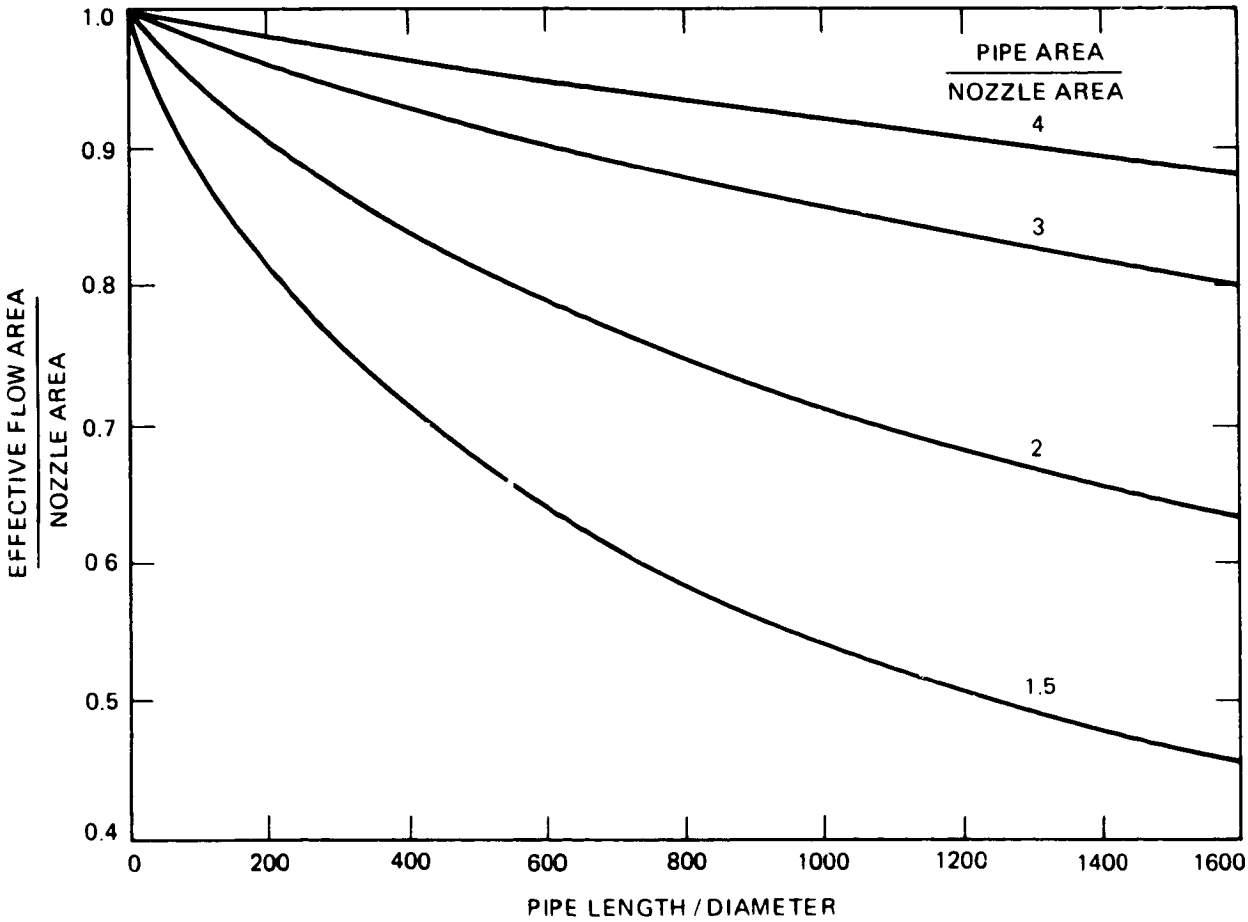

Figure 30. Effective flow area of pipe and nozzle combinations

For the main branch the ratio of pipe area to effective nozzle area is 412/71 = 5.8 and the L/D is 160. From Fig. 30 the reduction factor is close to 1.0. The total volume of the pipes is 2100 cm^3. A single pipe of 412 mm^2 length and 5.1 m length has the same volume.

Thus, a single branch system equivalent to the two-branch system of Fig. 23 consists of a 412-mm^2, 5.1-m long pipe and a 71 mm^2 nozzle. When these values are used as inputs to program HFLOW the result is a single curve of mass discharged versus time. The mass discharged from each nozzle in the multibranch system is obtained by multiplying the total mass discharged by the fraction of total nozzle area for each nozzle, namely 47/71 for Branch 1 and 24/71 for Branch 2. The mass discharge curves obtained in this way are compared in Fig. 31 with the curves from the multibranch run of the computer program. The masses discharged are about the same for the two program runs, and the discharge time for the single-branch approximation is about the same as for the earliest-emptying branch of the two-branch system. Thus, the single-branch approximation appears to be a valid approach to simplifying the computations.

C. Discharge Time Graphs

To provide a convenient way of estimating discharge times, the computer program can be run for a range of pipe sizes and orifice sizes and the results plotted in a graph for each bottle size and set of initial conditions. Figure 32 presents such a graph for a 3750 cm^3 bottle with 3.2 kg of Halon at 5.2 MPa initial pressure and 20°C initial temperature. Discharge time is plotted as a function of pipe length for four nozzle areas and several values of pipe/nozzle area ratio. As would be expected, the discharge times decrease as nozzle area increases, and the discharge times increase with pipe length.

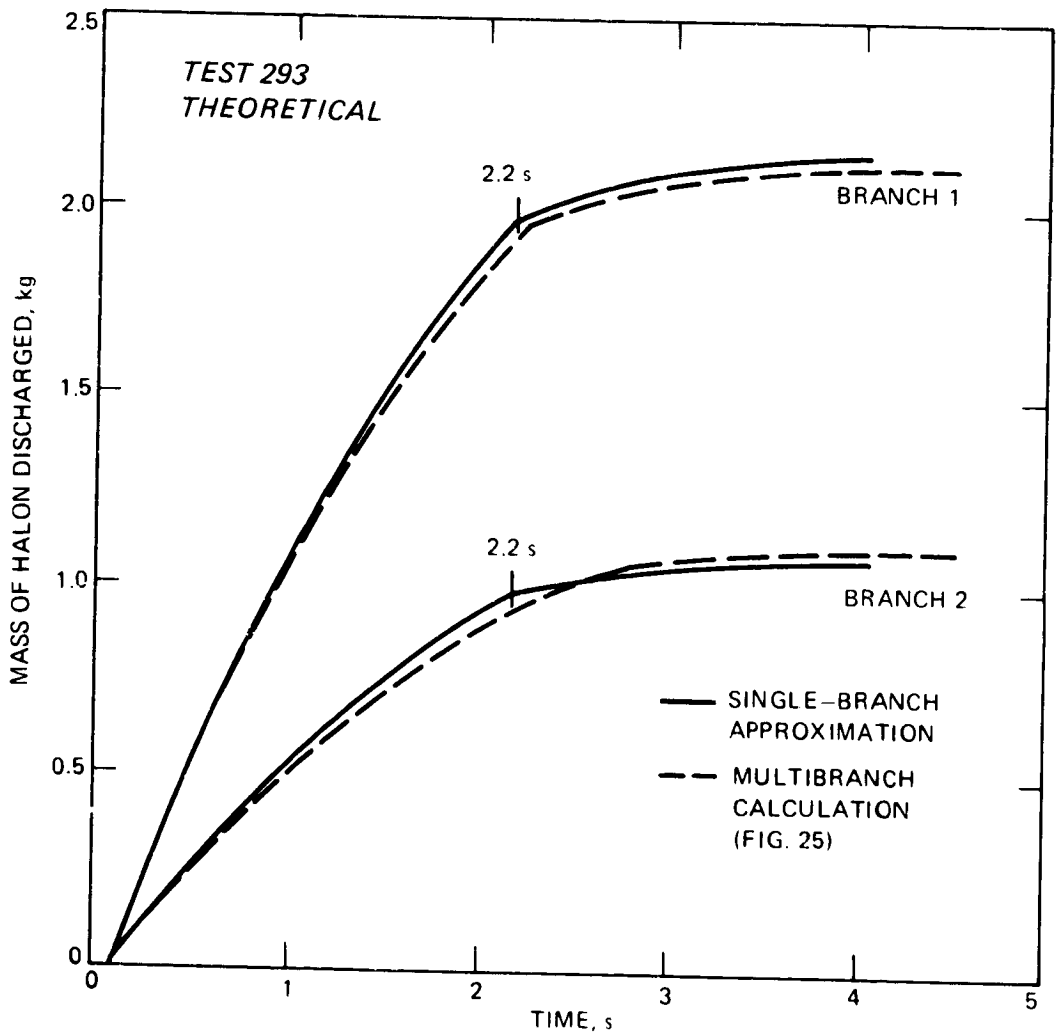

Figure 31. Comparison, for distribution system 1 and equivalent single-branch system, between theoretical discharge flows

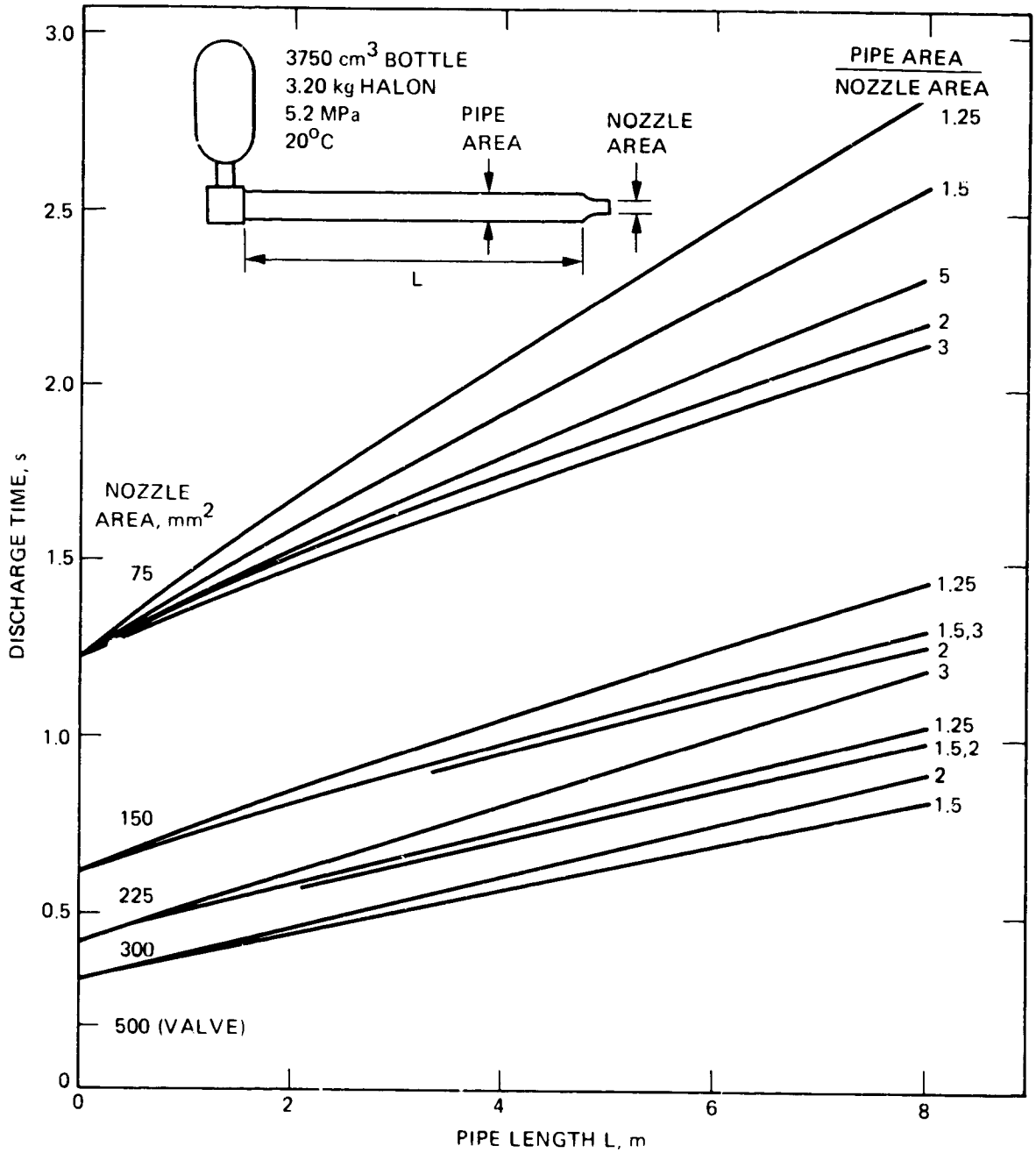

Figure 32. Liquid discharge time for single-branch flow systems

The discharge time for the two-branch system of Fig. 23 is estimated by using the effective nozzle area of 71 mm^2, the pipe area of 412 mm^2, and the effective pipe length of 5.1 m. Fig. 32 shows that for a 75 mm^2 nozzle area and a pipe/nozzle area ratio of 5.8 the discharge time at 5.1 m length is about 2.0 s. For small changes in nozzle area the discharge time is proportional to area; thus, the discharge time for a nozzle area of 71 mm^2 is 75/71 x 2.0 = 2.1, which is close to the value given by the computer program in Fig. 31.

For the flow system of Fig. 27, the effective nozzle area for each branch, from Fig. 30, is 105 mm^2. The total pipe volume is 3990 cm^3, the pipe/nozzle area ratio is 2, and the effective single-pipe length is 9.7 m. From Fig. 32, interpolating for 210 mm^2 area and extrapolating to 9.7 m length, the discharge time is about 1.2 s, in agreement with Fig. 28.

Thus, a graph of the type shown in Fig. 32 provides useful estimates of discharge time. The computer program could be used to generate a set of more detailed graphs, with additional values of nozzle area, for each initial bottle condition of interest.

D. Optimum Pipe Diameters

It can be seen from Fig. 32 that there is an optimum pipe area, giving minimum discharge time, for each nozzle area. At larger pipe areas than optimum the discharge time is increased because of the pressure loss in filling the large pipe volume. At smaller pipe areas than optimum the discharge time is increased because of the friction pressure drop in the pipe.

Figure 33 illustrates the effect of varying pipe/nozzle area ratio. Pressure-time curves are plotted for five different pipe areas at a fixed nozzle

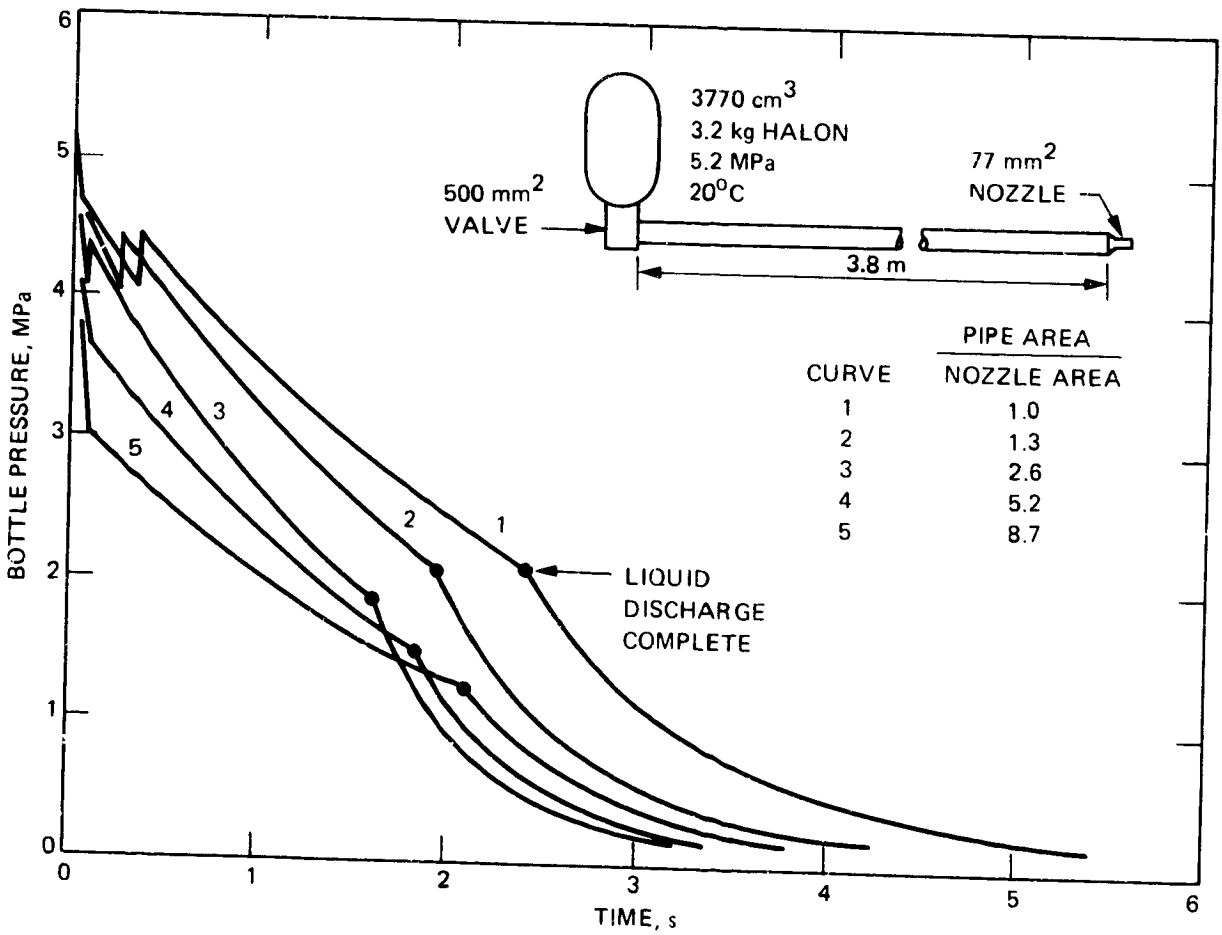

Figure 33. Effect of pipe/nozzle area ratio on discharge time

area of 77 mm^2. In Curve 1 the pipe has the same area as the nozzle and the discharge time is 2.4 s. Increasing the pipe area to 1.3 times the nozzle area gives a higher flow rate and a lower discharge time of 1.9 s. With a pipe area 2.6 times the nozzle area, the discharge time is further reduced to 1.6 s. However, at a pipe area of 5.2 times the nozzle area, the loss in pressure due to filling the pipe begins to dominate and the discharge time increases to 1.8 s. At a pipe area of 8.7 times the nozzle area, the discharge time is further increased to 2.1 s. Thus, the optimum ratio of pipe area to nozzle area is about 2.6 at this pipe length and nozzle area.

Figure 32 shows that the optimum pipe/nozzle area ratio decreases with increasing nozzle area. The optimum area ratio ranges from 3.0 at 75 mm^2 nozzle area to 1.5 at 300 mm^2 nozzle area. However, an area ratio of 2.0 gives nearly minimum discharge time at all nozzle areas.

If a Halon distribution system is built with optimum pipe areas (twice the nozzle area is close enough), then the estimation of discharge time can be further simplified to a single curve for each nozzle area. Furthermore, the discharge times can be normalized by nozzle area to factor out the first-order effect of nozzle area. Figure 34 shows such a graph. The product of nozzle area and discharge time is plotted as a function of pipe length for four different nozzle areas. For the Fig. 33 conditions of 77 mm^2 nozzle area and 3.8 m pipe length, for example, Fig. 34 shows that the product of nozzle area and discharge time is 128 mm^2-s. Therefore, the discharge time is 128/77 = 1.7 s, in agreement with the minimum discharge time from Fig. 33.

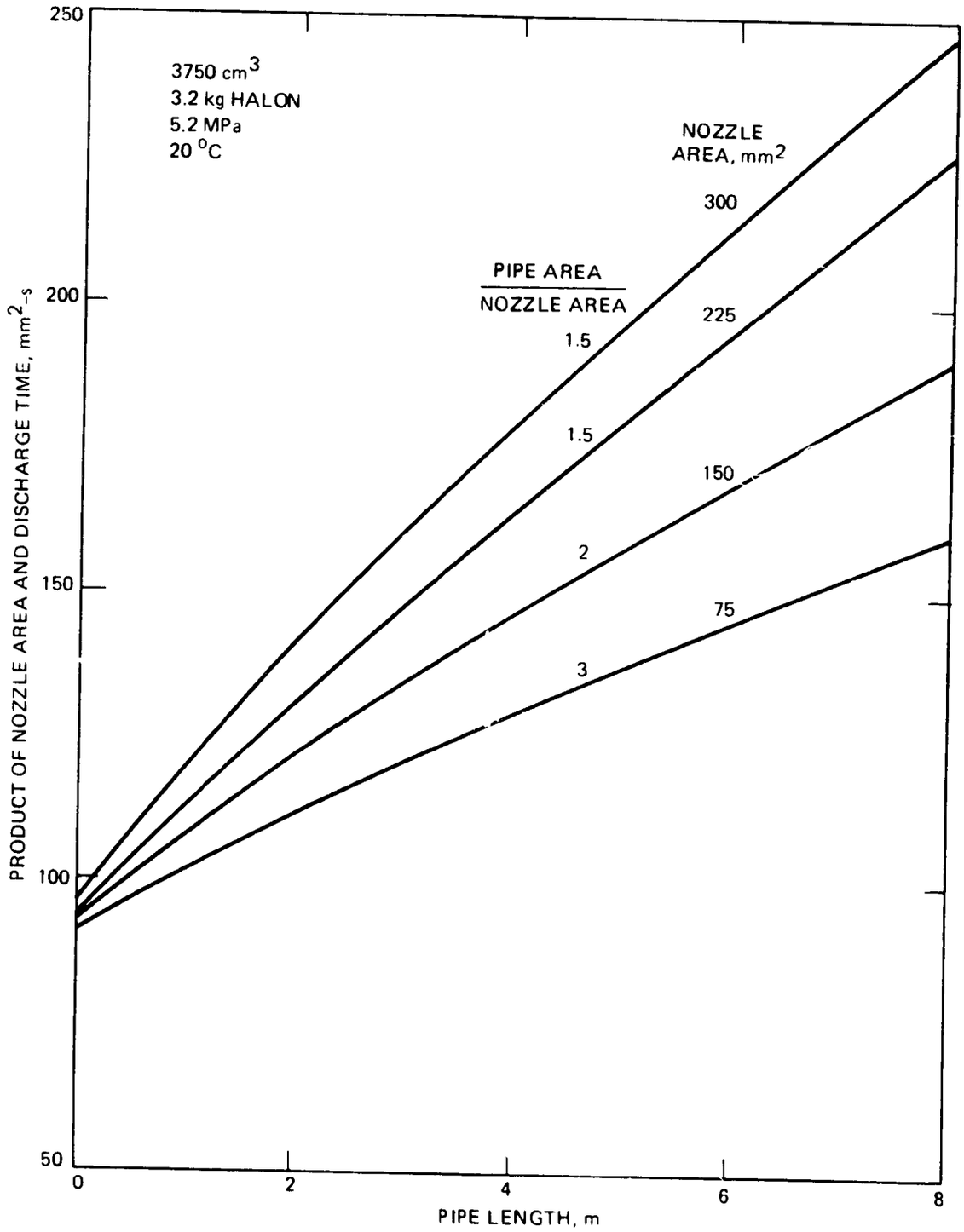

Figure 34. Discharge time with optimum pipe/nozzle area ratios

E. Discharge Time Formula

The curves in Fig. 34 can be approximated by straight lines fitted by the following formula:

$$\text{Discharge Time} = \frac{95 + (4.6 + 0.047\ A)L}{A} \quad \text{seconds}$$

where A is the nozzle area in mm^2 and L is the pipe length in m. For a multibranch system, area A is the sum of the effective areas of the branches (calculated from Fig. 30) and length L is the length of pipe having the total volume of the system. For the system of Fig. 27, for example, which has close to optimum pipe sizes, A = 210 mm^2 and L = 9.7 m. The formula gives a liquid discharge time of 1.1 s, 15 percent less than the value given by the computer program in Fig. 28.

F. Comparison With NFPA Method

The National Fire Protection Association has presented a method of sizing pipes and nozzles for Halon 1301 fire extinguishing systems (Ref. 8), and manufacturers have published handbooks for applying the NFPA method at particular initial pressures (Ref. 9).

The procedures of the NFPA method are, in effect, the same as the ones used here in converting multibranch systems to single-branch systems: the nozzle areas (corrected for pipe pressure drop) are added to give a single nozzle area, and the pipe volumes are added to give a single pipe volume.

Reference 9 presents a sample calculation for a Halon system with two bottles feeding six nozzles. The system is sketched in Fig. 35. The aim of the calculation in Ref. 9 is to size the nozzles and pipes for a "10 second discharge time".

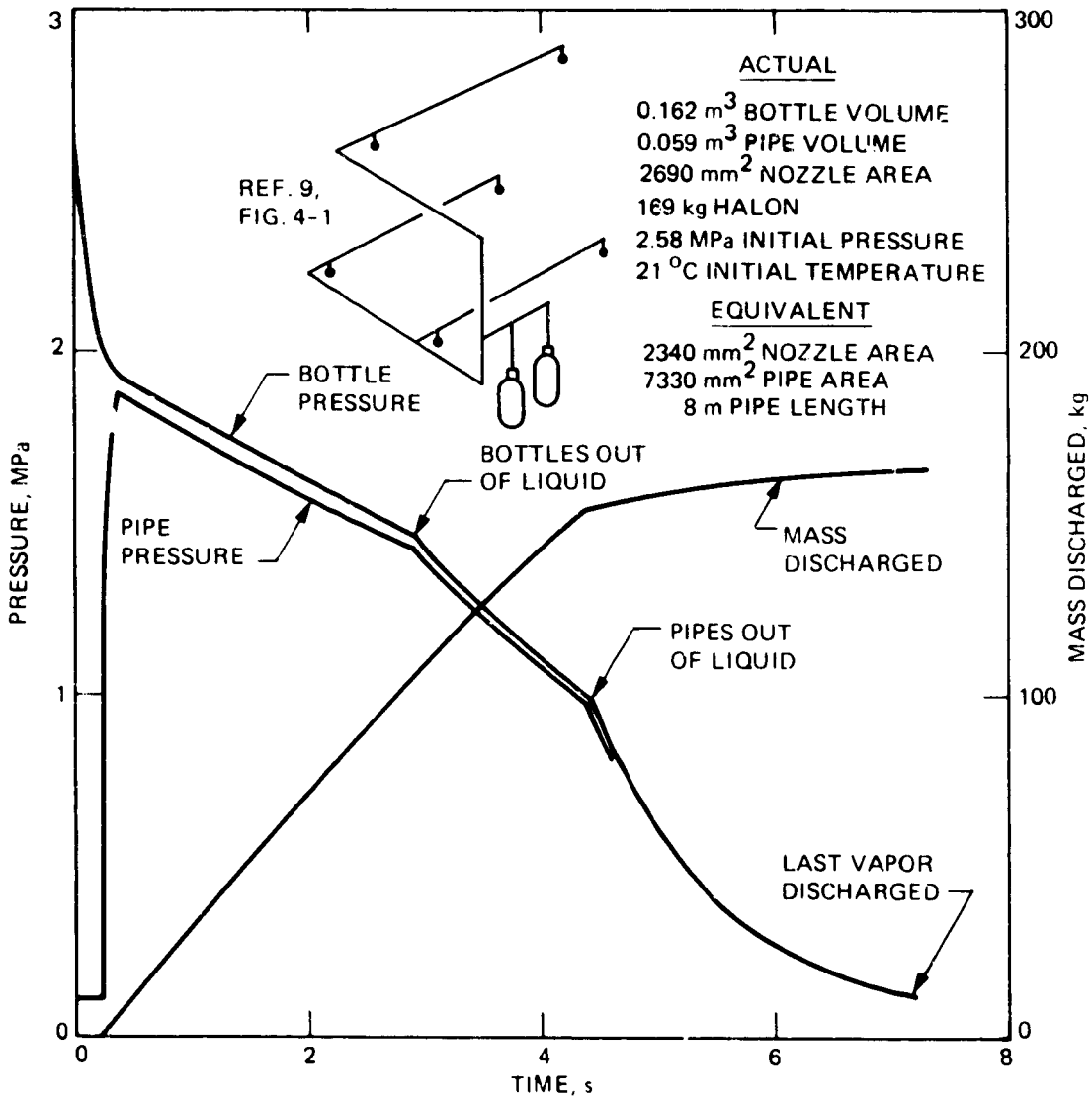

Figure 35. HFLOW predictions for Halon system analyzed by NFPA method in Ref. 9

From Fig. 30 the branches have area reduction factors from 0.82 to 0.92. The total effective area of the six nozzles is 2340 mm^2. The choice of equivalent pipe length and diameter is arbitrary so long as the volume equals the total pipe volume; 8 m length and 7330 mm^2 area are chosen. Figure 35 shows the pressure-time curves predicted by program HFLOW. The time required for discharge of the entire amount of Halon, including vapor, is 7.2 s, which is consistent with the 10 s design value. However, the liquid discharge is complete at 4.3 s, and 90 percent of the Halon has been discharged by that time. Thus, it may be possible to use smaller pipes and nozzles than calculated by the NFPA method for a given discharge time.

G. Summary

The computer program HFLOW provides accurate calculations of Halon discharge flow for single-branch systems. Multibranch systems can be handled as equivalent single-branch systems. The results of computer runs can be plotted for convenient estimation of discharge times.

The optimum pipe/nozzle area ratios for minimum discharge times are 1.5 to 3.0, depending on nozzle area, and an area ratio of 2.0 will give near-minimum discharge times in all cases. For such ratios, the time, in seconds, required for discharge of the liquid (about 90 percent of the total Halon) from a system with a 3750 cm^3 bottle containing 3.2 kg of Halon at 5.2 MPa and 20°C is given by $[95 + (4.6 + 0.047\ A)L]/A$ where A is the nozzle area in mm^2 and L is the pipe length in m.

IV. HALON DISPERSION NOZZLES

A. Liquid Atomization and Acceleration

About half of the mass of Halon leaving a discharge nozzle is liquid. The atomization and acceleration of this liquid affects the way the Halon travels after leaving the nozzle. Fortunately, two-phase nozzle flow is well understood (Ref. 10). The liquid acceleration mechanism is slip between the gas and liquid which, at the same time, atomizes the liquid to small drops.

Applying the theory of Ref. 10 to the Halon nozzle discussed previously (Fig. 14), it is possible to replace the isentropic velocity plotted in Fig. 14 with the actual gas and liquid velocities and to calculate the drop size. Figure 36 shows the results. The liquid atomizes to droplets of 15 μm diameter by the time the flow reaches the throat. With such small drops the liquid is accelerated efficiently, and the liquid velocity stays at about 90 percent of the gas velocity.

B. Orifice Nozzles

Halon nozzles used in the past have had converging or straight passages only, with no diverging section. In such "orifice nozzles" the exit velocity is only about 30 percent of the velocity attainable at atmospheric pressure, as can be seen from Fig. 36. The Halon continues to accelerate outside the nozzle, but with uncontrolled spreading and with less effective liquid acceleration than would be provided by a diverging section.

To disperse the Halon into the compartment to be flooded, orifice nozzles use slots or holes aimed in the desired direction. The nozzles may also have

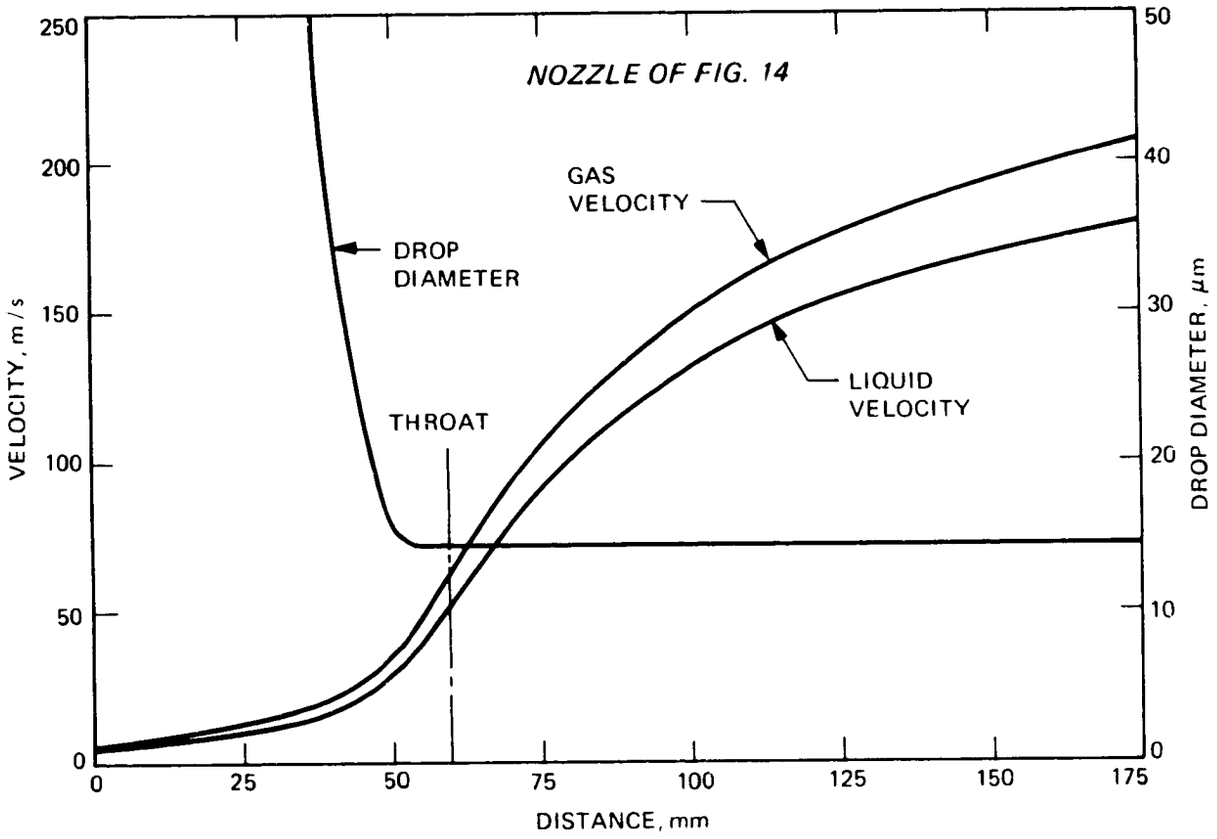

Figure 36. Theoretical drop breakup and slip in a Halon nozzle

deflectors downstream to re-direct the flow leaving the nozzle. Three such nozzles were tested, and they are shown in Fig. 37. The "beehive" nozzle had slots cut in one side of a cylinder and a hole in the end. The "splitter" nozzle had two bars in front of a straight orifice to divide and spread the flow. The "showerhead" nozzle had 31 holes drilled at angles of 15, 45, and 60 degrees from center in an effort to provide hemispherical coverage. The total orifice area was 1370 mm^2 for the beehive nozzle, 790 mm^2 for the splitter nozzle and 157 mm^2 for the showerhead nozzle.

The three nozzles were tested with water and nitrogen mixtures for visual and photographic observation and with Halon using high-speed movies. Figure 38(a) shows the beehive nozzle operating with water and nitrogen. The flow leaves as a flat sheet from the slots on the side and as a jet from the end. Figure 38(b) is a movie frame of the beehive nozzle in a Halon test, at a time 8 ms after the start of flow. The view is toward the hole in the end of the nozzle, showing the main Halon sheet flat on, traveling to the right. The beehive nozzle is effective only in producing a planar flow directed to one side of the nozzle.

Figure 39(a) shows the splitter nozzle operating with water and nitrogen. The deflector bars produce four jet lobes spreading at about 20 degrees from center. Figure 39(b) shows the splitter nozzle with Halon at 2 ms from the start of flow. Four diverging Halon lobes can be seen. The splitter nozzle is effective in producing a slightly divergent discharge flow.

The showerhead nozzle is shown operating with water and nitrogen flow in Fig. 40(a). The flow initially spreads at 60 degrees but pulls inward to a cylindrical spray downstream. With Halon flow, Fig. 40(b), the showerhead nozzle has an even more pronounced pulling-in effect, yielding a jet that has no more spreading than the flow from the bottle valve alone, as previously shown in

Figure 57. Orifice-type distribution nozzles tested: (a) beehive nozzle, (b) Splitter nozzle, and (c) Showerhead nozzle

Figure 38. Flow test of the beehive nozzle: (a) With water and nitrogen

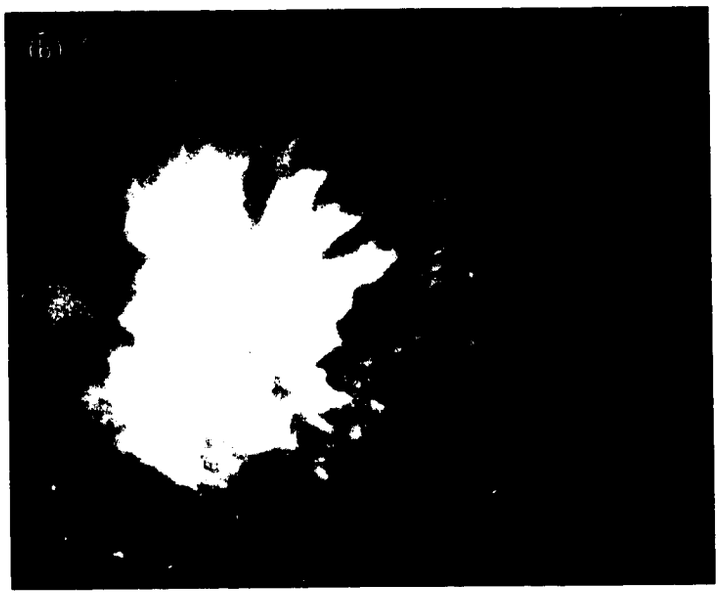

Figure 38. Flow test of the beehive nozzle: (b) With Halon

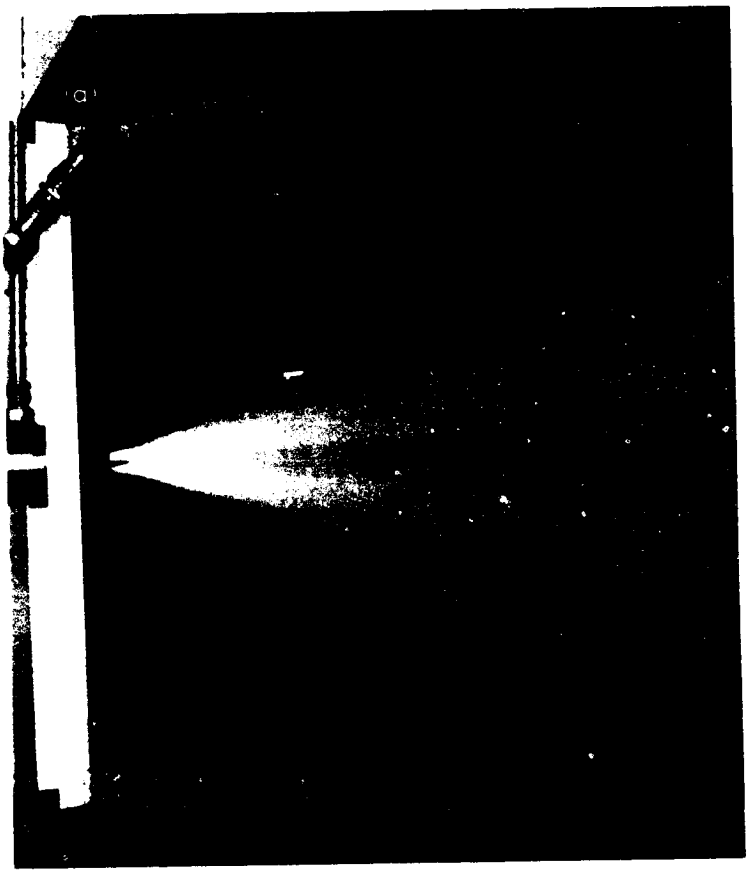

Figure 39. Flow test of the splitter nozzle: (a) With water and nitrogen

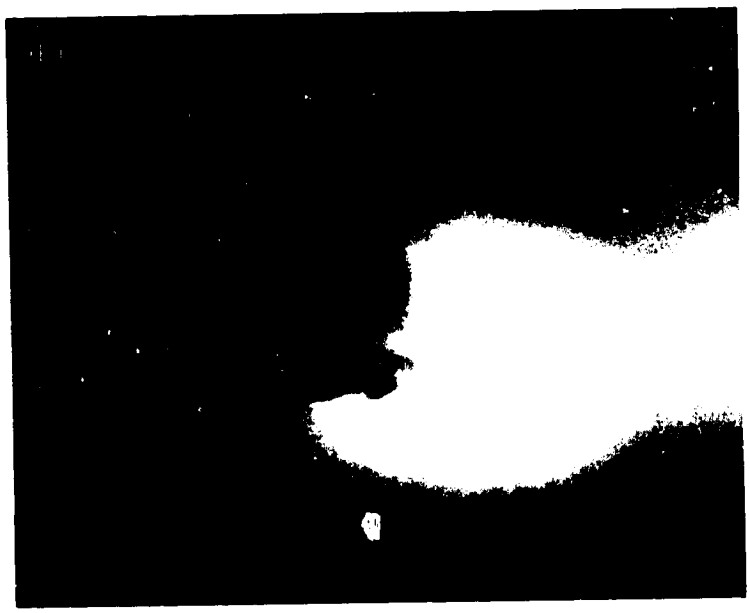

Figure 39. Flow test of the splitter nozzle: (b) With Halon

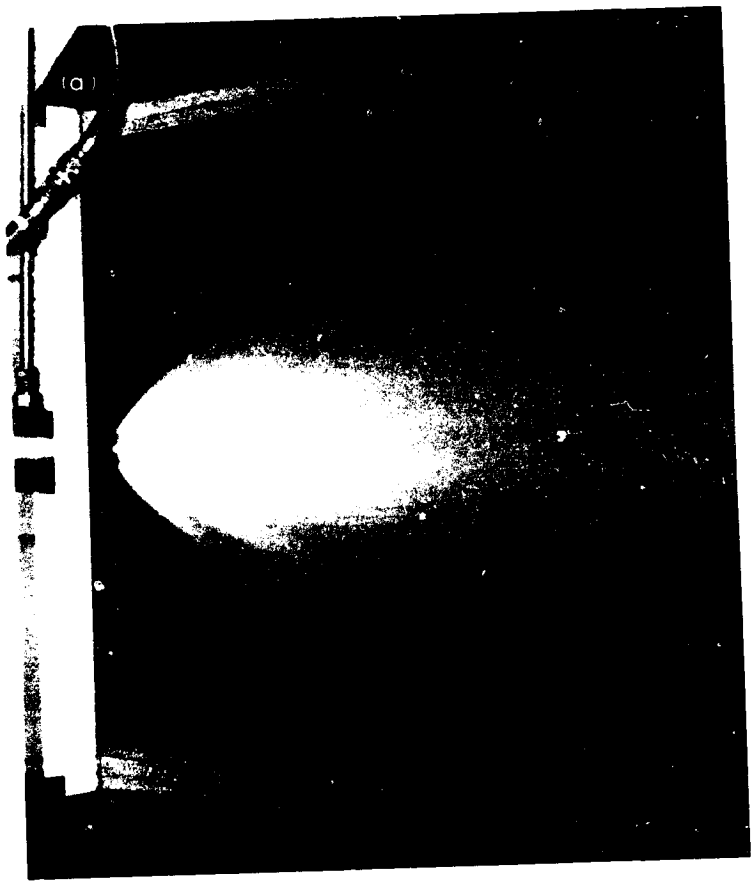

Figure 40. Flow test of the showerhead nozzle: (a) With water and nitrogen

Figure 40. Flow test of the showerhead nozzle: (b) With Halon

Fig. 1.

The reason that the showerhead nozzle fails to produce a spreading flow is simply that continuity prevails. At atmospheric pressure the Halon has a certain velocity and density that defines a fixed flow area. The Halon cannot expand to a larger area without going to lower than atmospheric pressure. When the momentum of the Halon attempts to carry the Halon to a larger flow area, the pressure in the Halon jet starts to drop below atmospheric, and the surrounding air pushes the flow inward.

C. Multicone Nozzle

Wide angle dispersion can be achieved only with discrete jets or sheets that penetrate the atmosphere but do not coalesce into a single flow stream. There must be air between the jets. The flow from a nozzle with hemispherical distribution will have fixed Halon flow area and increasing air-gap area as the Halon travels away from the nozzle.

The problem with the showerhead nozzle was thought to be the straight orifices which discharged the Halon at throat pressure and allowed the Halon jets to spread without restraint and merge to exclude air gaps. To avoid this effect, a new nozzle was designed with converging-diverging passages. The diverging sections would give controlled, narrow-angle expansion to atmospheric pressure and produce jets that would penetrate the air without merging.

A nested annular nozzle configuration was chosen for ease of fabrication. The resulting "multicone" nozzle, Figs. 41 and 42, has eight converging-diverging annular nozzles at angles of 15 to 85 degrees from center. The total throat area is 600 mm^2 and the exit area is 9000 mm^2, giving an expansion ratio

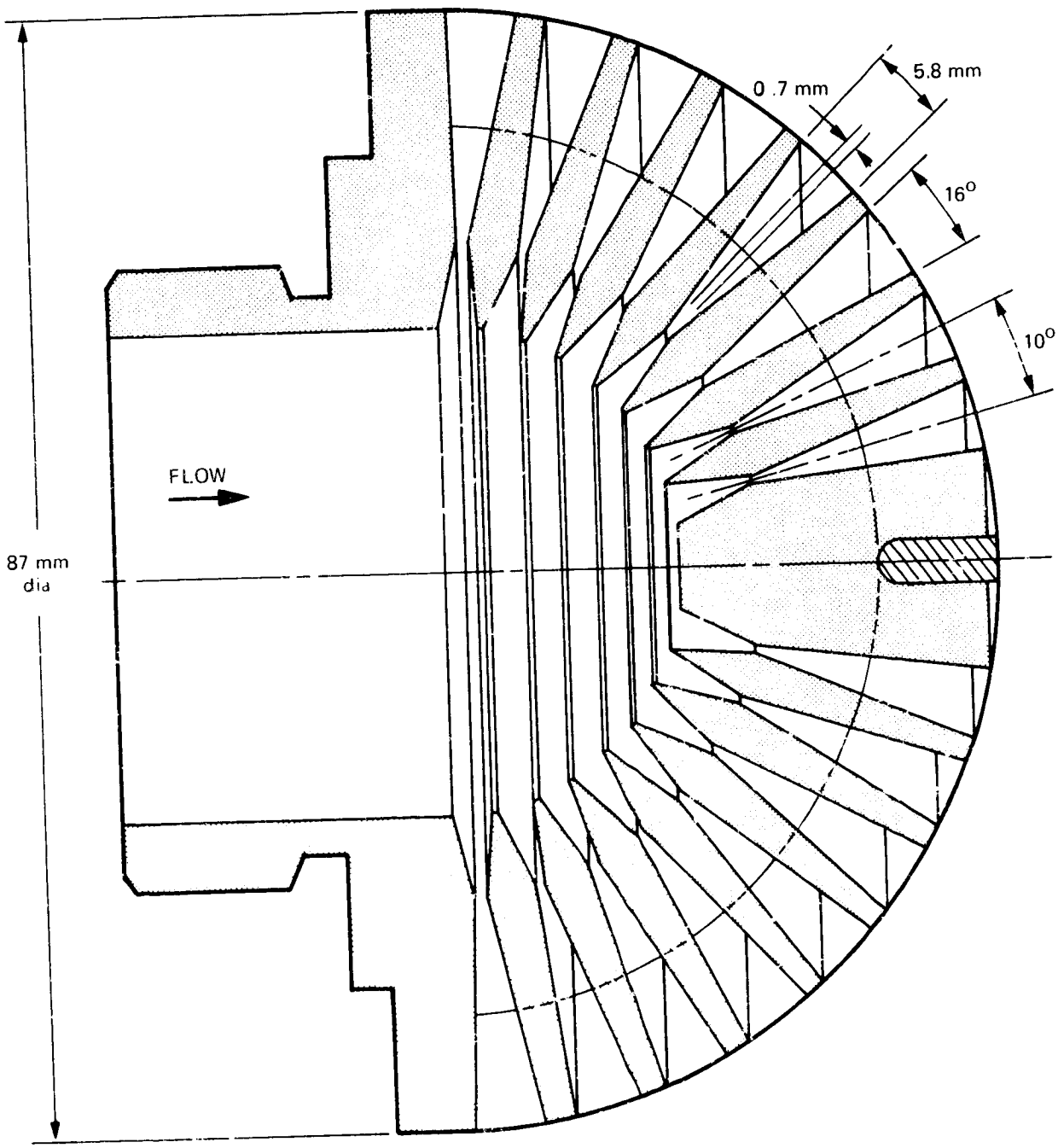

Figure 41. Multicone nozzle design

(a)

Figure 42. Multicone nozzle: (a) Parts

(b)

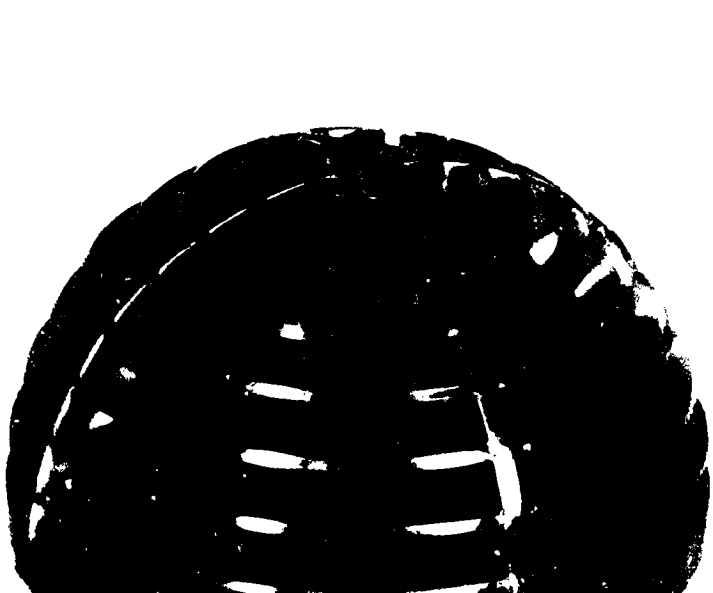

Figure 42. Multicone nozzle: (b) Assembly

of 15. The nozzle exit occupies 75 percent of the hemispherical exit surface, allowing an initial 25 percent air gap area; at a distance of 1.0 m from the nozzle the Halon jets occupy only 1.4 percent of a hemispherical surface, and the distance between jet centers is 175 mm.

The nozzle is held together by two hoops. These hoops give an undesired interruption of the flow; a center support post could be used instead.

Figure 43(a) shows the multicone nozzle operating with water and nitrogen flow as viewed from between the support hoops, and Figure 43(b) shows the flow as viewed edge-on to a support hoop. The flow shows little tendency to pull inward to a cylindrical jet. However, the support hoops produce a 25 degree gap in the flow.

Figure 44 shows movie frames of Halon flow from the multicone nozzle. The Halon spreads at a large angle, and the nozzle achieves the desired hemispherical distribution except for the gaps due to the support hoops.

Figure 45 is a movie frame of a fire suppression test conducted by Dr. Harry T. Johnson at NASA White Sands Test Facility. Two multicone nozzles, one on the lower left and one on the lower right, spray Halon 1301 away from the camera and toward a diesel fuel fire in a simulated tank crew compartment. The gaps in the flow due to the support hoops are very pronounced. Otherwise, the Halon is spreading satisfactorily over a wide angle. The fire was extinguished in 150 ms.

D. Personnel Impact Hazards

Personnel struck by discharging Halon could be injured either by the total force or by the high velocity and low temperature of the flow.

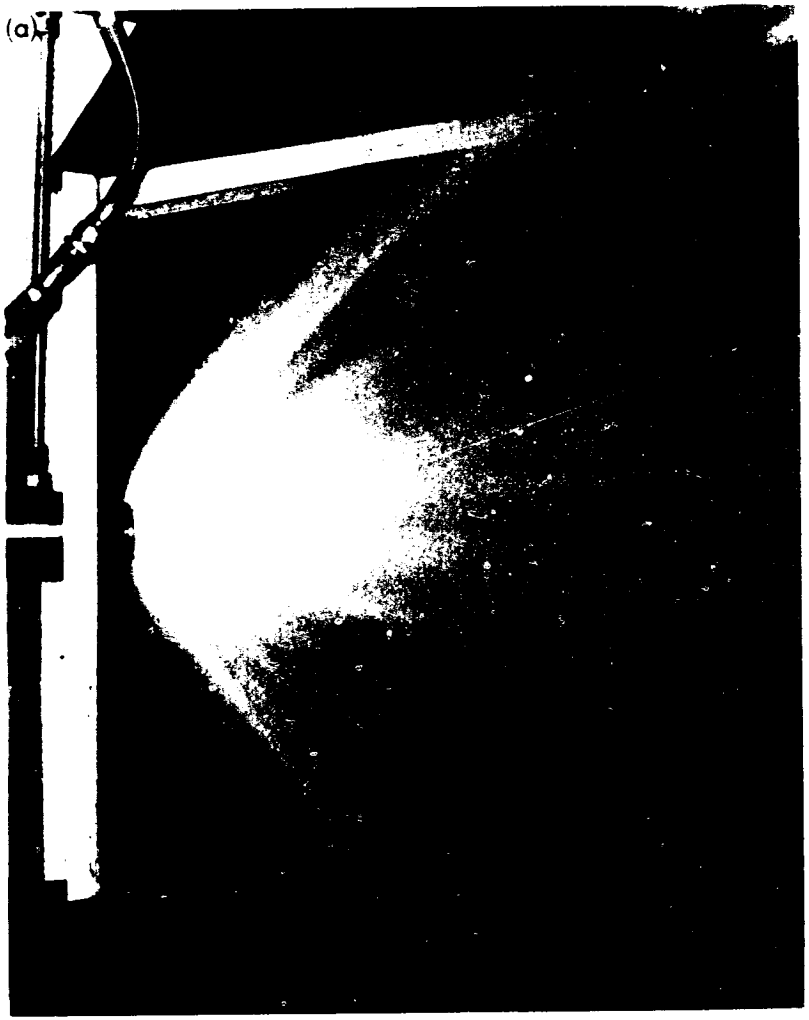

Figure 43. Flow test of the multicone nozzle with water and nitrogen: (a) Viewed between the support hoops

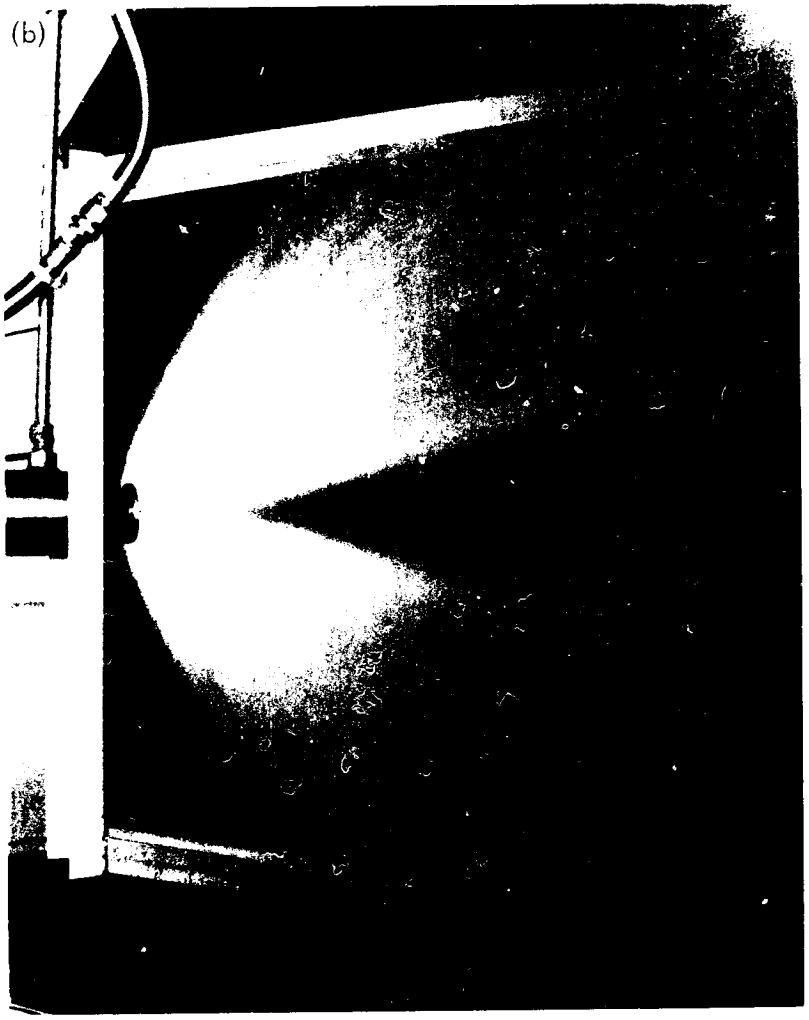

Figure 43. Flow test of the multicone nozzle with water and nitrogen: (b) Viewed edge-on to a support hoop

Figure 44. Halon flow test of the multicone nozzle at: (a) 0 ms

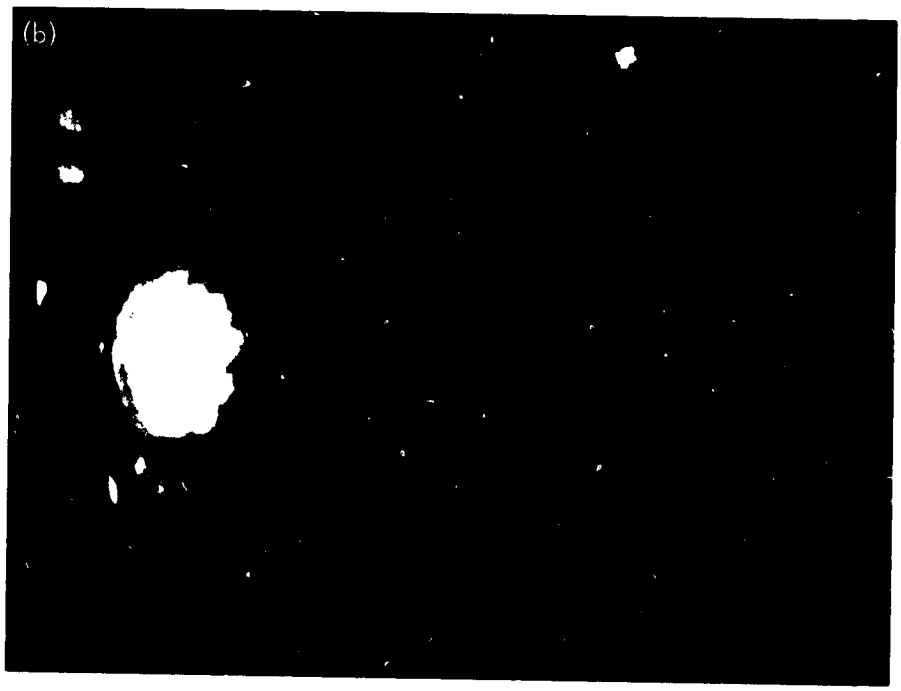

Figure 44. Halon flow test of the multicone nozzle at: (b) 1 ms

Figure 44. Halon flow test of the multicone nozzle at: (c) 4 ms

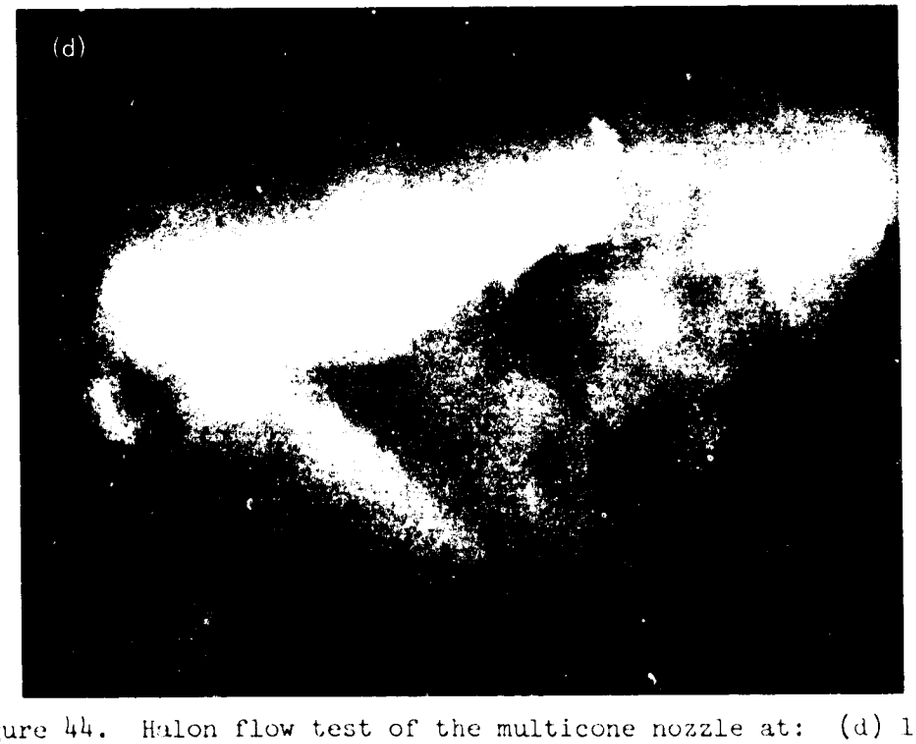

Figure 44. Halon flow test of the multicone nozzle at: (d) 12 ms

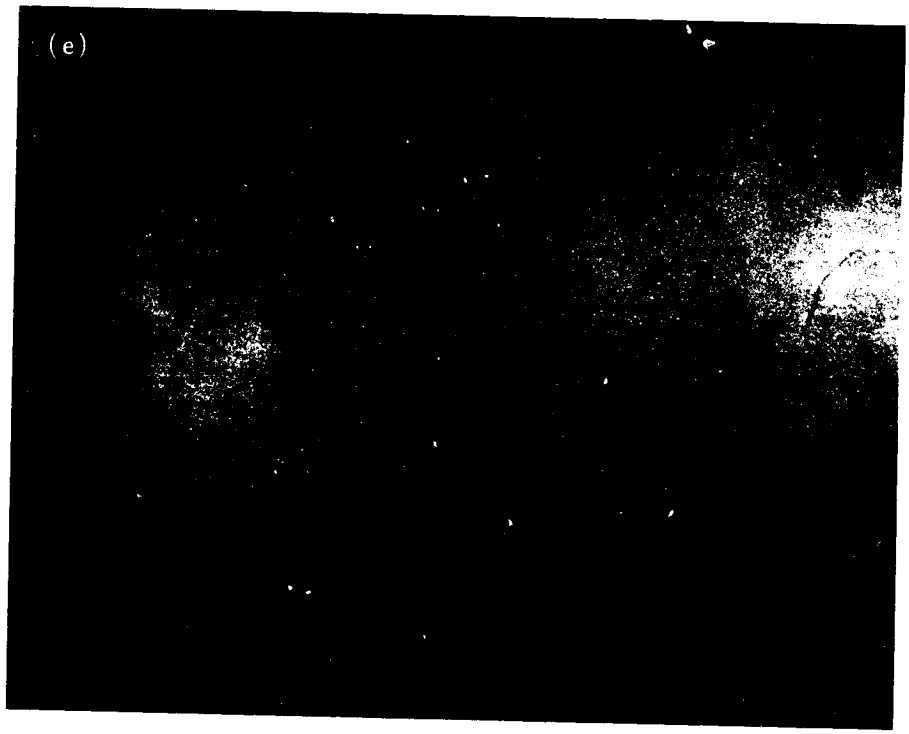

Figure 44. Halon flow test of the multicone nozzle at: (e) 50 ms

Figure 45. Fire suppression test of two multicone nozzles

Total force measurements were made using the apparatus shown in Fig. 46. A target plate mounted on a load cell was placed downstream of the bottle valve. The maximum force occurred at the start of discharge when the flow rate was about 15 kg/s. The isentropic Halon velocity at 5.2 MPa bottle pressure is 220 m/s. The theoretical peak force is thus 15x220 = 3300 N = 740 lbf. The peak forces measured were higher, about 4000 N. With a wide-dispersion nozzle a person standing more than about 0.5 m from the nozzle would be struck by only a fraction of the flow, and the force would be much less.

Based on past experience with water-and-nitrogen nozzles (Ref. 10), impingement of two-phase flow on bare skin is uncomfortable but not injurious. To simulate Halon flow conditions with water and nitrogen a nozzle with a 20 mm exit diameter was operated at an exit velocity of 140 m/s. The flow rate was 0.6 kg/s and the void fraction of the jet was 0.99. Placing a hand in the jet gave a sensation of a bundle of needles being pressed into the skin, but there were no injurious effects. It can be concluded that impingement of Halon flow would not be injurious from the standpoint of drop penetration. The low temperature would be an additional hazard.

E. Summary

Halon can be dispersed by simple nozzles with orifices, slots, or deflectors if nothing more is desired than a few jets or sheets of Halon. Uniformly filling a large volume with Halon flow is more difficult, because numerous closely-spaced Halon jets or sheets are required and there must be air gaps between the streams. A multicone nozzle design achieved the desired air penetration of multiple Halon sheets, and gave a hemispherical distribution

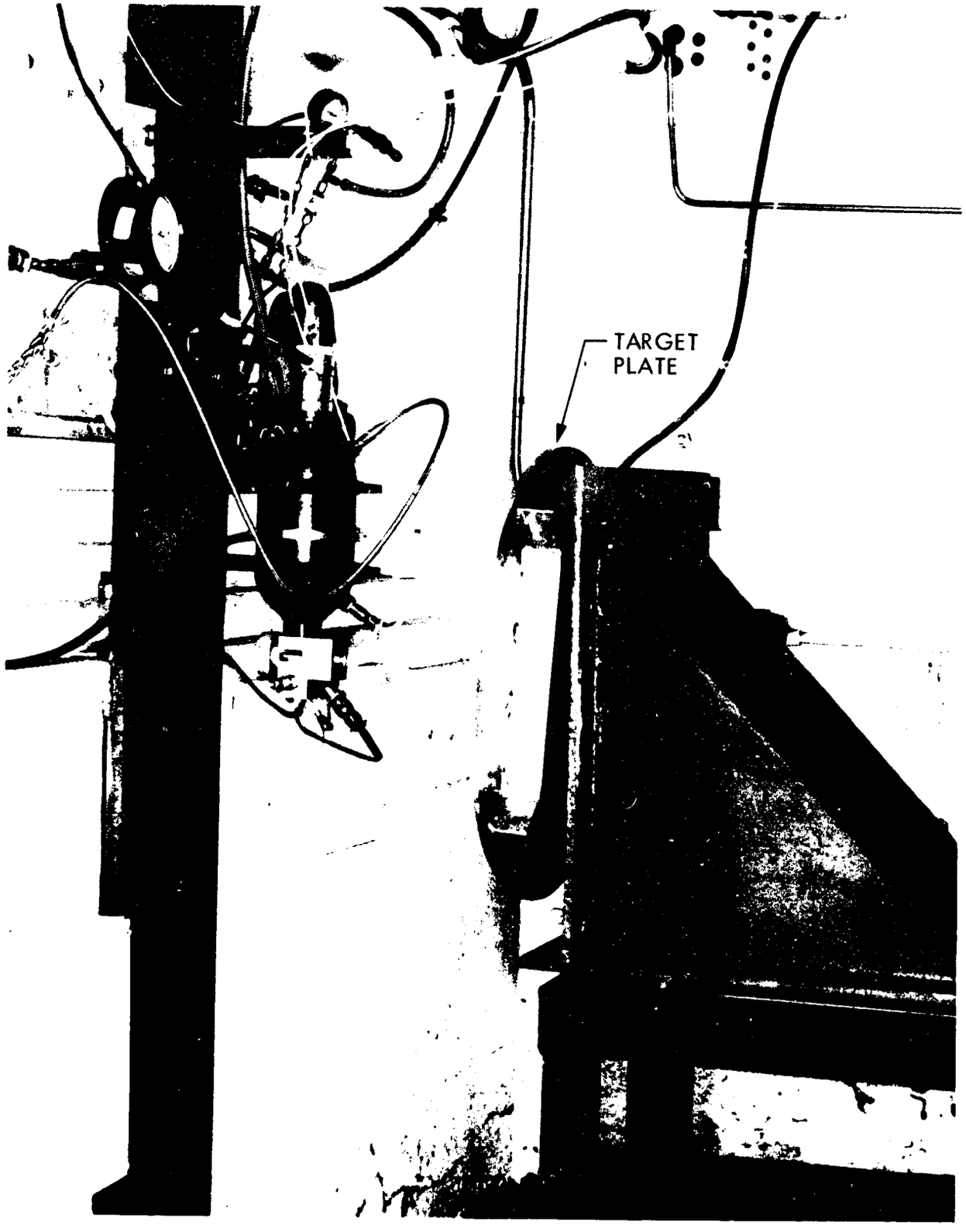

Figure 46. Test arrangement with impact force target

except for gaps due to support struts. A center-supported multicone nozzle design would eliminate the gaps.

The impact force of Halon leaving a bottle was 4000 N, but the force with a dispersion nozzle would be less. The impact of water-and-nitrogen flow on skin at a velocity similar to Halon discharge conditions was found to be uncomfortable but not injurious.

REFERENCES

1. Malcolm, J.E., Vaporizing Fire Extinguishing Agents, Report No. 1177, U.S. Army Engineer Research and Development Laboratories, Ft. Belvoir, Va., Aug. 18, 1950.

2. Fryburg, G., Review of Literature Pertaining to Fire Extinguishing Agents and to Basic Mechanisms Involved in their Action, NACA TN-2102, National Aeronautics and Space Administration, Washington, DC, May 1950.

3. Larson, E.R., "Halogenated Fire Extinguishants: Flame Suppression by a Physical Mechanism?", ACSC Symposium Series 1975, Vol. 16, pp. 376-402.

4. Sheinson, R.S., Gellene, G.I., Williams, F.W., and Hahn, J.E., "Quantification of Fire Suppressant Action on Liquid Pool Fires", Chemical and Physical Processes in Combustion, Proceedings of the 1978 Fall Technical Meeting of the Eastern Section of the Combustion Institute, Pittsburgh, PA., December 1, 1978, pp. 18-1 - 18-4.

5. Parks, D.J., Alvares, N.J., and Beason, D.G., Fundamental Flame-Speed Measurements in Combustion Gases Containing CF_3Br, Preprint UCRL-82181, Lawrence Livermore Laboratory, Livermore, Calif., March 1979.

6. Rozniecki, E., Conversion of M60 Engine Compartment Fixed Manual CO_2 Fire Extinguisher System to Halon-1301, Technical Report No. 12432, U.S. Army Tank-Automotive Research and Development Command, Warren, Mich., April 1979.

7. Moran, K.M., and Zydowicz, M.P., Halon 1301 Fire Suppression System Tests, Report No. D-921, Jet Propulsion Laboratory, Pasadena, Calif., Aug. 1983 (Internal Document).

8. Standard on Halogenated Fire Extinguishing Agent Systems--Halon 1301 Document No. 12A, National Fire Protection Association, Boston, Mass., 1973.

9. 360 psi Total Flooding Halon 1301 Fire Extinguishing Systems Design Manual, Document No. F-41426B, Walter Kidde & Company, Inc., Wake Forrest, N.C., Aug. 1975.

10. Elliott, D.G., and Weinberg, E., Acceleration of Liquids in Two-Phase Nozzles, Technical Report 32-987, Jet Propulsion Laboratory, Pasadena, Calif., July 1, 1968.

11. Thermodynamic Properties of DuPont Halon 1301 Fire Extinguishant, Bulletin T-1303, E.I. DuPont de Nemours & Co., Petrochemicals Dept., Wilmington, Del., 1966.

12. DuPont Halon 1301 Fire Extinguishant, Bulletin B-29D, E.I. DuPont de Nemours & Co., Organic Chemicals Dept., Wilmington, Del., 1977.

13. Ford, C.L., Specific Volumes and Vapor Pressures of Solutions of Nitrogen in Freon FE 1301, E.I. DuPont de Nemours & Co., Freon Products Division, Wilmington, Del., 1978.

14. Ford, C.L., Equations Used in Computer Program "SUPER", E.I. DuPont de Nemours & Co., Freon Products Division, Wilmington, Del., 1979.

15. Hirt, C.W., Oliphant, T.A. Rivard, W.C., Romero, N.C., and Torrey, M.D., SOLA-LOOP: A Nonequilibrium, Drift-Flux Code for Two-Phase Flow in Networks, Report No. L-7659, Los Alamos National Laboratory, Los Alamos, New Mexico, 1979.

16. Campbell, J.R., Rivard, W.C., and Sicilian, J.M., SOLA-NET: A Program for Water-Steam-Air Hydraulics in Pipe Networks, Interim Report, Flow Science, Inc., Los Alamos, New Mexico, June 1982.

APPENDIX A. DERIVATION OF THEORETICAL MODEL

A. Assumptions

The two-phase mixture of Halon liquid, Halon vapor, and nitrogen that flows out of the bottle is assumed to be a homogeneous mixture as it flows through the discharge piping and nozzles. The mixture behaves as a single-phase compressible fluid with a density that is a function of temperature and pressure, and all parts of the mixture have the same velocity. Inside the bottle the fluid has two layers, with the liquid confined to the lower layer.

The flow in the bottle and pipes is assumed to be adiabatic, because the bottle and pipe wall areas are too small to transfer an amount of heat that would vaporize enough additional liquid to significantly affect the flow.

A key simplifying assumption is that the discharge flow rate out of the system at each instant of time is equal to the steady-state flow rate that would exist if the bottle conditions were held constant at the values for that instant. The flow rate out of the bottle and into the piping system is then found by adding the rate of storage change in the piping system to the discharge flow rate, but the discharge flow rate itself is not a true transient calculation. This "quasi-steady" approximation is accurate during most of the discharge time, for piping volumes that are not greatly larger than the bottle volume. The approximation breaks down during initial pressurization of the piping system, when the storage rate dominates, and this process is treated by a different procedure.

B. Two-Phase Mixture Properties

The Halon-nitrogen mixture is a two-phase, two-component mixture. The nitrogen will be designated "component A" and the Halon "component B", with subscripts a and b, respectively.

By Henry's Law, the mole fraction of nitrogen in the liquid phase is proportional to the partial pressure of tne nitrogen, p_a.
Thus,

$$\frac{m_{a\ell}/W_{a\ell}}{m_{a\ell}/W_{a\ell}+(m_\ell - m_{a\ell})/W_{b\ell}} = Hp_a \qquad (1)$$

where m_ℓ is the liquid mass, $m_{a\ell}$ is the mass of dissolved component A, $W_{a\ell}$ and $W_{b\ell}$ are the molecular weights of A and B, respectively, and H is the mole fraction dissolved per unit pressure of A (the inverse of Henry's Law constant).

Solving for $m_{a\ell}/m_\ell = \alpha$ (the concentration of dissolved nitrogen) the result is

$$\alpha = \frac{(W_{a\ell}/W_{b\ell})\ Hp_a}{1 + (W_{a\ell}/W_{b\ell} - 1)\ Hp_a} \qquad (2)$$

The partial pressure p_b of component B is equal to the vapor pressure p_{bo} of pure B multiplied by the mole fraction of B in the liquid (Raoult's Law).

$$p_b = (1 - Hp_a)p_{bo} \qquad (3)$$

The total pressure is

$$p = p_a + p_b \qquad (4)$$

Combining Eqs. (3) and (4) the nitrogen partial pressure is

$$p_a = \frac{p - p_{bo}}{1 - Hp_{bo}} \tag{5}$$

The effective molecular weight W_g of the gas phase, such that the gas density is given by $W_g\, p/RT$ where R is the universal gas constant, is

$$W_g = \frac{W_{ag}p_a + W_{bg}p_b}{p} \tag{6}$$

The mass fraction of Halon vapor in the gas phase is

$$\beta = \frac{W_{bg}p_b}{W_g p} \tag{7}$$

The mass ratio of component A (gaseous nitrogen plus dissolved nitrogen) to component B (Halon liquid plus vapor) is the "component ratio" r_c, defined by

$$r_c = \frac{m_{a\ell} + m_{ag}}{m_{b\ell} + m_{bg}} \tag{8}$$

The mass ratio of gas to liquid, in terms of r_c and the concentrations α and β, is

$$r_m = \frac{r_c - \alpha(1+r_c)}{1 - \beta(1+r_c)} \tag{9}$$

If $\rho_{a\ell}$ and $\rho_{b\ell}$ are the densities of dissolved nitrogen and liquid Halon, respectively, then the density of the Halon-nitrogen solution is

$$\rho_\ell = [(\alpha/\rho_{a\ell}) + (1 - \alpha)/\rho_{b\ell}]^{-1} \tag{10}$$

The specific enthalpies of the gas and liquid phases are the sums of the contributions from the components:

$$h_g = (1-\beta)\, h_{ag} + \beta h_{bg} \tag{11}$$

and

$$h_\ell = \alpha h_{a\ell} + (1-\alpha) h_{b\ell} \tag{12}$$

The specific internal energies of the gas and liquid phases are found by subtracting the pressure-volume product from the enthalpy:

$$u_g = h_g - \frac{p}{\rho_g} \tag{13}$$

$$u_\ell = h_\ell - \frac{p}{\rho_\ell} \tag{14}$$

The two-phase mixture density, in terms of the phase densities, is

$$\rho_{mix} = \frac{1 + r_m}{\frac{r_m}{\rho_g} + \frac{1}{\rho_\ell}} \tag{15}$$

As a given mass m_t of the two-phase mixture proceeds through the flow system, the component ratio r_c remains constant but the mass ratio r_m changes and the gas and liquid flow rates change according to

$$m_g = \frac{r_m}{1 + r_m}\, m_t \tag{16}$$

and

$$m_\ell = m_t - m_g \tag{17}$$

C. Fluid Expansion in the Bottle

At some intermediate pressure p_1 during discharge the mass of fluid in the bottle is m_1 and the volume of fluid is the bottle volume v_{bot}. When the bottle pressure drops to a lower value p_2 the mass m_1 expands to a larger volume equal to m_1/ρ_{mix2}, where ρ_{mix2} is the density of the mixture (consisting of the liquid layer and the ullage gas) at pressure p_2 and temperature T_2, with T_2 to be determined. The volume of fluid that must leave the bottle during the expansion from p_1 to p_2 is

$$v_{out} = \frac{m_1}{\rho_{mix2}} - v_{bot} \tag{18}$$

If the average density of the fluid in the liquid layer during the expansion from p_1 to p_2 is ρ_{out}, then the mass of fluid discharged is $m_{out} = \rho_{out} v_{out}$. To satisfy conservation of energy the change in the internal energy of the fluid in the bottle must equal the enthalpy of the fluid leaving. Thus,

$$U_1 - U_2 = m_{out} h_{out} \tag{19}$$

where h_{out} is the specific enthalpy of the fluid leaving.

The new temperature T_2 is the value that causes Eq. (19) to be satisfied. Once T_2 is found, all of the bottle conditions at the new pressure level p_2 are known, and the amount of fluid m_{out} discharged to reach p_2 is known.

Assumptions must be made about the location of the nitrogen bubbles in calculating the density ρ_{out} and enthalpy h_{out} of the fluid leaving the bottle. To decide the best assumption, predictions for Test 146 were made for two limiting cases: (1) no bubble rise, with all of the released nitrogen remaining

trapped in the liquid layer, and (2) complete bubble rise, with all of the released nitrogen moving to the ullage. Fig. A-1 shows the comparison with data for the two assumptions. If complete bubble rise is assumed, the predicted discharge time is too short. The assumption of no bubble rise gives good agreement with the observed discharge time and is the assumption adopted in the model.

In the model the dissolved nitrogen is held in solution until the nitrogen release pressure is reached. Fig. A-2, step 1-2, shows an example of the bottle conditions that satisfy Eqs. (18) and (19) for expansion without nitrogen release. If the nitrogen is then released from solution with no mass discharged, the conditions determined by Eq. (19) are shown in step 2-3. The next expansion step, with equilibrium dissolved nitrogen concentration, is shown in step 3-4. These illustrations show the detailed bookkeeping necessary in calculating two-phase, two-component expansion processes.

D. Nozzle Flow

In a nozzle the pressure drop is balanced by velocity increase. For a small pressure change dp the change in velocity is given by

$$d(V^2) = \frac{2\,dp}{\rho_{mix}} \tag{20}$$

If Eq. (20) is integrated over a finite pressure decrease from p_1 to p_2, and the mixture density is evaluated from Eq. (15) with gas density calculated from the perfect gas equation, a convenient equation for velocity increase, accurate for substantial pressure differences, is

$$V_2^2 - V_1^2 = \frac{2}{1 + r_{mm}} \left(\frac{r_{mm}\, p_m}{\rho_{gm}} \ln\frac{p_1}{p_2} + \frac{p_1 - p_2}{\rho_m} \right) \tag{21}$$

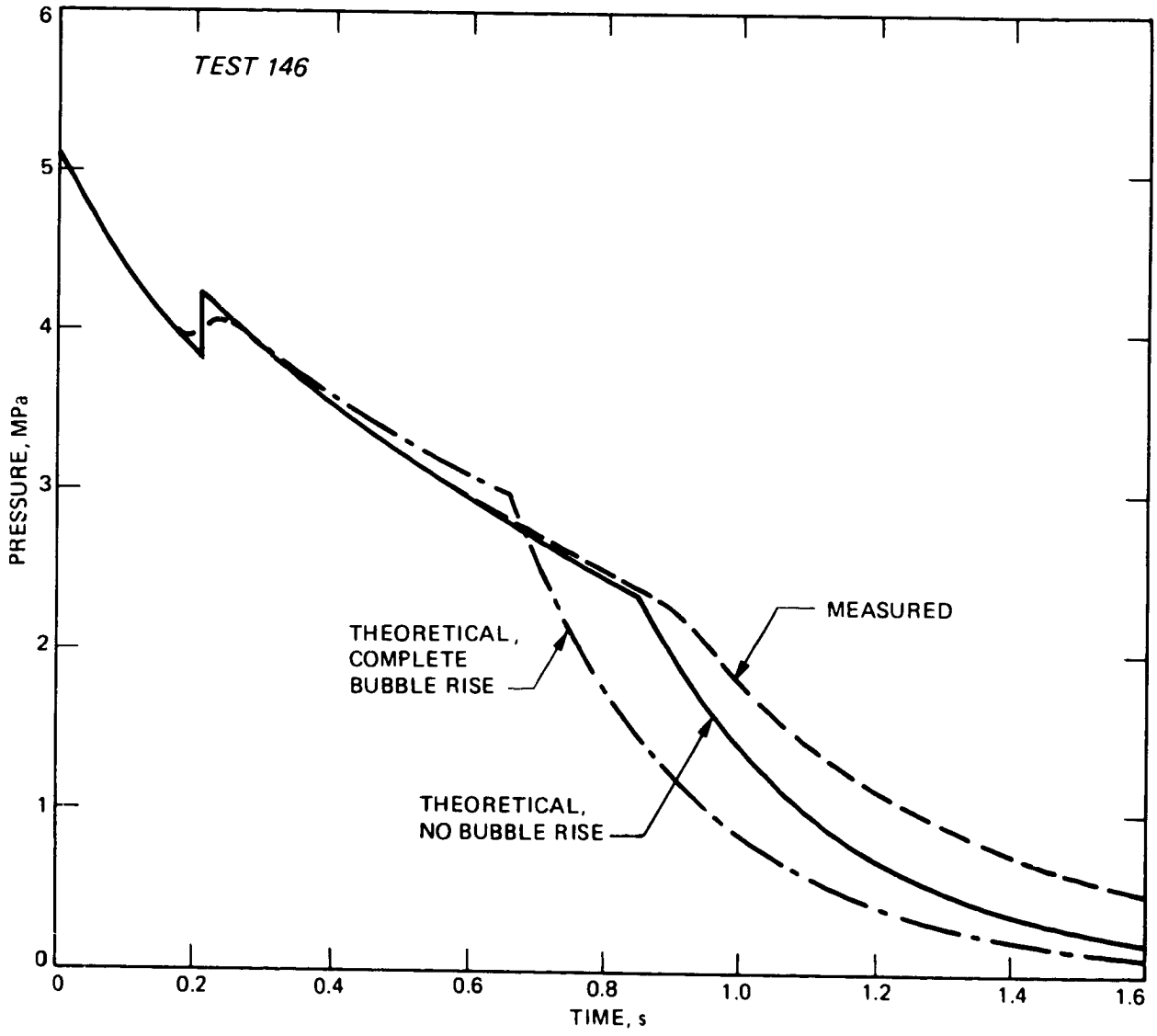

Figure A-1. Comparison, for no bubble rise and complete bubble rise, between experimental and theoretical pressure-time curves

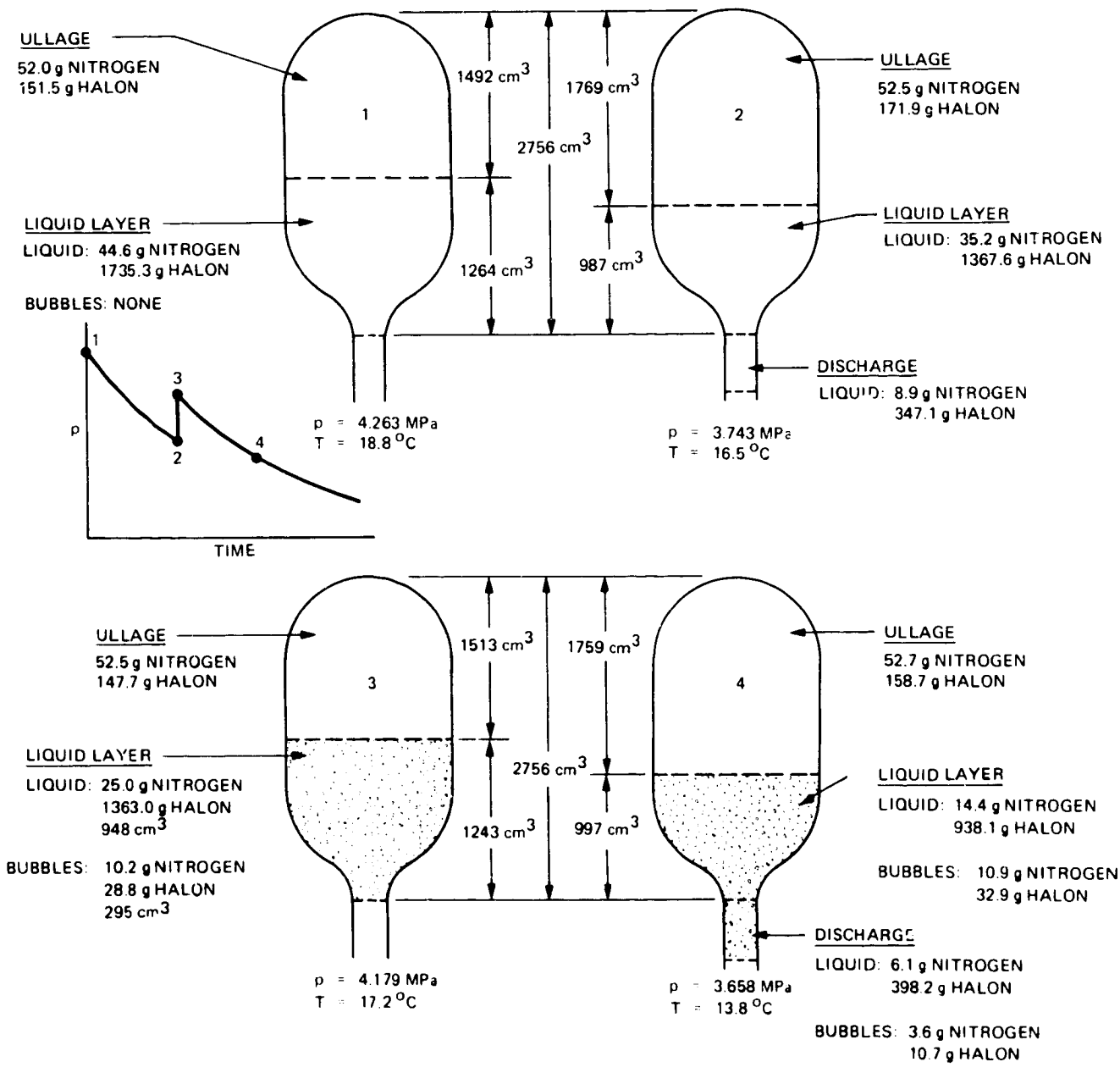

Figure A-2. Typical bottle conditions at four successive stages of Halon discharge

where r_{mm}, p_m, ρ_{gm}, and $\rho_{\ell m}$ are the arithmetic mean values of gas/liquid ratio, pressure, gas density, and liquid density, respectively, over the interval from p_1 to p_2.

The temperature T_2 at pressure p_2 is found by guessing T_2, using that guess in evaluating the mean values in Eq. (21), and then seeing if the enthalpy change of the fluid is equal to the kinetic energy change $(V_2^2 - V_1^2)/2$. Temperature T_2 is iterated until the kinetic energy change from Eq. (21) agrees with the enthalpy change.

At the end of each pressure step the flow area for given flow rate $\dot{m}$ is found from

$$A_2 = \frac{\dot{m}}{\rho_{mix_2} V_2} \tag{22}$$

The smallest value of area found is the throat area A_t. If the actual nozzle has throat area A, then the choked flow rate is $\dot{m}A/A_t$.

E. Pipe Flow

In a pipe the pressure drop is balanced mainly by wall friction. For a pressure decrease from p_1 to p_2 the velocity changes from V_1 to V_2, with V_2 given by continuity:

$$V_2 = \frac{\dot{m}}{\rho_{mix_2} A_{pipe}} \tag{23}$$

The mean wall shear for the section of pipe between p_1 and p_2 is

$$\tau_w = 0.5 \, \rho_{mixm} \, V_m^2 \, C_f \tag{24}$$

where ρ_{mixm} is the mean mixture density, V_m^2 is the mean-square velocity, and C_f is the friction coefficient.

The friction retarding force on the fluid in the length of pipe Δx between p_1 and p_2 is $\tau_w \pi D_{pipe} \Delta x$. This force is balanced by the pressure drop and fluid momentum change. The pipe length needed for the required friction force is

$$\Delta x = \frac{A_{pipe} (p_1 - p_2) + \dot{m}(V_1 - V_2)}{\tau_w \pi D_{pipe}} \qquad (25)$$

The new temperature T_2 is found in the same way as for a nozzle, iterating on temperature until the enthalpy decrease equals the kinetic energy increase.

As the flow proceeds down a long pipe the distance increment Δx required to provide enough friction to balance a given pressure difference $p_1 - p_2$ decreases. When a zero or negative Δx is found this means that sonic conditions have been reached. The pipe length at that point is the maximum length possible for the given flow rate.

F. Abrupt Enlargement

Between the valve and the nozzle or pipe inlet the flow area abruptly increases. The kinetic energy decrease downstream of the valve throat is converted to heat. To calculate the slight temperature rise downstream of the valve the downstream temperature is iterated until the kinetic energy decrease equals the enthalpy increase.

G. Flow Rate Calculation for Series Components

During discharge the Halon flows subsonically through several restrictions before reaching sonic conditions at the final restriction. For example, the Halon flows through the bottle valve and may then flow through a pipe inlet nozzle and a pipe before reaching the discharge nozzle throat. To calculate the flow rate through such a series string a flow rate must be guessed. The sonic

flow area required after the flow has encountered the various pressure losses can then be calculated. If the required area is larger than the actual throat area of the discharge nozzle then a smaller flow rate must be guessed. The flow rate is iterated until the required and actual throat areas agree.

The final flow restriction moves from one component to the next during filling of the piping system. The flow-rate search is first done with the bottle valve area as the throat area, then with the pipe inlet orifice, then with successive positions in the pipe, and finally with the discharge nozzle. The position of the fluid front, which determines which flow restriction is controlling, is calculated from the fluid front (sonic) velocity and elapsed time.

H. Elapsed Time Calculation

For each pressure increment p_1 to p_2 the average flow rate $\dot{m}_{dis}$ at the discharge restriction is calculated as described above. The change in stored mass Δm_{sto} is found at the same time by integrating the fluid density over the pipe volume at the two pressures and finding the difference. The mass of fluid m_{out} that left the bottle between p_1 and p_2 is already known from the bottle calculations. The time increment Δt between pressures p_1 and p_2 must be such that the sum of the discharged mass $\dot{m}_{dis}\Delta t$ plus the storage increase Δm_{sto} is equal to the mass leaving the bottle. Thus, the time increment between p_1 and p_2 is

$$\Delta t = \frac{m_{out} - \Delta m_{sto}}{\dot{m}_{dis}} \qquad (26)$$

I. Pipe Pressurization

Between the time the Halon reaches the end of the pipe and the time the pipe reaches peak pressure the storage change predominates and a different procedure for calculating elapsed time is used. The flow rate into the pipe at

the time the liquid reaches the end of the pipe is $\dot{m}_{in1}$. The first flow rate out of the discharge nozzle, with just the pipe sonic exit pressure applied to the nozzle, is $\dot{m}_{out1}$. The mass stored in the pipe at this time is m_{sto1}.

The pressure at the time of peak pipe pressure is guessed and the corresponding discharge flow rate $\dot{m}_{out2}$ is calculated. Since the pipe pressure is not changing at that instant, having just reached its peak, the pipe inlet flow rate is equal to the outlet flow, $\dot{m}_{in2} = \dot{m}_{out2}$. The mass stored at that time is m_{sto2}.

The average inlet flow rate during pressurization is $\dot{m}_{inm} = (\dot{m}_{in1} + \dot{m}_{in2})/2$ and the average outlet flow rate is $\dot{m}_{outm} = (\dot{m}_{out1} + \dot{m}_{out2})/2$.

The average net flow rate into the pipe is $\dot{m}_{inm} - \dot{m}_{outm}$, and that flow rate times the filling time Δt_{fill} is equal to the storage increase $m_{sto2} - m_{sto1}$. Thus, the time increment between the arrival of the liquid front at the end of the pipe and the instant of peak pipe pressure is

$$\Delta t_{fill} = \frac{m_{sto2} - m_{sto1}}{\dot{m}_{inm} - \dot{m}_{outm}} \tag{27}$$

The mass Δm_{bot} discharged from the bottle during the time increment Δt_{fill} is the product of the average inlet flow rate $\dot{m}_{inm}$ and Δt_{fill}. From the bottle calculations the bottle pressure existing when that much mass has left the bottle is known and can be compared with the guessed bottle pressure at the time of peak pipe pressure. If the two pressures do not agree a new bottle pressure is guessed and calculations starting with $\dot{m}_{out2}$ are repeated until the results converge.

J. Multibranch Calculations

For multibranch calculations the pressure at the junction between the main pipe and the branch pipes is calculated from the previous flow rate. Each

branch is then calculated as though the junction conditions were the bottle conditions for that branch. The branch flow rates and branch storage masses are added and applied to the exit of the main branch and the calculations then completed in the same way as for a single-branch system.

K. Summary

The model consists of two sections: a bottle section that calculates bottle outlet conditions as a function of mass discharged and a flow section that calculates flow rate as a function of bottle outlet conditions. The flow rate calculations assume steady flow and determine flow rates from sonic flow conditions at the final flow restriction prevailing at the time. Adding the pipe storage changes gives the bottle discharge mass for each pressure increment, from which the elapsed time can be determined. For the pipe pressurization step the elapsed time is obtained from the average of the net flow rates at the beginning and end of pressurization.

APPENDIX B. HALON AND NITROGEN PROPERTIES

Thermodynamic properties of Halon 1301 are tabulated in Ref. 11 and physical and transport properties in Ref. 12. Measurements of specific volumes and vapor pressures of solutions of nitrogen in Halon 1301 are reported in Ref. 13. Based on Ref. 13, Du Pont developed a computer program called "SUPER" for calculation of nitrogen-pressurized Halon 1301 properties; the equations used in program SUPER are given in Ref. 14.

Using the equations and tabulations of Refs. 11 to 14 and other sources, property subroutines were written for program HFLOW and for the modified version of SOLA-LOOP (Appendix C). The equations used are the following:

1. Nitrogen Specific Volume

The equation of state for gaseous nitrogen from Ref. 14 is

$$p = \frac{R_o T}{W(v-0.015313)} - \frac{99.164}{v(v+0.015313)\sqrt{T}} \qquad (1)$$

where p is the nitrogen pressure in psia, T is the temperature in R, v is the specific volume in ft^3/lb, R_o is the universal gas constant (10.73152 psi-ft^3/mole-^oR), and W is the molecular weight (28.016). The gas constant for nitrogen is $R = R_o/W = 0.38305$.

The equation of state can be rearranged for iterative solution as follows:

$$\Delta p = \frac{C_{11}}{v(v+C_{12})\sqrt{T}} \qquad (2)$$

$$v = \frac{RT}{p + \Delta p} + C_{12} \qquad (3)$$

where $C_{11} = 99.164$ and $C_{12} = 0.015313$.

To start the solution, an initial guess at specific volume is calculated from the perfect gas law.

$$v_0 = RT/p \tag{4}$$

Then v_o is substituted in Eq. (2) to find the small pressure correction Δp, and a new volume v is found from Eq. (3). The answer converges rapidly with successive iterations.

It is convenient to express the specific volume in terms of an effective molecular weight that gives the correct specific volume when substituted in the perfect gas equation. The effective molecular weight is

$$W_g = \frac{R_o T}{vp} \tag{5}$$

2. Dissolved Nitrogen Specific Volume

The partial specific volume of nitrogen dissolved in Halon 1301 is given by Ref. 14 as

$$v = C_{21} + C_{22} \ln (C_{23} - t) \tag{6}$$

where v is the increase in volume of a nitrogen-Halon solution in ft^3 per lb of dissolved nitrogen and t is the temperature in ^oF. The constants are C_{21} = 0.24094456, C_{22} = -0.04021084 and C_{23} = 152.96.

3. Nitrogen Enthalpy

The enthalpy of nitrogen over the range 0 to 600 psi and -80° F to 80° F can be represented by

$$h_g = C_{31}\, p + C_{32}(300-T) + C_{33}\, p(300-T) + C_{34}\, p(300-T)^2 \tag{7}$$

where h_g is the enthalpy in J/g-mole, p is the pressure in atm, and T is the temperature in K. The constants are C_{31} = -5.8462, C_{32} = -28.96, C_{33} = -0.0428, and $C_{34} = -0.3788 \times 10^{-3}$.

4. Halon 1301 Saturation Pressure

The saturation pressure of Halon 1301 from Ref. 14 is

$$\log_{10} p = C_{11} + C_{12}/T^2 + C_{13}/T + C_{14}T + C_{15}T^2 \qquad (8)$$

where p is the pressure in psi and T is the temperature in R. The constants are $C_{11} = 7.322506$, $C_{12} = -44295.0$, $C_{13} = -1795.678$, $C_{14} = -0.00438339$, and $C_{15} = 0.312584 \times 10^{-5}$.

5. Halon 1301 Vapor Density

From the Ref. 11 tabulation of saturated vapor density an effective molecular weight can be calculated that varies from 153.77 at -76°F to 202.02 at 76°F (the actual molecular weight of Halon 1301 is 148.93). When the effective molecular weights are substituted in the perfect gas law together with the saturation pressure from Eq. (8), the density agrees with the Ref. 11 tabulation. A curve fit to the effective molecular weight that agrees within 0.1 percent is given by

$$W_g = C_{21} + C_{22}t + C_{23}t^2 + C_{24}t^3 \qquad (9)$$

where t is the temperature in °C. The constants are $C_{21} = 178.10867$, $C_{22} = 0.74214272$, $C_{23} = 0.008111179$, and $C_{24} = 0.42822036 \times 10^{-4}$.

6. Halon 1301 Liquid Density

From Ref. 14 the saturated liquid density is

$$\rho_\ell = C_{31} + C_{32}(T_c-T) + C_{33}(T_c-T)^{1/2} + C_{34}(T_c-T)^{1/3} + C_{35}(T_c-T)^2 \qquad (10)$$

where ρ_ℓ is the density in lb/ft^3, T is the temperature in R and T_c is the critical temperature of 612.27 R. The constants are $C_{31} = 46.50$, $C_{32} = 0.039808$, $C_{33} = 0.82202$, $C_{34} = 9.30627$, and $C_{35} = 0.922 \times 10^{-6}$.

7. Halon 1301 Vapor Enthalpy

A curve fit to the Ref. 11 tabulation of saturated vapor enthalpy that agrees within 0.04 percent is given by

$$h_g = C_{41} + C_{42}t + C_{43}t^2 + C_{44}t^3 \quad (11)$$

where h_g is the enthalpy in Btu/lb-^oF and t is the temperature in ^oC. The constants are C_{41} = 53.635704, C_{42} = 0.10834558, C_{43} = $-0.69031717 \times 10^{-3}$, and C_{44} = $-4.1710027 \times 10^{-6}$.

8. Halon 1301 Liquid Enthalpy

A curve fit to the Ref. 11 tabulation of saturated liquid enthalpy that agrees within 0.1 percent is given by

$$h_\ell = C_{51} + C_{52}t + C_{53}t^2 + C_{54}t^3 \quad (12)$$

where h_ℓ is the enthalpy in Btu/lb-^oF and t is the temperature in ^oC. The constants are C_{51} = 12.690278, C_{52} = 0.33714354, C_{53} = 0.5673509×10^{-3} and C_{54} = 1.671468×10^{-6}.

9. Henry's Law Constant

From Ref. 14 the Henry's Law Constant is given by

$$H = C_{61} + C_{62}t + C_{63}t^2 + C_{64}t^3 \quad (13)$$

where H is the partial pressure of nitrogen (in psia) per mole fraction of dissolved nitrogen, and t is the temperature in ^oF. The constants are C_{61} = 4763.8683, C_{62} = 3.9464357, C_{63} = -0.016242350, and C_{64} = $-0.4445893 \times 10^{-3}$.

10. Halon 1301 Liquid Viscosity

The Ref. 12 tabulation of Halon 1301 liquid viscosity can be represented by

$$\mu_\ell = 0.112 + 3.11\times10^{-5}(150-t)^{1.673} \qquad (14)$$

where μ_ℓ is in centipoise and t is the temperature in ^{o}F.

11. Halon 1301 Vapor Viscosity

The Ref. 12 tabulation of Halon 1301 vapor viscosity can be represented by

$$\mu_g = 0.0137 + 3\times10^{-5}t \qquad (15)$$

where t is the temperature in ^{o}F.

12. Halon 1301 Surface Tension

An equation that follows the fourth-power rule and fits the Ref. 12 data at $0^{o}F$ and $70\ ^{o}F$ is

$$\sigma = 6.6\times10^{-8}(\rho_\ell-\rho_g)^4 \qquad (16)$$

where σ is the surface tension in dyne/cm and ρ_ℓ and ρ_g are the liquid and vapor densities in lb/ft^3.

13. Conversion to SI Units

The conversion factors to SI units for these properties are:

psi x 6894.76 = Pa

lb/ft^3 x 16.01846 = kg/m^3

Btu/lb x 2326.0 = J/kg

centipoise x 10^{-3} = $N-s/m^2$

dyne/cm x 10^{-3} = N/m

APPENDIX C. FLOW CALCULATIONS WITH THE SOLA-LOOP PROGRAM

A group at the Los Alamos National Laboratory (LANL) developed a computer program called SOLA-LOOP for calculation of transient two-phase flow in piping networks (Ref. 15). The program was written for steam and water. We prepared a modified version of SOLA-LOOP with Halon 1301 and nitrogen properties replacing the steam and water properties. The modified program was run on the LANL computer from a terminal at JPL.

The SOLA-LOOP program divides the piping system into many small segments and solves the continuity, momentum, and energy equations for each segment at each time step. There are no restrictions on the geometry of the piping system. With sufficiently small segments and small time steps the results should be highly accurate.

Predictions of the modified SOLA-LOOP program were compared with test results for the single-branch system of Fig. 18. Figure C-1 shows the results for Test 174, with a 77 mm^2 nozzle. The agreement is very good. The SOLA-LOOP program not only follows the average pressure decay curves accurately but shows the pressure oscillations following the filling of the pipe, although with some exaggeration.

Figure C-2 compares the theoretical and experimental pressures for Test 177, with no orifice on the end of the pipe. The SOLA-LOOP program correctly shows the gradual pressure rise at the pipe exit, because the model includes the effect of air in the pipe ahead of the flow.

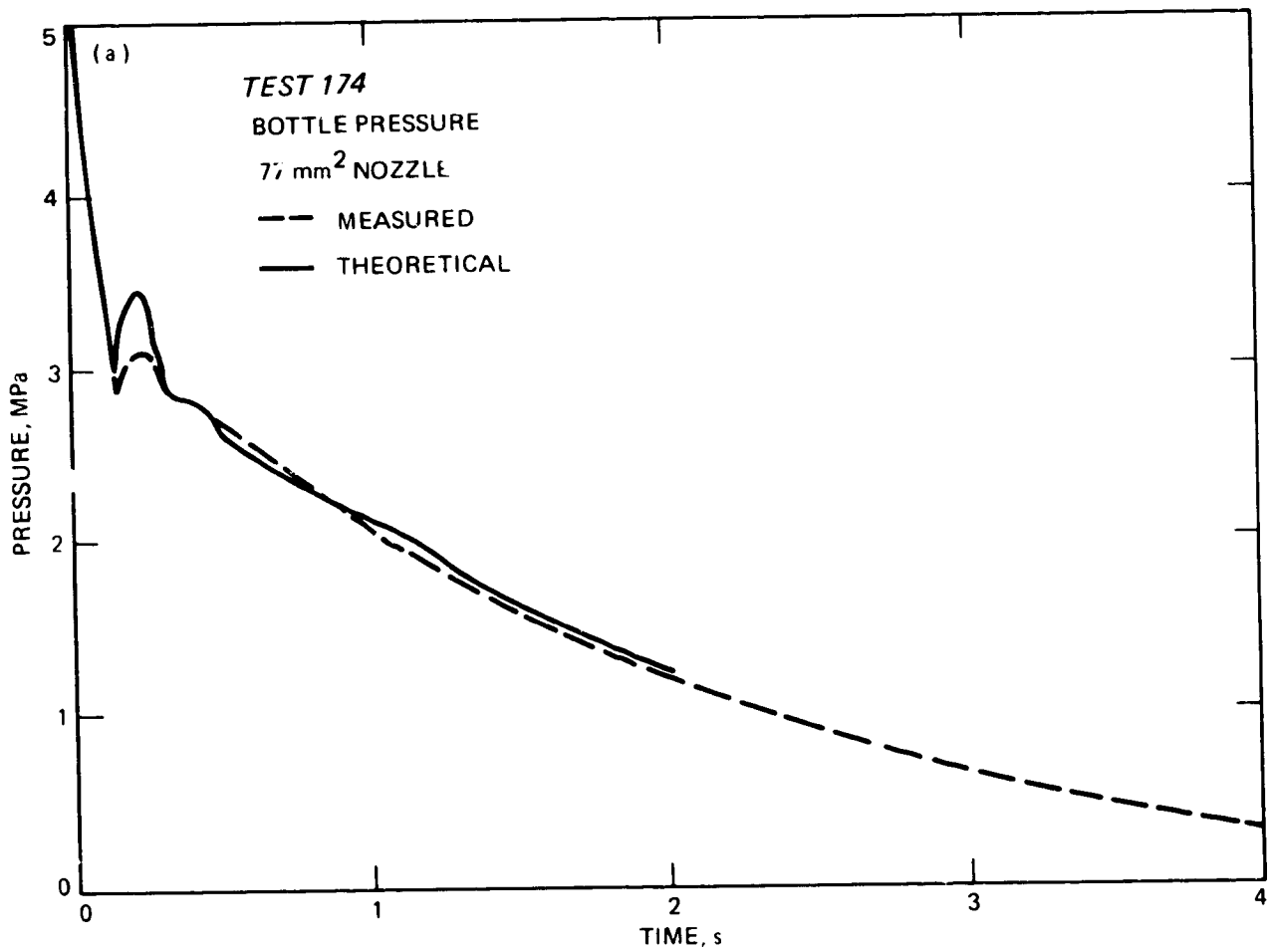

Figure C-1. Comparison, for discharge through a pipe and nozzle, between: (a) Bottle pressure SOLA-LOOP predictions and data

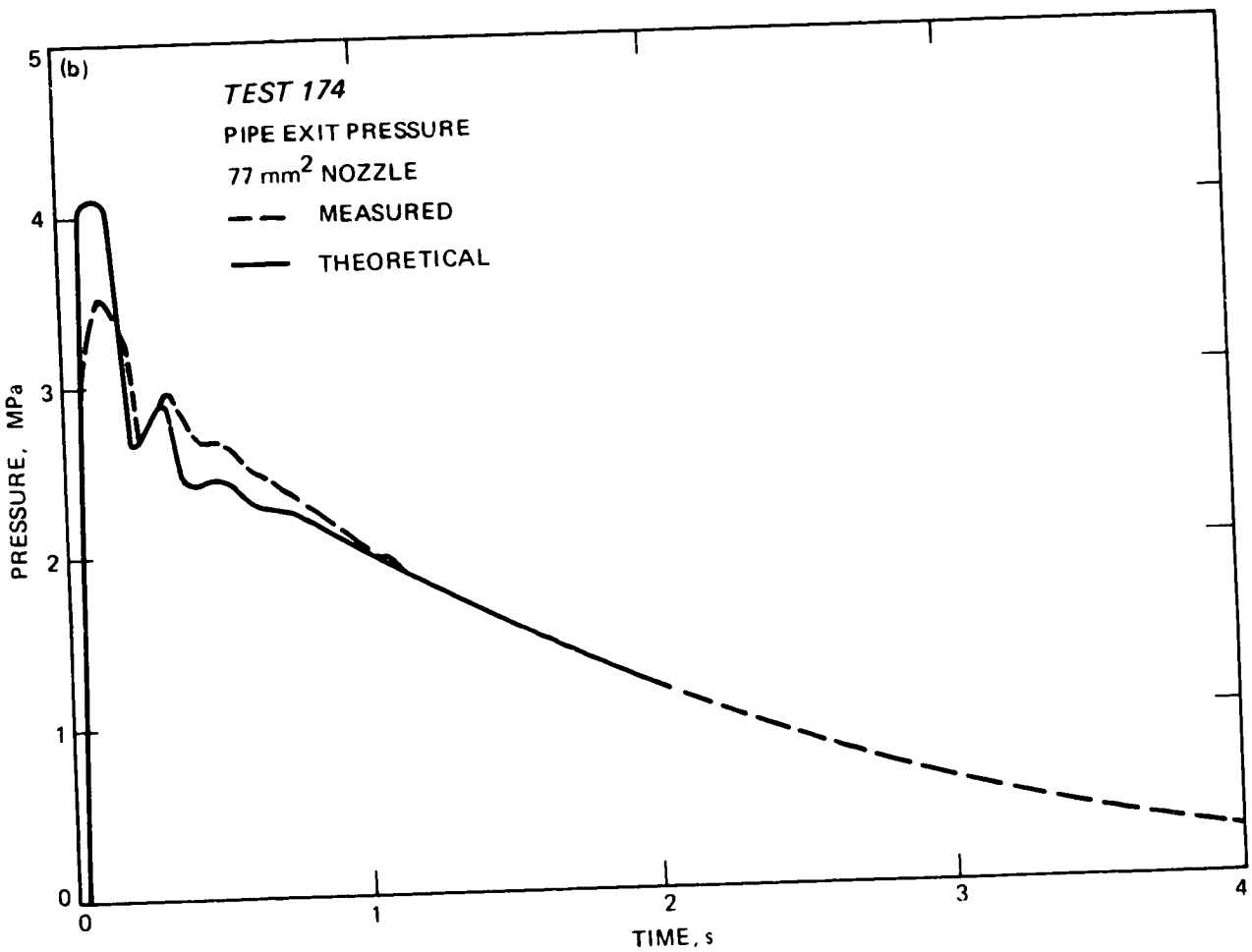

Figure C-1. Comparison, for discharge through a pipe and nozzle, between: (b) Pipe exit pressure SOLA-LOOP predictions and data

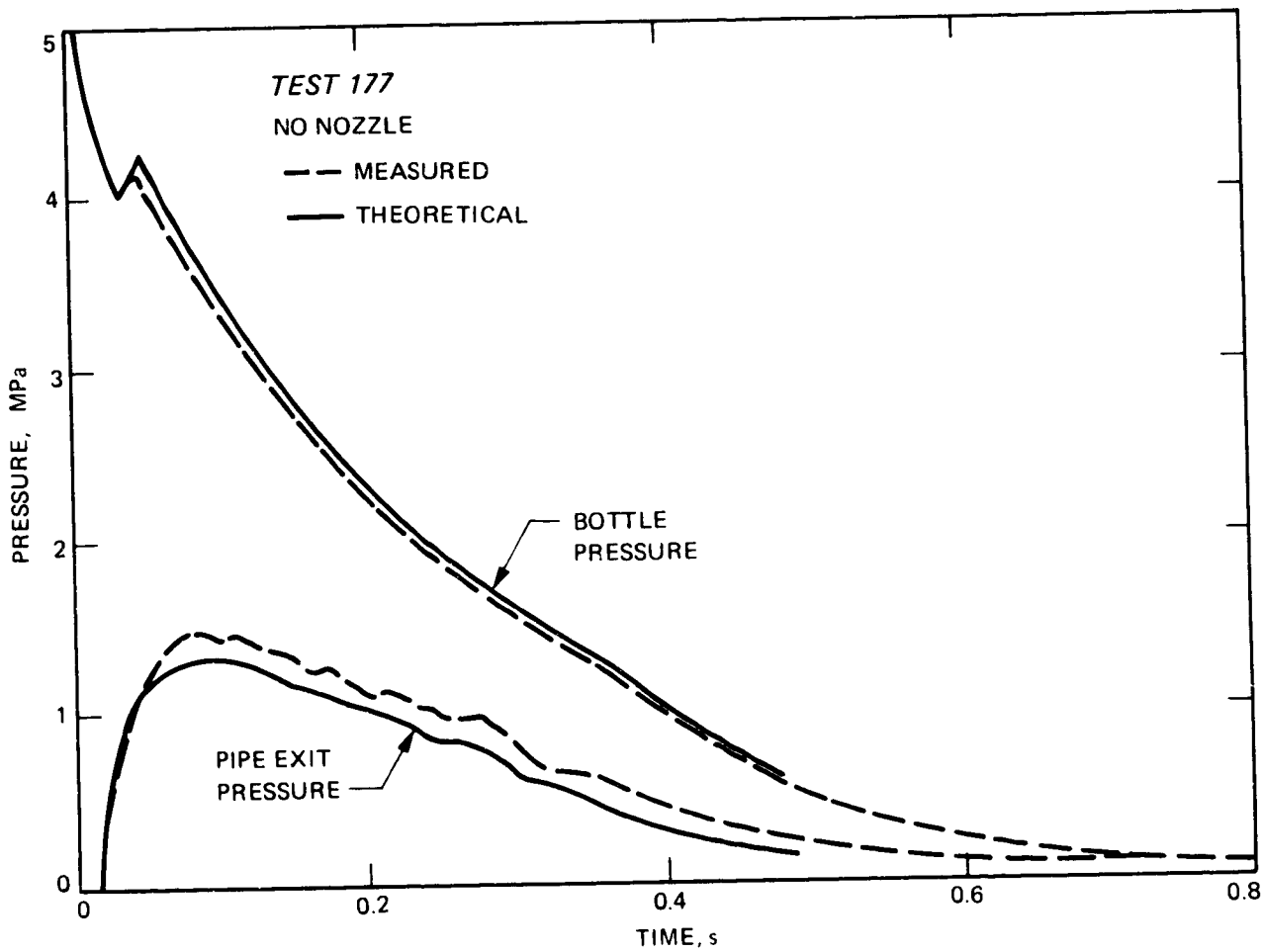

Figure C-2. Comparison, for discharge through a pipe without a nozzle, between SOLA-LOOP predictions and data

Computing time and cost for the SOLA-LOOP program on the LANL CDC-7600 computer ranged from 30 s and $4, for computing the flow from a bottle through an orifice, to 11 minutes and $90 for a three-branch distribution system.

An improved version of the SOLA-LOOP program, called "SOLA-NET", is now available (Ref. 16). Adding Halon properties to that program would probably give the most accurate Halon flow program possible at the present.

APPENDIX D. TEST SUMMARY

In addition to the tests run for comparison with the theoretical models, about 150 tests were made with flow through the bottle valve only. These tests were referred to as the "short system tests". Two different bottle sizes were used, with valves from four different manufacturers. Four different Halon fill densities were used. Table D-1 lists the short-system test numbers for each combination of conditions.

The bottle pressure used for each short-system test was the value that would have been reached on heating or cooling a standard-condition bottle (70°F and 750 psig) to the test-cell temperature. That pressure was obtained from the graphs shown in Figs. D-1(a) and (b).

The results of each test consisted of plots of pressure, temperature, and target force versus time. These plots are voluminous and are available separately.

A summary of test conditions and results is presented in Table D-2 for the short-system tests and also for the tests used in developing the models. An estimate of liquid discharge time is given for those tests where a slope break could be identified.

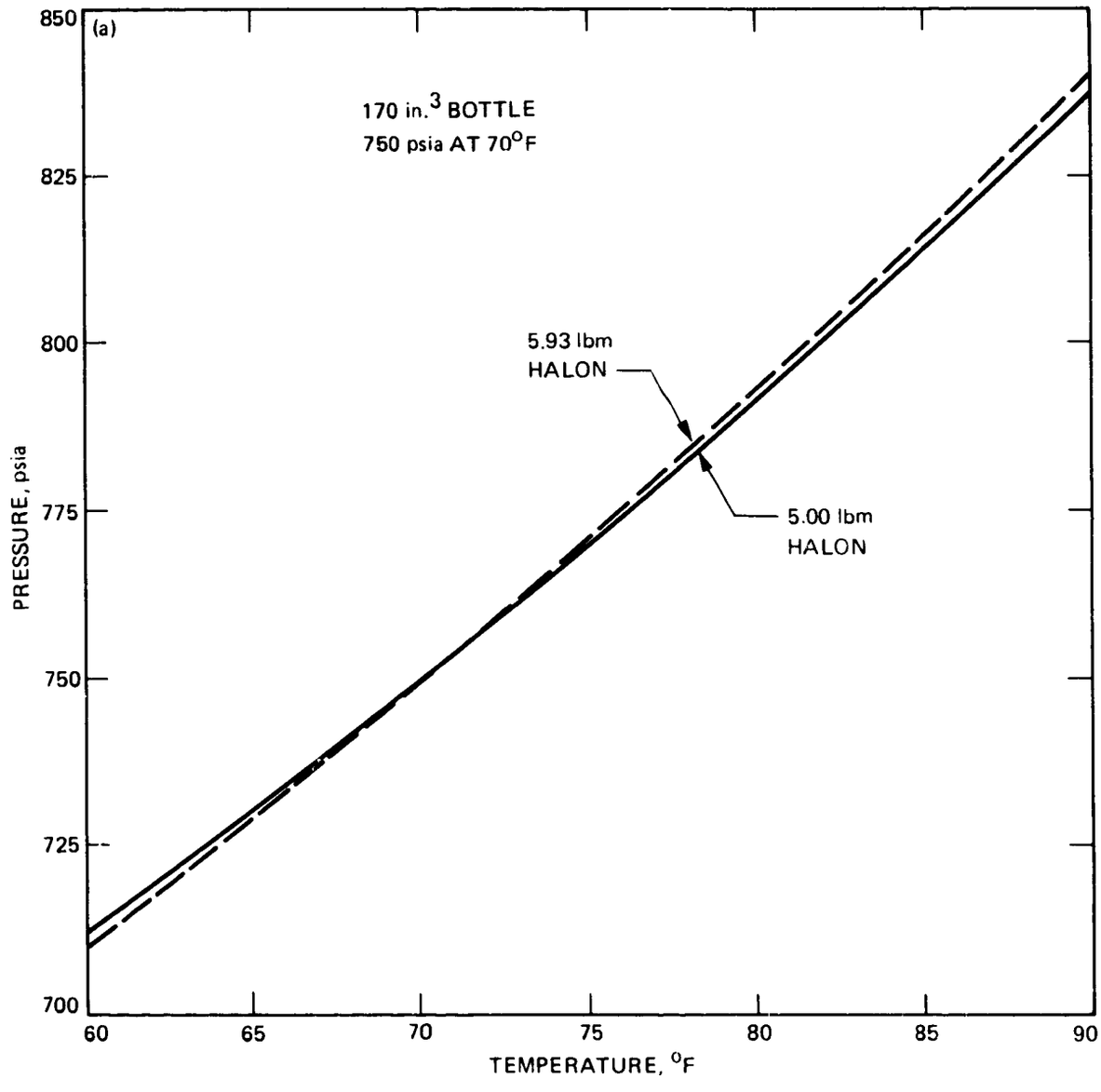

Figure D-1. Curves used for setting bottle pressures in the short-system tests: (a) With a 170-in^3 bottle

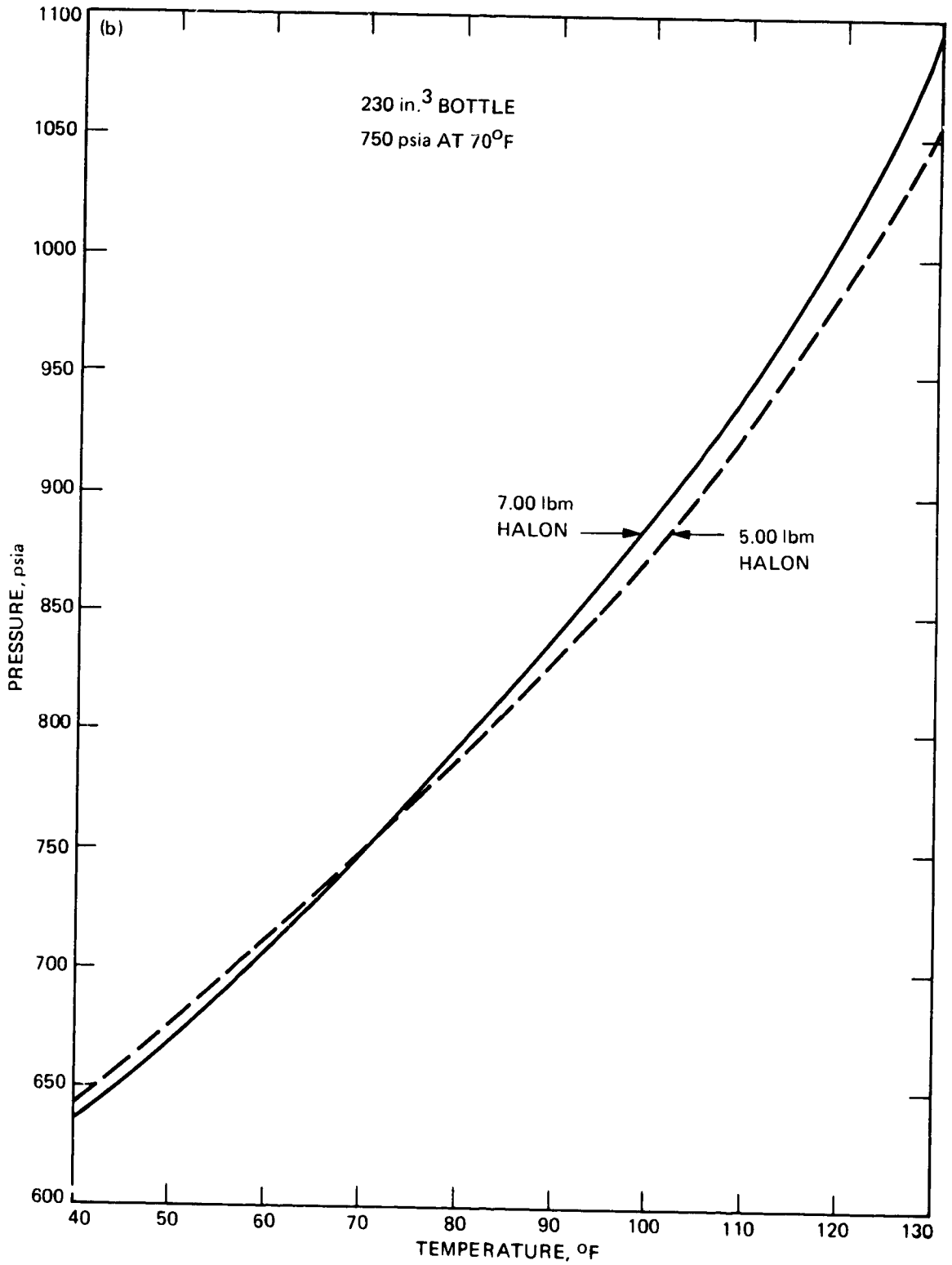

Figure D-1. Curves used for setting bottle pressures in the short-system tests: (b) With a 230-in^3 bottle

Table D-1. Short-System Test Numbers

DESIRED TEST CONDITION			CROWN VALVE		HTL VALVE		HRM VALVE		MAROTTA VALVE	
Bottle Volume $in.^3$	Halon fill density lb/ft^3	Temperature ^oF	1	2	1	2	1	2	1	2
230	38	70	68-71		81-84		c0-63		275-278	
170	60	70	52-55		118 119 136 159		132-135		124-127	
170	50	70	46-49		167 121 123 160		108-111		128-131	
230	53	70	72-75	76-79	138-140 168	141 150-152	56-59	64-67	279 282	285-288
		120	90-93	86-89	169-172	153 156-158	98-101	94-97	283 284	290

Table D-2. Test Summary[a]

Test No.	Valve	Bottle Volume, $in.^3$	Halon Fill, lbm	Fill Density, lbm/ft^3	Initial Pressure, psia	Initial Liquid Temp, °F	Nitrogen Release Pressure, psia	Liquid Expulsion Time, ms
46	CR-1	169.0	4.98	50.9	785	85	605	90
47	CR-1	169.0	5.02	51.3	743	65	460	100
49	CR-1	169.0	5.25	53.7	750	62	432	100
50	CR-2	169.0	5.37	54.9	787	75	570	---
51	CR-2	169.0	5.05	51.7	771	72	700	---
52	CR-2	169.0	6.15	62.9	725	61	455	---
53	CR-2	169.0	5.94	60.7	751	64	460	150
54	CR-2	169.0	5.91	60.4	752	66	480	---
55	CR-2	169.0	6.08	62.2	748	68	538	---
56	HR-1	231.5	6.98	52.1	769	68	525	150
57	HR-1	231.5	7.04	52.5	747	72	490	140
58	HR-1	231.5	7.07	52.8	782	74	541	160
59	HR-1	231.5	7.13	53.2	769	74	549	160
60	HR-1	231.5	5.06	37.8	775	78	561	100
61	HR-1	231.5	5.02	37.5	778	75	559	110
62	HR-1	231.5	5.05	37.7	745	67	490	---
63	HR-1	231.5	5.08	37.9	763	67	525	---
64	HR-2	231.5	6.99	52.2	737	64	464	150
65	HR-2	231.5	7.00	52.3	739	65	465	160
66	HR-2	231.5	7.00	52.3	733	66	480	150
67	HR-2	231.5	6.98	52.1	750	65	490	150
68	CR-1	229.3	5.08	37.9	717	60	430	80
69	CR-1	229.3	5.05	37.7	744	64	460	80
70	CR-1	229.3	4.93	36.8	720	63	400	80
71	CR-1	229.3	5.07	37.8	732	61	411	80
72	CR-1	229.3	6.98	52.6	739	63	620	150
73	CR-1	229.3	7.10	53.5	736	62	451	150
74	CR-1	229.3	7.10	53.5	733	62	450	150
75	CR-2	229.3	7.02	52.9	650	53	265	---
76	CR-2	229.3	6.88	51.8	737	63	475	---
77	CR-2	229.3	6.88	51.8	737	62	450	---
78	CR-2	229.3	7.05	53.1	781	67	535	150
79	CR-2	229.3	6.97	52.5	735	67	483	140
81	HT-1	229.6	5.04	37.9	732	59	433	90
82	HT-1	229.6	5.05	38.0	761	66	491	80
83	HT-1	229.6	5.11	38.5	745	64	470	80
84	HT-1	229.6	5.18	39.0	751	64	474	80
85	CR-2	229.3	6.92	52.1	968	113	---	---
86	CR-2	229.3	7.07	53.2	1043	118	970	---
87	CR-2	229.3	7.17	54.0	1017	123	911	---
88	CR-2	229.3	6.99	52.6	1022	125	960	---
89	CR-2	229.3	7.00	52.7	1005	124	964	---
90	CR-1	229.3	7.01	52.8	985	119	941	---
91	CR-1	229.3	7.13	53.7	1003	124	909	---

Table D-2. Test Summary (Contd.)

Test No.	Valve	Bottle Volume, $in.^3$	Halon Fill, lbm	Fill Density, lbm/ft^3	Initial Pressure, psia	Initial Liquid Temp, °F	Nitrogen Release Pressure, psia	Liquid Expulsion Time, ms
92	CR-1	229.3	7.13	53.7	982	123	---	---
93	CR-1	229.3	7.15	53.8	1028	120	980	---
94	HR-2	231.5	7.01	52.3	989	121	---	---
95	HR-2	231.5	6.97	52.0	1034	123	945	---
96	HR-2	231.5	7.03	52.5	969	120	---	---
97	HR-2	231.5	7.10	53.0	1050	120	974	---
98	HR-1	231.5	6.81	50.8	1007	124	958	---
99	HR-1	231.5	7.04	52.5	999	119	---	---
100	HR-1	231.5	7.05	52.6	975	120	950	---
101	HR-1	231.5	7.08	52.8	997	122	970	---
102	HR-1	231.5	6.92	51.7	802	65	581	170
103	HR-1	231.7	6.97	52.0	781	67	560	---
104	HR-1	231.7	7.18	53.5	797	76	600	---
105	HR-1	231.7	7.14	53.5	848	70	682	190
106	HR-1	231.7	7.07	52.7	841	80	680	180
107	HR-1	170.7	5.01	50.7	805	81	634	100
108	HR-1	170.7	5.01	50.7	839	88	687	100
109	HR-1	170.7	4.99	50.5	796	79	624	110
110	HR-1	170.7	4.99	50.5	801	78	630	100
111	HR-1	170.7	5.10	51.6	775	70	550	120
118	HT-1	168.2	5.95	61.1	820	83	667	150
119	HT-1	168.2	5.96	61.2	821	84	675	140
121	HT-1	168.2	5.12	52.6	783	74	590	90
122	HT-1	168.2	4.99	51.3	826	85	680	80
123	HT-1	168.2	4.97	51.1	830	89	680	80
124	MR-1	168.7	6.12	62.7	853	91	730	200
125	MR-1	168.7	5.88	60.2	771	73	560	190
126	MR-1	168.7	5.90	60.4	790	77	605	190
127	MR-1	168.7	5.91	60.5	787	81	570	180
128	MR-1	168.7	4.98	51.0	806	81	631	140
129	MR-1	168.7	4.99	51.1	802	80	632	140
130	MR-1	168.7	4.93	50.5	806	77	631	140
131	MR-1	168.7	5.05	51.7	751	72	479	130
132	HR-1	170.7	5.92	60.0	780	76	575	170
133	HR-1	170.7	5.96	60.3	794	67	586	170
134	HR-1	170.7	5.99	59.7	831	86	654	150
135	HR-1	170.7	5.93	60.0	793	74	619	150
136	HT-1	168.2	5.96	60.6	792	77	615	140
137	MR-1	229.4	6.96	52.4	803	86	680	120
138	HT-1	229.6	7.05	53.1	806	72	601	160
139	HT-1	229.6	7.09	57.9	801	78	638	200
140	HT-1	229.6	7.34	55.2	835	73	680	140
141	HT-1	229.6	7.05	53.1	816	82	637	140
145	HT-1	168.2	4.36	44.8	798	83	615	---
146	HT-1	168.2	5.13	52.7	750	71	530	850

Table D-2. Test Summary (Contd.)

Test No.	Valve	Bottle Volume, $in.^3$	Halon Fill, lbm	Fill Density, lbm/ft^3	Initial Pressure, psia	Initial Liquid Temp, °F	Nitrogen Release Pressure, psia	Liquid Expulsion Time, ms
150	HT-2	229.6	7.06	53.1	813	77	635	160
151	HT-2	229.6	6.94	52.2	811	77	625	160
152	HT-2	229.6	7.02	52.8	806	72	625	---
153	HT-2	229.6	7.01	52.8	970	155	---	---
154	HT-2	229.6	6.99	52.6	940	108	800	160
155	HT-2	229.6	6.82	51.3	800	101	670	160
156	HT-2	229.6	7.16	53.9	962	124	---	---
157	HT-2	229.6	7.00	52.7	990	160	---	---
158	HT-2	229.6	6.97	52.5	975	120	---	---
159	HT-1	168.2	5.94	61.0	880	128	750	---
160	HT-1	168.2	5.03	5.17	880	105	775	90
166	MR-2	229.4	7.15	53.9	764	71	561	---
167	HT-1	168.2	5.17	53.1	777	71	571	100
168	HT-1	229.6	7.01	52.8	790	74	605	150
169	HT-1	229.6	7.02	52.8	1012	125	950	---
170	HT-1	229.6	7.01	52.8	1021	159	961	---
171	HT-1	229.6	6.98	52.5	970	125	905	---
172	HT-1	229.6	7.02	52.8	985	129	930	---
173	HT-1	229.3	7.03	53.0	764	68	550	800
174	HT-1	229.3	6.95	52.4	761	80	588	2000
175	HT-1	229.3	7.01	52.8	756	79	590	540
177	HT-1	229.3	7.02	52.9	757	78	586	360
275	MR-1	229.4	5.02	37.8	723	54	577	100
276	MR-1	229.4	4.96	37.4	735	61	470	90
277	MR-1	229.4	5.10	38.4	736	61	479	90
278	MR-1	229.4	4.96	37.4	767	61	520	100
279	MR-1	229.4	7.03	53.0	746	62	593	200
280	MR-1	229.4	6.98	52.6	736	65	507	200
281	MR-1	229.4	7.01	52.8	744	65	518	200
282	MR-1	229.4	7.05	53.1	701	61	446	---
283	MR-1	229.4	7.04	53.0	1149	145	800	200
284	MR-1	229.4	7.13	53.7	1210	151	740	170
285	MR-2	229.4	6.95	52.4	746	65	480	---
286	MR-2	229.4	6.95	52.4	754	67	510	---
287	MR-2	229.4	6.95	52.4	751	69	512	---
288	MR-2	229.4	7.04	53.0	745	69	510	---
289	MR-2	229.4	7.23	54.5	795	81	600	210
290	MR-2	229.4	4.99	37.6	1490	146	1380	---
293	HT-1	229.3	7.00	52.5	783	75	---	---
294	HT-1	229.3	7.05	53.1	761	72	---	---

[a] All tests used the bottle valve only, except for the following: tests 145 and 146 used a 0.389-in. diameter nozzle; test 173 used a 3.8-m pipe with a 0.610-in. diameter nozzle; test 174 used a 3.8-m pipe with a 0.389-in. diameter nozzle; test 175 used a 3.8-m pipe with a 0.844-in. diameter nozzle; test 177 used a 3.8-m pipe with no nozzle; test 293 used distribution system no. 1; and test 294 used distribution system no. 2.